An overexcited plant immunoreceptor: a hybrid FLS2 receptor that is active without flagellin

Dissertation

der Mathematisch-Naturwissenschaftlichen Fakultät

der Eberhard Karls Universität Tübingen

zur Erlangung des Grades eines

Doktors der Naturwissenschaften

(Dr. rer. nat.)

vorgelegt von

M.Sc. Yan Wang

aus Beijing, China

Tübingen

2022

Gedruckt mit Genehmigung der Mathematisch-Naturwissenschaftlichen Fakultät der Eberhard Karls Universität Tübingen.

Tag der mündlichen Qualifikation:	04.07.2022
Dekan:	Prof. Dr. Thilo Stehle
1. Berichterstatter/-in:	Prof. Dr. Georg Felix
2. Berichterstatter/-in:	Prof. Dr. Rosa Lozano-Durán

Summary

Perception of bacterial flagellin by the receptor kinase AtFLS2 is a classic model for studying the molecular functioning of plant immunoreceptors. Although FLS2 receptors with a conserved ectodomain consisting of 28 leucine-rich repeats (LRRs) occur in a broad range of plant species, these FLS2 homologs display species-specific characteristics with respect to the affinity and specificity for the peptide ligand flg22 and derivatives thereof. SlFLS2 from tomato, for example, has higher affinity for flg22 than AtFLS2 and is able to recognize the shortened ligand peptide flg15. In previous work, chimeric receptors with LRR subdomain swaps between AtFLS2 and SlFLS2 were generated to investigate the LRRs responsible for the species-specific features (Mueller et al., 2012). Most of these chimeric receptors indeed proved functional and exhibited characteristics for either SlFLS2 or AtFLS2.

However, Sl15-24, one of the hybrids with the LRRs 15-24 from SlFLS2 replacing the corresponding LRRs in AtFLS2, showed constitutive activation of defence responses even in the absence of ligand. Interestingly, this autoactivation depended strictly on the co-receptor AtBAK1/AtSERK3. None of the other SERKs from *A. thaliana*, even when overexpressed, did cause autoactivation. Intriguingly also, in mutants lacking AtBAK1 the Sl15-24 hybrid behaved as a functional flg22-receptor much like AtFLS2, inducing a full set of responses when treated with its ligand flg22. Additionally, Sl15-24-induced autoactivation could be supressed by the negative regulators BIR2, BIR3 and BIR4 which are known to negatively regulate AtBAK1 and prevent flg22-dependent activation of AtFLS2. These results strongly suggest that the Sl15-24 hybrid interacts with AtBAK1 to trigger cellular responses in the absence of ligand. However, Sl15-24 and AtBAK1 do not form a stable complex in a manner comparable to the ligand (flg22)-induced complex between AtFLS2 and AtBAK1. Since the autoactivation process depends on functional kinase domains on Sl15-24 and AtBAK1, this suggests transient interaction between these partners to be sufficient for the induction process.

With further swapping constructs we narrowed the LRRs required from SlFLS2 for causing autoactivation to the LRRs 18-24. However, importantly, extending the swap to the LRRs 11-24 abolished the autoactivation effect and resulted in fully functional, ligand-dependent FLS2 receptor chimeras. Thus, autoactivation occurs only in chimeras that have 18-24 from SlFLS2 in combination with LRRs 7-14 from AtFLS2.

Zusammenfassung

In *Arabidopsis thaliana* ist die Wahrnehmung des Peptidliganden flg22 durch die Rezeptorkinase AtFLS2, zusammen mit dem Ko-Rezeptor AtBAK1/AtSERK3, ein klassisches Modell zur Untersuchung der molekularen Funktionsweise pflanzlicher Immunrezeptoren. Obwohl FLS2-Rezeptoren in Pflanzen konserviert sind, weisen sie artspezifische Eigenschaften auf. Frühere Studien zeigten, dass SlFLS2 aus Tomate eine höhere Affinität zu flg22 hat, als AtFLS2. SlFLS2 ist zudem in der Lage, das verkürzte Ligandenpeptid flg15 zu erkennen. In früheren Arbeiten wurden chimäre FLS2-Rezeptoren mit Sequenz-Austausch zwischen AtFLS2 und SlFLS2 generiert, um jene LRRs zu identifizieren, die für die artspezifischen Merkmale verantwortlich sind (Mueller et al., 2012).

Sl15-24, einer dieser chimären Rezeptoren, bei dem die LRRs Nummer 15 bis 24 von SlFLS2 die entsprechenden LRRs in AtFLS2 ersetzen, wies eine bemerkenswerte Eigenschaft auf: Sl15-24 war auch in Abwesenheit eines Liganden konstitutiv aktiv. Interessanterweise zeigten genetische Experimente, dass diese Autoaktivierung in *A. thaliana* strikt von AtBAK1/AtSERK3 abhängt. In Abwesenheit von AtBAK1 verhielt sich diese Chimäre wie ein funktioneller Flagellin-Rezeptor, welcher, wie AtFLS2, mit den üblichen Immunantworten auf Behandlungen mit flg22 reagierte. Darüber hinaus wurde die Autoaktivität von Sl15-24 durch die Überexpression negativer Regulatoren von AtBAK1 (*i.e.* von BIR2, BIR3 und BIR4) unterdrückt. Diese Ergebnisse sind starke Hinweise dafür, dass der chimäre FLS2-Rezeptor Sl15-24 mit AtBAK1 interagiert, um zelluläre Antworten auch in Abwesenheit des Liganden auszulösen. Bisher konnte jedoch keine stabile Komplexbildung zwischen Sl15-24 und AtBAK1 in der Weise gefunden werden, wie dies bei dem flg22-induzierten Komplex zwischen AtFLS2 und AtBAK1 der Fall ist. Da der Autoaktivierungsprozess von der Funktionalität beider Kinasen, der des chimären Rezeptors und des Ko-Rezeptors, abhängt, deutet dies darauf hin, dass eine vorübergehende Interaktion zwischen diesen Partnern für den Induktionsprozess ausreichend sein könnte.

Mit weiteren Austauschkonstrukten haben wir die Autoaktivität-verursachenden LRRs von SlFLS2 auf die LRRs Nummer 18 bis 24 eingeengt. Erstaunlicherweise bewirkte die Ausweitung des Austausches von SlFLS2 LRRs auf die LRRs 11–24 keine Autoaktivierung. Stattdessen waren diese Chimären voll funktionsfähige und ligandenabhängige FLS2-Rezeptoren. Somit trat also die Autoaktivierung nur bei solchen Chimären auf, welche sowohl die LRRs Nummer 18-24 von SlFLS2, als auch die LRRs Nummer 7-14 von AtFLS2 aufwiesen.

Table of Contents

1 Introduction

1.1 General introduction to plant immunity

Pathogenic microbes occur in the environment surrounding plants at all times. Unlike animals, plants neither can move to escape from invasion nor do they have circulating immune cells to deal with it. To survive under constant attack plants employ a broad set of constitutive and inducible defence mechanisms (Jones and Dangl, 2006, Boller and Felix, 2009).

Conceptually, plants inducible defence systems, often summarized as plant innate immunity, can be separated into two layers, pattern-triggered immunity (PTI) and effector-triggered immunity (ETI), respectively. Both layers are important, utilizing a series of immune responses to fight off pathogenic invasion (Boller and Felix, 2009, Zipfel, 2014, Yu et al., 2017). The activation of PTI is achieved by the perception of molecular patterns that signal the presence of potential pathogens (or other dangers) by large families of surface localised pattern recognition receptors (PRRs) (Zipfel and Felix, 2005). These molecular patterns detected by PRRs can be either derived from the pathogens, thus often termed PAMPs or MAMPs for pathogen- or microbe-associated molecular patterns, or they get released from host tissue as damage-associated molecular pattern (DAMPs) in the course of pathogen attacks.

Activated PRRs trigger intracellular signalling and a broad range of defence responses that confer resistance to host plants. Production of reactive oxygen species (ROS) and the stress hormone ethylene are part of this responses that are often used to monitor PAMP perception by PRRs (Boller and Felix, 2009). However, successfully adapted pathogens evolved means to evade or overcome this first line of host defences provided by PTI (Jones and Dangl, 2006). Such pathogens often apply an array of effector molecules to interfere with PTI responses and block the immune system (Dangl et al., 2013). However, as results of co-evolutionary processes, plants evolved a second layer of immunodetection systems that relies on the detection of effectors (Jones and Dangl, 2006, Boller and Felix, 2009). Unlike PTI, ETI relies on intracellular receptors detecting pathogen-derived effectors and more intensive immune responses, often accompanied with host cell death that effectively restricts the spreading of pathogens (Lolle et al., 2020, Cui et al., 2015, Dangl et al., 2013). Previously, PTI and ETI were considered to be separate, independent mechanisms, however, recent evidence suggests

that PTI and ETI share common downstream components and are partially overlapping (Yuan et al., 2021a, Ngou et al., 2021, Yuan et al., 2021b, Pruitt et al., 2021).

1.2 PTI signal perception—ligand recognition by PRRs

PRRs can be classified into two types: receptor-like kinase (RLK) and receptor-like protein (RLP)(Shiu and Bleecker, 2003, Shiu and Bleecker, 2001a). RLKs consist of an extracellular domain (ECD) for ligand recognition, a single-spanning transmembrane domain (TMD) and a cytoplasmic Ser/Thr kinase domain (KD) (Gust and Felix, 2014, Shiu and Bleecker, 2001b, Ma et al., 2016). Ligand binding to the receptor-like kinase triggers a complex formation with a further RLK that acts as a co-receptor and allows for the activation of the KDs and induction of downstream signalling (Gou and Li, 2020, Chinchilla et al., 2007, Song et al., 2021, Albert et al., 2020). In *A. thaliana* the co-receptor is one of the five so-called somatic embryogenesis receptor-like kinase (SERKs), notably AtSERK3 which is also named brassinosteroid insensitive 1-associated receptor kinase 1 (AtBAK1, hereafter AtBAK1) (Chinchilla et al., 2009, Domínguez-Ferreras et al., 2015, Ma et al., 2016). RLPs are similar to RLKs but lack a kinase domain (Boller and Felix, 2009, Couto and Zipfel, 2016). Instead, most RLPs of *Arabidopsis* form a constitutive complex with the RLK suppresser of BIR1 (SOBIR1) that acts as a common adaptor kinase and allows downstream signalling together with co-receptors like AtBAK1 (Gust and Felix, 2014, Couto and Zipfel, 2016, Boller and Felix, 2009). According to the structure of their extracellular domain, PRRs can also be categorised into different receptor classes, for instance leucine-rich repeat (LRR)-RLK/RLP, lysin motif (LysM)-RLK/RLP, epidermal growth factor (EGF)-RLK/RLP et cetera (Bohm et al., 2014).

Besides, PRRs can also be grouped according to the type of ligand they detect. For instance, receptors for bacterial patterns include the flagellin sensing 2 (FLS2) detecting bacterial originated flagellin-derived peptide flg22 and elongation factor Tu receptor (EFR) that detects the elf18 ligand representing the N-terminus of bacterial elongation factor Tu (Chinchilla et al., 2006, Chinchilla et al., 2007, Gómez-Gómez and Boller, 2000, Zipfel et al., 2006). For fungal derived elicitors, chitin is recognized by chitin elicitor receptor kinase 1 (CERK1)/ lysin motif receptor kinase 5 (LYK5) in *A. thaliana* and chitin oligosaccharide elicitor-binding protein (CEBiP) in rice (Liu et al., 2012, Cao et al., 2014, Kaku et al., 2006, Hayafune et al., 2014). Another example is that tomato ethylene-inducing xylanase receptor 1 and 2 (SlEIX1 and SlEIX2) recognize fungal xylanase (Ron and Avni, 2004, Bar et al., 2010). AtRLP23 recognises the Necrosis and ethylene-inducing peptide 1-like proteins (NLPs)

derived from bacterial, fungal and oomycetes (Albert et al., 2015). Moreover, PRRs can also perceive plant-derived elicitors. For example, LRR-RLK AtPep receptor PEPR1 and 2 (AtPEPR1/AtPEPR2) and tomato systemin receptor 1 and 2 (SlSYR1/SlSYR2) perceive the endogenous proteinatious Atpeps and systemin, respectively (Yamaguchi et al., 2010, Yamada et al., 2016, Wang et al., 2018). Wall-associated kinase 1 (WAK1) might perceive the putative oligogalacturonides (OGs) from plant cell wall (Brutus et al., 2010).

1.3 Mechanism of receptor activation—FLS2 as an example

Like the other RLKs, FLS2 consists of an ECD, a TMD and an active Ser/Thr KD (Gómez-Gómez and Boller, 2000). Normally, the ECD of FLS2 contains 28 LRR motifs with the LRR consensus sequence IPxxLxxLxxLxxLxLxxNxL (T/S) Gx (x represents for any amino acid, Figure 1.3.1A) (Mueller et al., 2012). Generally, the ECD of a receptor is responsible for perceiving extracellular ligand and the KD for cytosolic downstream signalling initiation (Zipfel and Oldroyd, 2017, Albert et al., 2020).

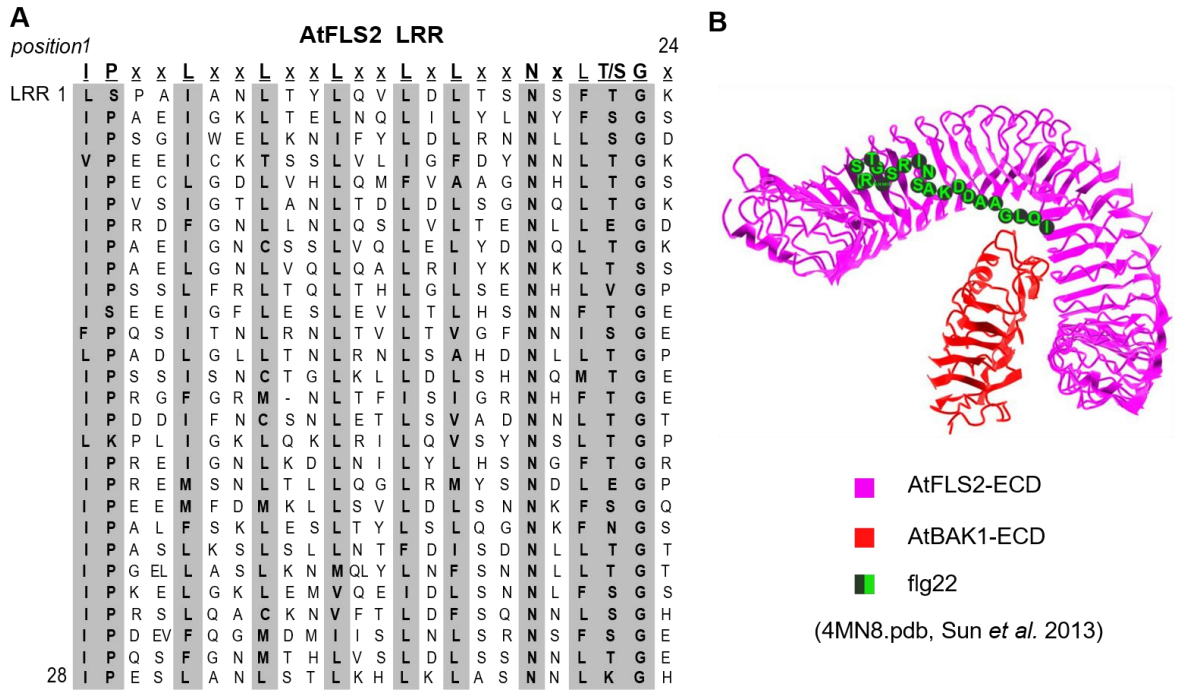

Figure 1.3.1 AtFLS2-LRR and AtFLS2-AtBAK1-flg22 complex

A) Amino acid sequence of AtFLS2 LRR. Gray shadow indicates conserved residue. B) Crystal structure of AtFLS2-AtBAK1-flg22 complex.

How does binding of a ligand to the ECD of an RLK lead to the activation of the cytoplasmic KD? The "address and message" concept was first proposed as a model for receptor activation in the animal field (Schwyzer, 1977). Basically, a part of ligand is responsible for being recognized by a receptor (binding/address) and the other part leads to the signal transduction of a receptor (activation/message). This concept also holds for flg22 and other ligands of plant receptors and has a molecular explanation by the binding of ligands to the receptors with their "address" part that then allows recruitment of co-receptors via their "message" part for activation of signalling (Meindl et al., 2000, Albert et al., 2010a).

Many studies were carried out to investigate the subdomain of AtFLS2 responsible for flg22 binding, culminating in the crystallographic structural analysis of Sun et al., (2013). The *fls2-24* mutant discovered in the original screen for flg22-insensitive lines carries a single point mutation with an exchange of Glycine 318 to Arginine located within LRR 10 of AtFLS2 (Gómez-gómez et al., 2001, Gómez-Gómez and Boller, 2000, Bauer et al., 2001, Mueller et al., 2012). This mutation completely abolished flg22 binding and functionality of the AtFLS2 receptor, but, interestingly, not when introduced into the tomato SlFLS2, as detected in a later study (Mueller, 2011). A further study applying alanine scanning on AtFLS2 indicated that the LRRs 9-15 are important for flg22 binding (Dunning et al., 2007). The LRR 17 of AtFLS2 was also claimed to be important for flg22 binding by testing the binding of flg22 to FLS2 variants observed in different *Arabidopsis* accessions (Vetter et al., 2012).

Studying the sequence requirements of the ligand peptide at its C-terminus, defined as the "message" part of flg22 in earlier studies, also helped to understand receptor activation. For instance, the peptides flg22-YWS and flg22-AYA, were found to bind to AtFLS2 but, rather than activating the receptor as agonists, they acted as competitive antagonists for unmodified flg22 (Mueller et al., 2012, Mueller, 2011, Bittel, 2010). These two examples clearly supported the "address and message" concept and indicated that the C-terminal 3 amino acids are important for AtFLS2 activation.

An important step in elucidating the molecular basis for the "message" function in receptor activation was the discovery that ligand binding leads to rapid complex formation of AtFLS2 with AtBAK1 *in vivo* and *in vitro* (Chinchilla et al., 2007, Schulze et al., 2010, Sun et al., 2013a), a process that was shown to be critical for AtFLS2-mediated responses (Chinchilla et al., 2007). AtBAK1 is also a LRR-RLK, yet the ECD of AtBAK1 only contains 5 LRRs (Hecht et al., 2001). The crystallographic study on ECDs of AtFLS2 and AtBAK1 revealed that flg22 binds to the groove of AtFLS2 across LRR 3 to LRR 16 (Figure 1.3.1B) (Sun et

al., 2013a). AtBAK1 indirectly interacts with AtFLS2 LRR16 and directly interacts with AtFLS2 LRR 18-20 and LRR23-26 under the "molecular glue" function of flg22 (Sun et al., 2013a). Glycine at the position 18 of flg22 was illustrated to be crucial for AtBAK1 recruitment (Sun et al., 2013a). The mutants flg22 peptides with the amino acid residue at position 18 changed from glycine to alanine or tyrosine were reported to have similar binding capacity like wildtype flg22 peptide to AtFLS2 (Sun et al., 2013a). However, no ligand-induced AtBAK1-AtFLS2 complex was observed upon the mutant flg22 treatment (Sun et al., 2013a).

1.4 PTI regulation-AtBAK1 and related

1.4.1 AtBAK1 and its homologs

AtBAK1 belongs to a small family of SERK proteins with five members in *A. thaliana* (Chinchilla et al., 2007, Hecht et al., 2001). Originally, AtBAK1 was identified as an interactor of plant developmental hormone brassinosteroid (BR) receptor brassinosteroid insensitive 1 (BRI1), therefore brassinosteroid insensitive 1-associated receptor kinase1 was named (Li et al., 2002). AtBAK1 forms a BR-induced complex with BRI1, allowing for the transphosphorylation of both KDs and leading to the initiation of BR downstream signalling (Nam and Li, 2002, Sun et al., 2013b, Wang et al., 2008). Besides AtBAK1, AtSERK1, AtSERK2 and AtSERK4 were also claimed to be positive regulators in the BR signalling pathway (Gou et al., 2012, Noguchi et al., 1999, Russinova et al., 2004), which suggested that AtSERKs might be redundant. However, the AtSERK5 from Col-0 seems not to contribute to the BR signalling pathway, possibly due to a leucine at position 401 instead of arginine that changes the Arg/Asp (RD) kinase motif that is commonly conserved in these kinases (He et al., 2007, Gou et al., 2012). Indeed, AtSERK5 in the accession Ler-0 has a non-mutated RD kinase motif and was observed to be a positive regulator in mediating BR signal transduction (Wu et al., 2015, Noguchi et al., 1999).

Later, the versatile role of AtSERKs was discovered in plant immunity represented by functioning as co-receptor of AtFLS2 in flg22 perception (Chinchilla et al., 2007, Schwessinger et al., 2011). Since then, AtSERKs have been reported as common co-receptors in immune signalling via diverse PRRs including EFR and PEPR1/2 (Roux et al., 2011, Tang et al., 2015). Moreover, the AtSERKs were also shown to act as co-receptors for RLKs

controlling plant growth and floral development (Lewis et al., 2010, Wang et al., 2015, Li et al., 2002, Ma et al., 2016).

1.4.2 AtBAK1 and the BIRs as its negative regulators

The BIRs, BAK1-interacting receptor-like kinases, are four structurally closely related LRR-RLKs that have been reported to interact with AtBAK1 constitutively in *planta*, and the ECD of BIRs were also found to interact with AtBAK1 ECD *in vitro* (Gao et al., 2009, Halter et al., 2014b, Ma et al., 2017). BIR2, BIR3 and BIR4 function as negative regulators of AtBAK1 and interact with AtBAK1 KD in yeast-two-hybrid experiments (Halter et al., 2014b, Imkampe et al., 2017). BIR1 was originally identified in a reverse genetic screen with *Arabidopsis* mutants carrying knockouts in genes which were upregulated 48 h post inoculation with *Pseudomunas syringae pv. Maculicola (P.s.m.)* (Gao et al., 2009). One of these mutants with a disruption in *At5g48380* showed dwarfism and extensive cell death. *At5g48380* encodes an RLK with an ECD consisting of 5 LRRs and interacts with AtBAK1, thus being dubbed BIR1. The dwarf phenotype of *bir1* can be partially suppressed by knocking out the common RLP adaptor kinase SOBIR1 (Liu et al., 2016). Interestingly, an interaction of AtBAK1 and SOBIR1 can be detected only when BIR1 was silenced, thus it was hypothesized that BIR1 plays a role in prohibiting complex formation between AtBAK1 and SOBIR1/RLP, thereby preventing downstream immune responses (Liu et al., 2016). However, AtFLS2-mediated PTI signalling pathway seems not affected by BIR1 (Liu et al., 2016). In contrast to BIR1, which has an active kinase, the other three BIRs in *A. thaliana* have pseudokinases (Blaum et al., 2014, Halter et al., 2014b, Imkampe et al., 2017). BIR2 and BIR3 were discovered in immunoprecipitates of AtBAK1-GFP, by proteomic analysis (Halter et al., 2014b). Genome analysis identified BIR4 as a further member of the BIR family (Gao et al., 2009, Halter et al., 2014b). BIR2 and BIR3 were both reported to interact with AtBAK1, thereby acting as negative regulators for the AtFLS2-mediated plant immunity pathway (Halter et al., 2014b, Blaum et al., 2014, Imkampe et al., 2017). Moreover, BIR3 was also stated to interact directly with AtFLS2 and negatively regulated BR signalling pathway (Halter et al., 2014b, Blaum et al., 2014, Imkampe et al., 2017).

1.5 PTI signal output : FLS2 as an example

Upon activation of their PRRs, plants implement multi-facetted immune responses. These include changes in ion fluxes across the plasmamembrane (PM) as early symptoms, production of active oxygen species in an oxidative burst, activation of MAPK-

cascades/CDPK (mitogen-activated protein kinase/calcium-dependent protein kinase induction) , ethylene production and massive reprogramming of gene expression (Felix et al., 1999, Nühse et al., 2000, Wendehenne et al., 2002, Apel and Hirt, 2004, Jeworutzki et al., 2010b, Zipfel and Robatzek, 2010). In Figure 1.5.1 (from the review of Yu et al) the timely ordered changes are summarized for the best-studied PRR AtFLS2 as an example (Yu et al., 2017).

Within seconds of flg22 treatment AtBAK1 is recruited to form a complex with AtFLS2 and the kinase of both partners trans-phosphorylate each other (Chinchilla et al., 2007, Schulze et al., 2010). Then the receptor-like cytoplasmic kinase (RLCK) botrytis-induced kinase 1 (BIK1) is phosphorylated and transduces the immune signal to the cytosol (Lu et al., 2010, Lin et al., 2014). Activated BIK1, in turn, opens calcium (Ca^{2+}) channels. Ca^{2+} acts as an important second messenger for multiple biochemical signalling pathways (Ranf et al., 2012, Thor and Peiter, 2014), such as opening of calcium-associated ion channels that leads to K^+ efflux and proton influx and results in extracellular alkalinization (Jeworutzki et al., 2010a, Gust et al., 2007). BIK1 also triggers the production of reactive oxygen species (ROS) and activates MAPK cascades that lead to altered expression of numerous genes (Felix et al., 1999, Mersmann et al., 2010, Asai et al., 2002). Among these responses are an increased biosynthesis of the stress hormone ethylene (Felix et al., 1999, Zipfel et al., 2004) and the transcriptional induction of defence-related genes, such as *flg22-induced receptor-like kinase 1* (*FRK1*) and *WRKY29* (Asai et al., 2002). As late responses, a range of other physiological changes such as stomata closure, callose deposition and seedling growth inhibition can be observed, occurring hours to days after addition of the ligand flg22 (Deger et al., 2015, Luna et al., 2011, Chinchilla et al., 2007).

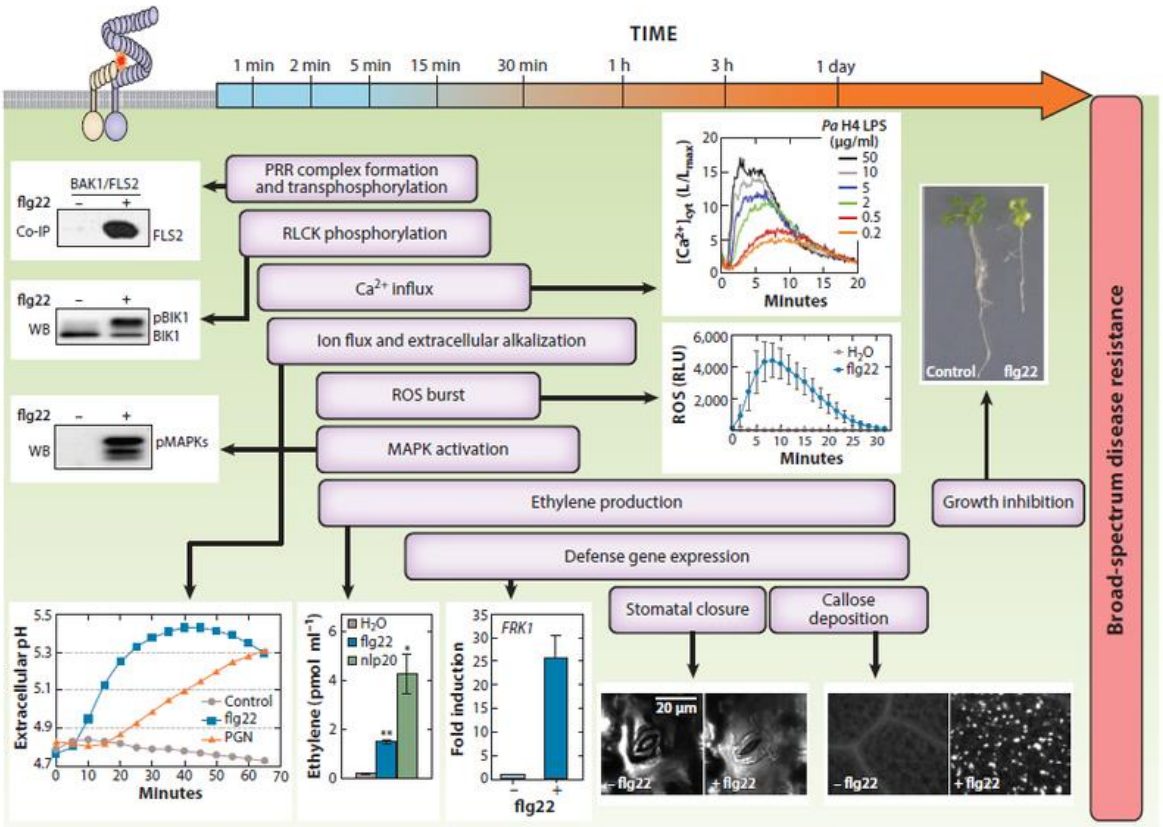

Figure 1.5.1 Time course of PTI outputs : AtFLS2 as example (Yu et al., 2017)

AtFLS2 and flg22 receptor-ligand pair is used as an example to illustrate the multi-layered immune responses after ligand perception, including: immunoreceptor complex formation and transphosphorylation, Ca^{2+} burst, apoplastic alkalinisation, ROS burst, ethylene production, defence gene reprograming, stomatal closure, callose deposition and seedling growth inhibition.

1.6 Domain swapping as a useful tool to dissect plant PRRs subdomains

Domain swapping has been applied in several studies to investigate ligand binding and kinase activation in plant PRRs. The first domain swapping example in plant PRRs was presented by fusion of ECD of BRI1 and KD of rice XA21, both of which are LRR-RLKs (He et al., 2000). Briefly, rice cells transformed with a chimeric construct of BRI1 and XA21 responded to brassinolide (BL) treatment with the typical immune responses of oxidative burst, defence gene upregulation and an increased rate of cell death. Much like the hybrid between BRI1 and XA21, BRI1 was also combined with EFR in a reciprocal way (Markus Albert unpublished data). Chimera containing BRI1 ECD and EFR TMD and KD responded to BL with ROS burst and the upregulation of an FRK1 immune marker. Vice versa, *A. thaliana* plants

expressing the hybrid of EFR ECD and BRI1 TMD-KD responded to the PAMP elf18 with increased growth (Markus Albert unpublished data).

Swapping of ligand-binding ECDs and KDs between AtFLS2 and EFR also resulted in fully functional receptors (Albert et al., 2010b, Brutus et al., 2010). While swapping the entire ECD resulted in functional receptors, shifting the swap site to a position leaving the last two of the LRRs with the TM and the KD resulted in non-functional receptors (Albert et al., 2010b). Similarly, $FLS2^{XL}$ from *V. riparia* was domain-swapped with VrFLS2 to map that the subdomain LRRs 12-18 from $FLS2^{XL}$ were crucial for $flg22^{Atum}$ binding (Fuerst et al., 2020). Besides, a chimeric approach was also used to generated hybrids consisting of ECD from BIR3 and KD from SERK-dependent immune/developmental LRR-RLKs, and these hybrids were able to trigger downstream signalling constitutively (Hohmann et al., 2020).

Domain swapping was not only applied to LRR-RLKs but to LRR-RLPs as well. Tomato LRR-RLP *Cladosporium fulvum* resistance protein-4 (Cf-4) and *Cladosporium fulvum* resistance protein-9 (Cf-9) recognise the fugal proteinaceous elicitors avirulence 4 (Avr4) and avirulence 9 (Avr9), respectively (Kruijt et al., 2005). Chimeras between Cf-4 and Cf-9 narrowed down the essential LRRs for receptor function involved in specific recognition to Avr4 or Avr9 (Wulff et al., 2001, Van der Hoorn et al., 2001, van der Hoorn et al., 2005).

ReMAX from *A. thaliana* recognizing eMAX from *Xanthomonads* showed no bioactivity upon eMAX treatment when ectopically expressed in *N. benthamiana* leaves (Jehle et al., 2013). However, functionality was achieved by creating a chimeric RLP in a way of combining the *Arabidopsis* ReMAX ECD with the juxtamembrane domain, the TMD and the C-terminus of the RLP EIX2 from tomato (Jehle et al., 2013). This indicated that the non-functionality of the authentic RLP ReMAX might have come from an incompatibility of this RLP with an essential component of response activation, such as the adaptor kinase SOBIR1, in the Solanaceous plant *N. benthamiana.* Interestingly, the versatility of chimeric approaches was also illustrated with swaps between structurally distinguishable receptors, for instance, EGF-RLK WAK1 and LRR-RLK EFR from *A. thaliana* (Brutus et al., 2010). The hybrid of WAK1 ECD fused with EFR KD was able to transduce the signal like EFR, inducing the stress hormone ethylene and upregulating elf18-induced defence marker genes while recognizing OGs. Likewise, the receptor consisting of EFR ECD and WAK1 KD was able to give a ROS burst upon elf18 treatment via WAK1 KD.

In a more intriguing approach, double reciprocal domain swapping was used to generate synthetic receptor and co-receptor pairs with either AtFLS2 or EFR (Albert et al., 2013a).

KDs of AtFLS2 or EFR were swapped reciprocal with the KD of AtBAK1, resulting in receptor pairs that showed the same responsiveness compared to the original receptor and co-receptor pairs. These results provided clear evidence that the formation of the heteromeric complex by AtFLS2 or EFR and AtBAK1, rather than representing a supporting or enhancing step, is an essential part of receptor activation. Additionally, these results are also in line with the crystallographic study of flg22, AtFLS2 and AtBAK1 ECDs forming a complex (Chinchilla et al., 2007, Sun et al., 2013a). The two reciprocal hybrid approaches provided a new sight for mapping receptor and co-receptor interaction sites, thereby brought better understandings of the receptor complex formation and activation mechanism.

1.7 Background for this work

1.7.1 Comparison of SlFLS2 and AtFLS2

FLS2 receptors are conserved among angiosperms and some gymnosperms, but these receptors show species-specific characteristics with respect to ligand perception and co-receptor preference (Albert et al., 2010a, Felix et al., 1999). FLS2 from *Arabidopsis* and FLS2

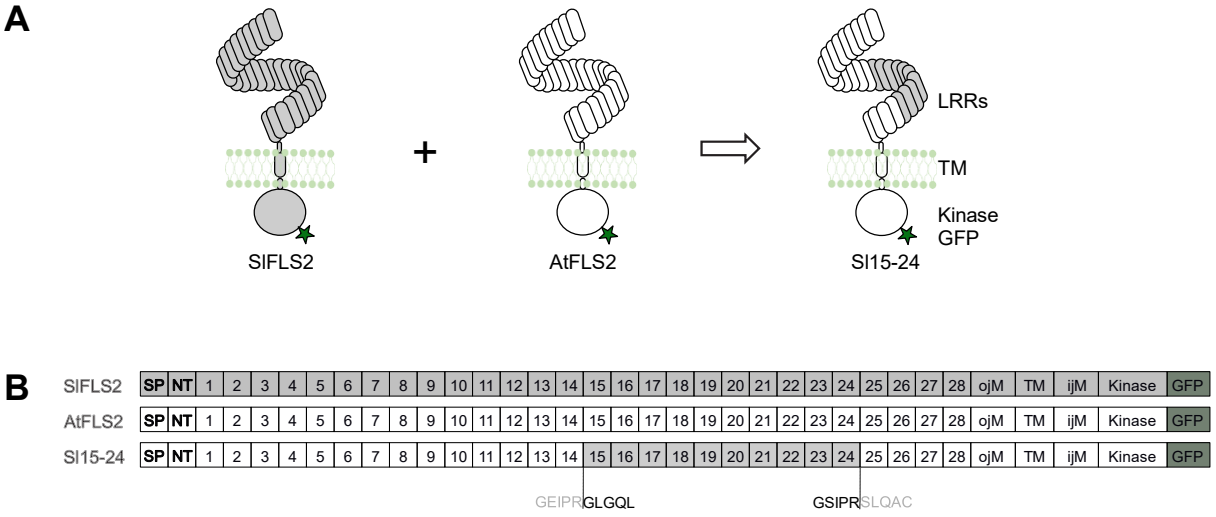

Figure 1.7.1 Sl15-24 domain swapping scheme

LRRs 15-24 from SlFLS2 were swapped into AtFLS2 substituting the corresponding LRRs. SlFLS2 is coloured in grey and AtFLS2 is in white. TM = transmembrane domain. A) Sl15-24 LRR swapping structural scheme. B) Sl15-24 LRR swapping overview and the sequence of switching points.

from tomato (SlFLS2), which share 55 % identical amino acids in their ECDs, perceive flg22

in a sensitive manner, but show distinct differences with respect to responsiveness and binding affinities for different flg22-derived variants (Mueller et al., 2012, Robatzek et al., 2007). SlFLS2 recognises the shortened flagellin-derived peptide flg15 and several C-terminally modified variants that are nonactive on AtFLS2 (Mueller et al., 2012). Also, for activating cytoplasmic signalling, AtFLS2 was observed to be strongly dependent on the co-receptor AtBAK1/AtSERK3, while SlFLS2 was not affected by the absence of AtBAK1 (Bittel, 2010, Mueller et al., 2012). For mapping the LRR subdomains/regions responsible for these differences in AtFLS2 and SlFLS2, hybrid receptors with precise swaps of specific LRRs were constructed (Figure 1.7.1, Sl15-24 as example) (Bittel, 2010).

These hybrid receptors were assayed for general functionality with the common flg22 ligand as well as with the flg22-variants that show preference for one of the FLS2 receptors (Bittel, 2010, Mueller et al., 2012). For example, the chimeric construct Sl19-24, AtFLS2 with its LRRs 19-24 replaced by the corresponding LRRs of SlFLS2, gained responsiveness to the C-terminally modified flagellin peptide flg22-AYA which acted as an antagonist of flg22 in cells with authentic AtFLS2 but as agonist in cells with SlFLS2 (Mueller et al., 2012). Similarly, as a second example, chimera Sl1-10, with LRRs 1-10 from SlFLS2 replacing the corresponding LRRs in AtFLS2, showed a clearly increased sensitivity to flg15 treatment compared to AtFLS2 (Mueller et al., 2012).

These data suggested that the species-specific properties of flagellin recognition of SlFLS2 can be introduced into AtFLS2 by LRR subdomain swapping. Intriguingly, one of the hybrids Sl15-24 (Figure 1.7.1), with LRRs 15-24 from SlFLS2 substituting the corresponding LRRs of the authentic AtFLS2, caught our eyes as an “overexcited” FLS2.

1.7.2 An “overexcited” FLS2

Why was Sl15-24 named “overexcited” FLS2? In contrast to all the other hybrids generated between AtFLS2 and SlFLS2 that were stably transformed into *Arabidopsis*, this Sl15-24 caused a dwarf phenotype and cell death in the T1 generation (Figure 1.7.2) (Bittel, 2010). Non-transformed plants were grown in parallel as controls, but the growth defect was not observed.

To confirm that this phenotype was indeed induced by the expression of Sl15-24, an estradiol inducible construct *pXVE::Sl15-24* was generated. The T2 generation of these transgenic lines were used for estradiol feeding experiments. As shown in Figure 1.7.3 A, after induction with 10 µM estradiol, the seedlings expressing Sl15-24 exhibited growth inhibition and necrosis,

whereas this phenotype occurred neither in wildtype plants treated with estradiol nor in *A. thaliana* transformed with *pXVE::Sl15-24* but without estradiol induction. Sl15-24 protein expression was verified via western blot with anti-FLS2 antibodies (Figure 1.7.3 B).

Figure 1.7.2 Expression of Sl15-24 affects *Arabidopsis* development (Bittel, 2010)

***A. thaliana fls2* mutant plants stably transformed with *p35S:: Sl15-24* and non-transformed *fls2* mutant plants were grown under short day conditions for 7-8 weeks. In comparison to *fls2* wildtype plants, Sl15-24 transgenic plants showed severe growth defect.**

Expression, notably overexpression, of elements of the immune system can lead to autoimmune-type of defence responses that eventually can lead to growth arrest and cell death (Domínguez-Ferreras et al., 2015, van der Burgh et al., 2019). We thus wondered whether the onset of estradiol-induced expression of Sl15-24 would be paralleled by defence responses like increased production of ethylene. In order to account for general effects of induced FLS2 expression we also used transformants with *pXVE::AtFLS2*. Within 12 h of treatment with 10µM estradiol, seedlings transformed with *pXVE::Sl15-24* but not seedling transformed with *pXVE::AtFLS2* responded with a clearly enhanced production of ethylene (Figure 1.7.3 C), suggesting that expression of Sl15-24 indeed caused immune responses in the absence of its ligand flg22 in *Arabidopsis*.

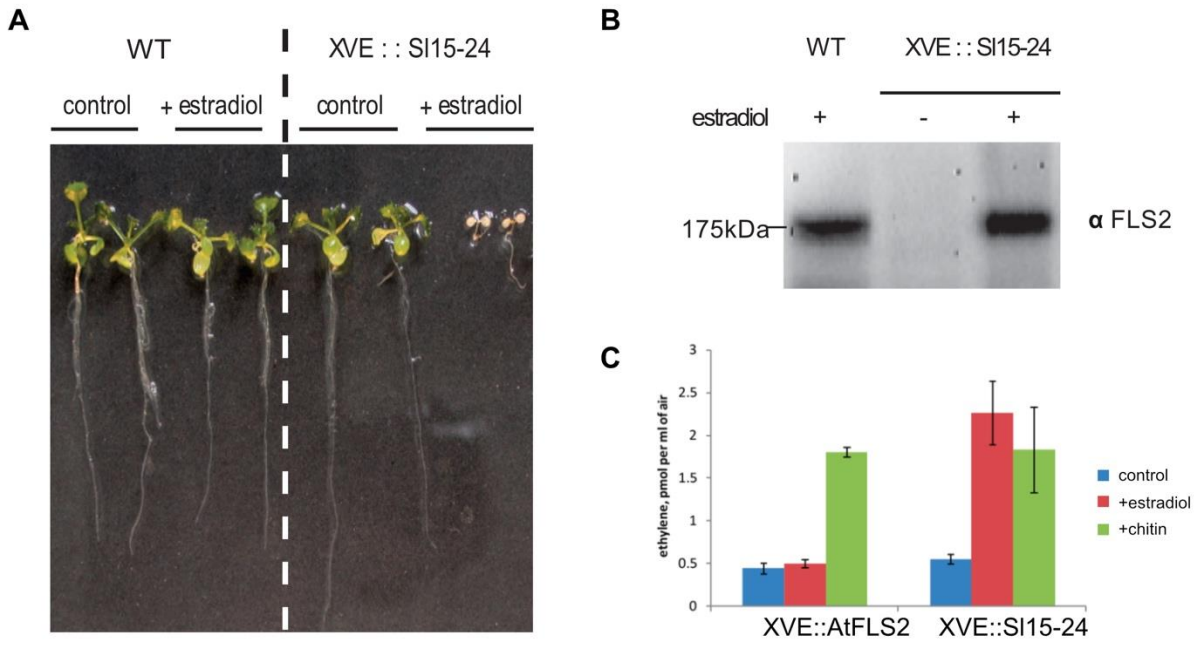

Figure 1.7.3 Expression of Sl15-24 causes necrosis and ethylene production in *Arabidopsis* seedling (Bittel, 2010)

A) Wild type and T2 generation of XVE::Sl15-24 seedlings were germinated for 6 days and then transferred to liquid MS medium supplemented with 10 µM estradiol or solvent as control. Seedlings were pictured 7 days after treatment. Western blot analysis of protein accumulation of seedling used in A) is shown in B). C) Ethylene production in XVE::AtFLS2/Sl15-24 transgenic seedlings induced with 100 mg/ml chitin or 10 µM estradiol for 12 h. Bars and error bars show means and standard deviations for n = 4.

The receptor activation process involving binding of flg22 to AtFLS2, complex formation with AtBAK1 and subsequent activation of intracellular signalling by the activated kinases has been illustrated via biochemical methods *in vivo*; and crystallographic evidence *in vitro* (Chinchilla et al., 2007, Sun et al., 2013a). Accordingly, it was hypothesized that Sl15-24 induced growth inhibition and ethylene production in *Arabidopsis* might depend on AtBAK1 (Bittel, 2010). To test this, *Sl15-24* was transformed into the *A. thaliana* mutants *bak1-7* and *bak1-5* lacking functional AtBAK1 or in a *fls2* mutant as a control. The *bak1-7* mutants is a knockout line with a T-DNA insertion in the coding region, whereas *bak1-5* carries a single amino acid change from cysteine to tyrosine at position 408, reported to have a dominant negative effect in PTI signalling without affecting its function as a co-receptor for BRI1 in development (Schwessinger et al., 2011). As illustrated in Figure 1.7.4, Sl15-24 did not induce growth defect in the two *bak1* mutants *bak1-7* and *bak1-5* but in the control plants

lacking FLS2. Thus, the Sl15-24 induced autoactivation is AtBAK1-dependent and the functioning of AtBAK1 in PTI signalling is necessary. In a repetition of this experiment the plants were transformed with *Sl15-24* driven under its endogenous AtFLS2 promoter. Again, no growth phenotype was observed in transformants of the two *bak1* mutants, but a strong growth inhibition was observed in plants with functional AtBAK1 (Supp. 1).

p35s::Sl15-24 (*fls2*) *p35s::Sl15-24* (*bak1-7*) *p35s::Sl15-24* (*bak1-5*)

Figure 1.7.4 Sl15-24 induced growth defect is AtBAK1-dependent

***p35s::Sl15-24* was stably transformed into *A. thaliana* lacking FLS2 (*fls2*) or BAK1 (*bak1-7*), or harbouring an impaired BAK1 in PTI (*bak1-5*) via *Agrobacterium* mediated transformation. Shown are representative examples of 7 weeks old T1 plants (Bittel, 2010).**

Further experiments were carried out with the estradiol-inducible system with the *pXVE::Sl15-24* construct transformed in *A. thaliana fls2* single mutants or *fls2* x *bak1-4* double mutants. In the *fls2* background with functional AtBAK1, the estradiol application caused growth arrest and necrosis (Figure 1.7.5 A, left panel) while the estradiol treatment of transformants in the *fls2* x *bak1-4* mutant had no effect (Figure 1.7.5 A, right panel). Thereby, the Sl15-24 protein accumulated in both types of transformants after the estradiol-treatment, reaching levels of FLS2 observed in wild-type seedlings (Figure 1.7.5 B). These data suggested that the seedling necrosis caused by Sl15-24 is AtBAK1 dependent.

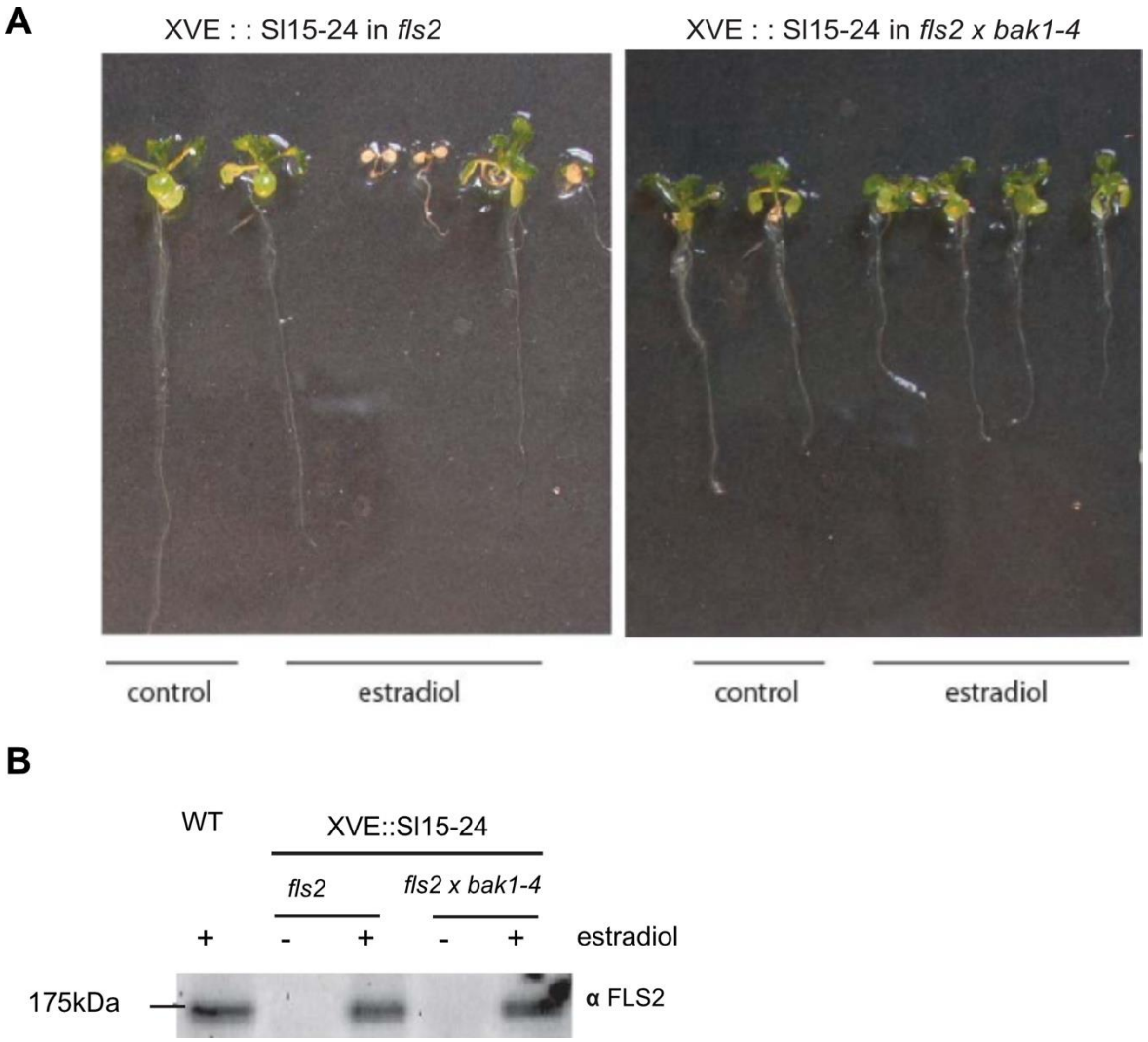

Figure 1.7.5 *bak1* rescues Sl15-24-caused *A. thaliana* seedling growth inhibition

A) T2 generation of *pXVE::Sl15-24* in *fls2* or *fls2* x *bak1-4* seedlings were germinated for 6 days and then transferred to liquid MS medium supplemented with 10 µM estradiol or solvent as control. Seedlings were pictured 7 days after treatment. B) Western blot analysis of protein accumulation of seedling used in A).

One interesting question that arose here is whether Sl15-24 harbours a binding site for flg22. To elucidate this, Sl15-24 or AtFLS2 receptors were immunoadsorbed to beads coated with anti-FLS2 antibodies and tested in competitive binding assays with radiolabelled flg22 (^{125}I-Tyr-flg22) and different concentrations of unlabelled flg22 (Figure 1.7.6 A). From these binding assays, the IC_{50} values, the concentration of unlabelled flg22 reducing binding of radiolabelled flg22 by 50 %, were estimated to be ~60 nM and ~ 20 nM for Sl15-24 and AtFLS2, respectively. In a further binding experiment, including a comparison with authentic

SlFLS2, binding of radio-ligand to Sl15-24 was only partially competed by 1 µM of the N-terminally shortened ligand flg15, analogous to the behaviour of AtFLS2 (Figure 1.7.6 B). In a next step, to further investigate the functionality of *Sl15-24*, it was transformed together with a Luciferase reporter gene under the pFRK1 promoter transiently into protoplasts lacking either AtFLS2 or both, AtFLS2 and AtBAK1, respectively. In protoplasts with functional AtBAK1, Sl15-24 induced a constitutive upregulation of luciferase activity even without flg22 treatment (Figure 1.7.6 C). In contrast, in protoplasts lacking functional AtBAK1 the expression of Sl15-24 did not cause autoactivation. Instead, it conferred responsiveness to flg22 but not flg15, indicating that Sl15-24 is a functional FLS2 receptor with a ligand preference for flg22 over flg15 like AtFLS2 (Mueller et al., 2012). In summary, Sl15-24 is a functional FLS2 with ligand binding characteristics similar to AtFLS2.

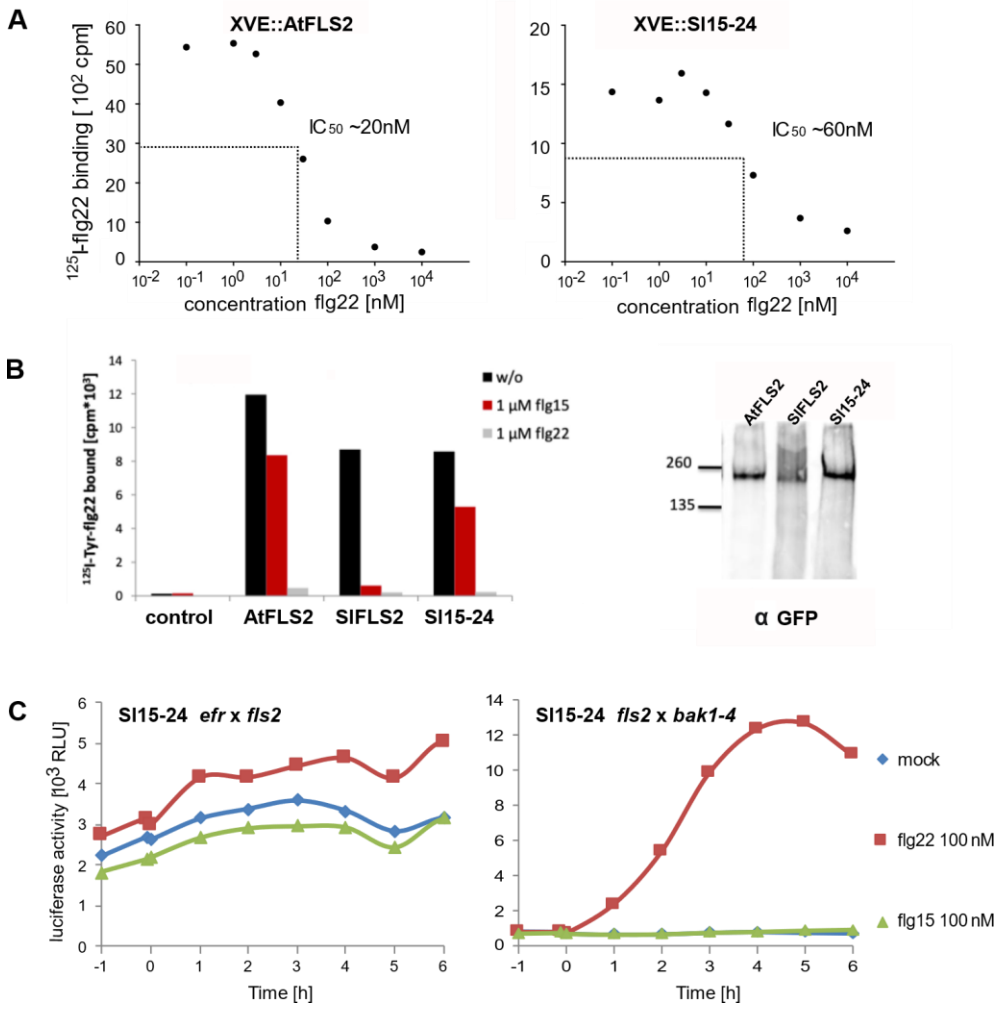

Figure 1.7.6 Sl15-24 is a functional FLS2 receptor responsive to flg22 (Katharina Mueller)

A) Competitive binding assays with 0.1 nM ^{125}I-Tyr-flg22 and different concentrations of unlabelled flg22 measured in immunoprecipitates of AtFLS2 and Sl15-24 expressed in transgenic plants induced with estradiol and purified with anti-FLS2 antibodies. IC_{50}, the concentration of unlabelled flg22 that results in 50% reduction of bound ^{125}I-Tyr-flg22. Cpm, counts per minute. B) Competitive binding assays with 0.1 nM ^{125}I-Tyr-flg22 and unlabelled flg22 or flg15 as competitors measured on GFP-trap incubated with solubilisates from *N. benthamiana* expressing AtFLS2-GFP, SlFLS2-GFP or Sl15-24-GFP. Protein expression was verified by western blot. C) *p35s::Sl15-24-GFP* was co-transformed with *pFRK1::Luciferase* into *A. thaliana* mesophyll protoplasts and luciferase activity was measured as described (Mueller et al., 2012). Sl15-24 expressed in *efr* x *fls2* background and *fls2* x *bak1-4* background protoplasts and luciferase activity were measured from -1 hour to 6 hour after treatment. Elicitors were added when t = 0. RLU, relative light units.

The kinase activity of AtFLS2 is critical to mediate flg22-induced downstream signalling (Asai et al., 2002, Albert et al., 2013b). The lysine at position 898 of AtFLS2, predicted to be involved in ATP binding, has been shown to be critical for receptor activation in earlier reports (Asai et al., 2002). In order to investigate whether the ligand-independent activity of Sl15-24 depends on its kinase activity, the 898 lysine of Sl15-24 was mutated to alanine and a *pXVE::Sl15-24 K898A* construct was transformed into *Arabidopsis* wild type plants (Bittel, 2010). Several independent lines of these transformants were all found not to respond with increased ethylene production and seedling growth inhibition when treated with estradiol (Figure 1.7.7A), although the Sl15-24 K898A protein accumulated in an estradiol-dependent manner (Figure 1.7.7B).

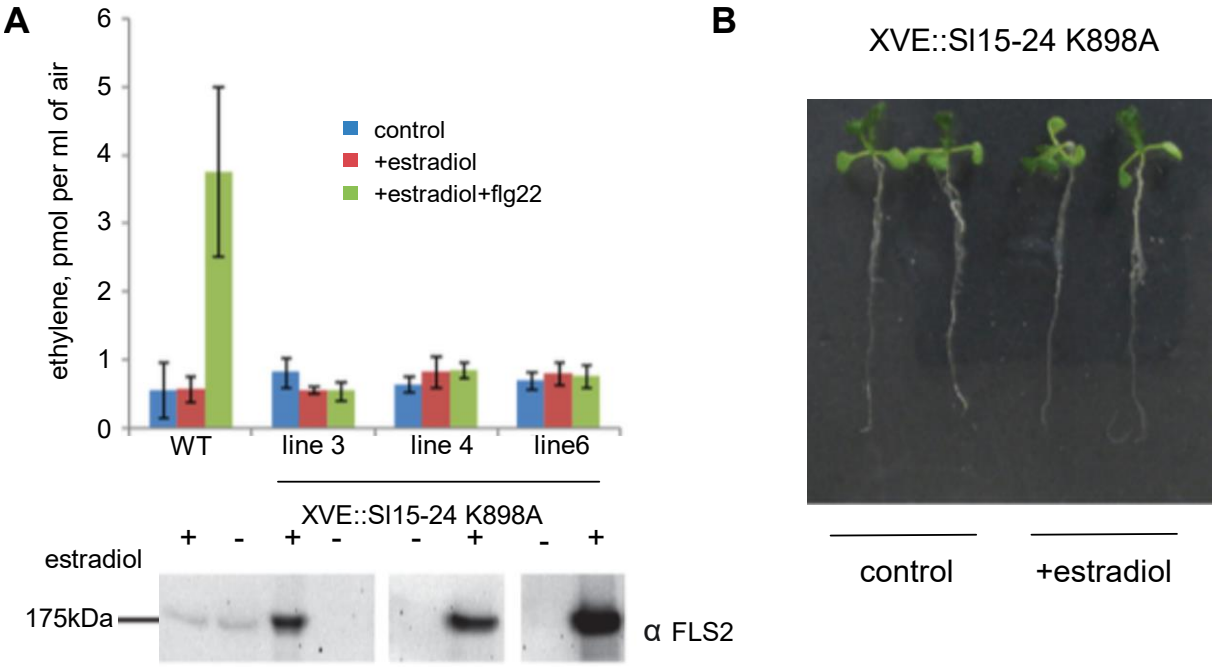

Figure 1.7.7 Ligand-independent activity of Sl15-24 is kinase dependent

A) K898A kinase-dead version of Sl15-24 is unable to induce ethylene production in absence of elicitors, nor responding to flg22 treatment. B) Sl15-24K898A seedlings do not show any growth defect.

So far, all the genetic evidence and molecular features of Sl15-24 support the hypothesis that Sl15-24 is a FLS2 receptor that gets activated in a ligand-independent manner in the presence of a functional AtBAK1 co-receptor. The most straightforward explanation would be that activation is caused by a ligand-independent interaction of Sl15-24 and AtBAK1. To obtain

evidence for a direct interaction of Sl15-24 and AtBAK1 co-immunoprecipitation (co-ip) experiments were performed with plants expressing Sl15-24 under constitutive or estradiol-inducible promoters in *Arabidopsis* plants with AtBAK1. Unexpectedly, however, such an interaction of Sl15-24 and AtBAK1 could not be reproducibly observed in several co-immunoprecipitation experiments that all showed the flg22-dependent interaction of the positive control with AtFLS2 experiments (Dr. Delphine Chinchilla personal communication). In Figure 1.7.8 an example of this failure is shown to illustrate the most frequently observed result, which was the absence of Sl15-24 in immunoprecipitates of AtBAK1, regardless of flg22 treatment.

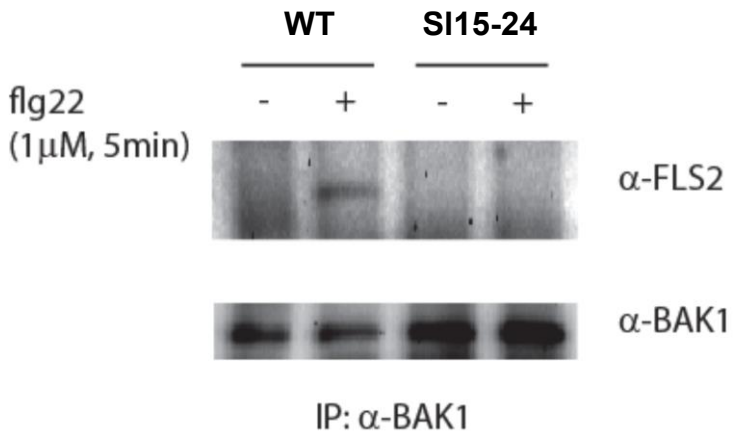

Figure 1.7.8 Sl15-24 does not interact with AtBAK1 in *A. thaliana*

Co-immunoprecipitation experiments were performed using anti-BAK1 antibodies on extracts of seedlings expressing Sl15-24 or AtFLS2 under the control of the XVE system. Seedlings were treated or not with 1 µM flg22 for 5 min. Input not shown. Provided by Dr. Delphine Chinchilla.

2 Aim of the work

PRRs play important roles in pathogen recognition for both animals and plants. In plant innate immunity, flg22-AtFLS2 is one of the best (or most thoroughly) studied ligand-receptor pairs. The crystal structure of the AtFLS2-flg22-AtBAK1 complex provided a clear picture on where the flg22 ligand binds to FLS2 and how this allows the formation of the ligand-receptor-co-receptor complex required for receptor activation (Sun et al., 2013a). In this context, however, the constitutive, ligand-independent activity of Sl15-24, a chimeric receptor with the LRRs 15-24 from tomato SlFLS2 replacing the corresponding LRRs in the ectodomain of AtFLS2, remains a riddle. Autoactivation of Sl15-24 depends on the functionality of its kinase and the presence of a functional AtBAK1 (Bittel, 2010). More intriguingly, in the absence of AtBAK1, Sl15-24 is a functional FLS2 receptor recognizing flg22.

In the present work, firstly, we aimed at investigating whether the Sl15-24 and AtBAK1 proteins interact physically, possibly in a manner that does not lead to a complex stable throughout immunoprecipitation. Secondly, we further characterised the molecular features of Sl15-24 and investigated the inhibitory function of BIRs on Sl15-24. Additionally, we further mapped the LRR regions which are responsible for the autoactivation of the chimeric receptors.

3 Materials and Methods

3.1 Plant material

3.1.1 *Arabidopsis thaliana*

Arabidopsis plants were grown in short-day phytochamber with 8 h light, 22 ºC, 40% - 65% relative humidity.

Genotype	**Comment**
Col-0	Wilde type
fls2	*fls2* (SAIL_691C4) in Col-0 background (Zipfel et al., 2004)
bak1-4	*bak1* (SALK_116202) T-DNA insertion line in Col-0 background (Kemmerling et al., 2007)
bak1-5	*bak1* dominant negative mutant in Col-0 background (Schwessinger et al., 2011)
bak1-7	*bak1* (GABI_213D09) T-DNA insertion line in Col-0 background (Bittel, 2010)
fls2 x *bak1-4*	*fls2* and *bak1-4* mutant in Col-0 background (Zipfel et al., 2004)
efr-1 x *fls2*	Crossing of *efr-1* (Zipfel et al., 2004) and *fls2* (Zipfel et al., 2006) mutant in Col-0 background (Nekrasov et al., 2009)
efr-1 x *fls2* x *bak1-5* x *serk4*	Crossing of *efr-1* x *fls2* and *bak1-5* x *serk4* mutant in Col-0 background (Albert et al., 2013)
sobir1-12	*sobir1*(SALK_050715) T-DNA insertion line in Col-0 background (Gao et al., 2009)
BIR2 OX	*p35s::BIR2-YFP* overexpression line in Col-0 background (Halter et al., 2014)

3.1.2 *Nicotiana benthamiana*

N. benthamiana plants were grown in greenhouse with 14 h light 25 ºC and 10 h dark 19 ºC.

3.2 Chemicals and Kits

Chemicals were ordered from Sigma-Aldrich (St. Louis, USA), Merck (Darmstadt, DE), Roche (Basel, CH), Duchefa (Haarlem, NL), Carl Roth (Karlsruhe, DE), Fluka (Buchs, CH) and kits from Thermo Scientific (Waltham, USA). MACHEREY-NAGEL (Düren, DE).

3.3 Peptides

Peptides were custom synthesized by different companies. Commonly, stock solutions containing 10 mM peptide were prepared in water and diluted in a solution containing 10 mg/ml BSA, 0.1 M NaCl to prevent adsorption of peptide to plastic surfaces.

peptide	**sequence**
Atpep1	ATKVKAKQRGKEKVSSGRPGQHN (Huffaker et al., 2006)
elf18	Ac-SKEKFERTKPKVNVGTIG (Kunze et al., 2004)
flg22	QRLSTGSRINSAKDDAAGLQIA (Felix et al., 1999)
flg15	RINSAKDDAAGLQIA (Felix et al., 1999)
Acri-flg22	Acri-QRLSTGSRINSAKDDAAGLQIA (Fuerst et al., 2020)

3.4 Bacterial strains

bacterial	**Growth condition**	**strain**
Agrobacterium tumefaciens	30 ºC incubator on LB agarose plate 30 ºC shaker 220 rpm in liquid LB medium	GV3101
Escherichia coli	37 ºC incubator on LB agarose plate 37ºC shaker 200 rpm in liquid LB medium	TOP10 (Thermo Scientific)
		XL1blue (Stratagene)

3.5 Cloning

3.5.1 Chimeric receptor constructs

Expression constructs for chimeric receptors were obtained either with Gateway cloning or Golden Gate cloning or the combination of both. For Gateway cloning, Phusion High-Fidelity DNA polymerase (Thermo Fisher) was used and chimeric receptors were created with overlapping extension PCR as described (Albert et al., 2010b). Amplified receptor constructs were directly ligated into pENTR D-TOPO entry vector (Invitrogen), followed by recombined into pK7FWG2.0 Gateway destination vector (VIB, University of Gent) which has a CaMV35S promoter and a C-terminal enhanced-GFP tag by LR reaction (LR clonase II, Invtrogen).

For Golden Gate cloning, separate parts of receptors were amplified with primers containing overhangings and BsaI recognition site and ligated into pJET1.2 blunt end vector (CloneJET PCR Cloning Kit, Thermo Fisher), followed by BsaI (Thermo Fisher) cut-ligation into LII BB10 expression vector as described (Binder et al., 2014).

For At15-24, Sl18-23, Sl18, Sl24, Sl18 & 24, a combination of Gateway and Golden Gate cloning was used. Separate parts of the chimeras were amplified with primers containing overhangings and BsaI recognition site and ligated into pJET1.2 blunt end vector, followed by BsaI cut-ligation into Golden Gate compatible pENTR vector. Then, the chimeras were recombined into pK7FWG2.0 destination vector via LR reaction.

The nucleotide sequence of all the amplified products were verified by Sanger sequencing (Eurofings or Microsynth) after insertion into a plasmid.

3.5.2 Mutagenesis

For AtFLS2 L663N and Sl15-24 N663L, AtFLS2 or Sl15-24 was recombined from pK7FWG2.0 destination vector into pDONR207 entry vector via BP reaction (BP clonase II, Invtrogen). Whole plasmid was amplified with primers containing overhangings introducing point mutation with Phusion High-Fidelity DNA polymerase (Thermo Fisher) (Liu and Naismith, 2008). Methylated template plasmid was digested with DpnI restriction enzyme (Thermo) for 1 h at 37 ºC. Mutation was confirmed by Sanger sequencing. Mutated constructs were recombined into pK7FWG2.0 again with LR clonase II.

3.5.3 Expression construct (all the tags are fused to C-terminus)

Gateway and classic cloning expression construct

construct	expression vector	promoter	tag	comment
AtFLS2	pK7FWG2.0			from Katharina Mueller
SlFLS2	pK7FWG2.0			from Katharina Mueller
S15-24	pK7FWG2.0			from Katharina Mueller
S15-24 kinase dead	pK7FWG2.0			from Katharina Mueller
S16-24	pK7FWG2.0			
S17-24	pK7FWG2.0			
S18-24	pK7FWG2.0			
S18-23	pK7FWG2.0	p35s	GFP	
S18-21	pK7FWG2.0			
S15-19	pK7FWG2.0			
S15-16	pK7FWG2.0			
S18-21	pK7FWG2.0			
S18	pK7FWG2.0			
S24	pK7FWG2.0			
S18 & 24	pK7FWG2.0			
S1-6	pK7FWG2.0			
S1-6/15-24	pK7FWG2.0			
S4-6/15-24	pK7FWG2.0			
AtFLS2 TM+20aa	pK7FWG2.0			
S15-24 TM +20aa	pK7FWG2.0			
BtF	pK7FWG2.0			from Markus Albert
S15-24 N663L	pK7FWG2.0			
AtFLS2 L663N	pK7FWG2.0			
AtSERK1	PGWB17			from Lisha Zhang
AtSERK2	PGWB17			from Lisha Zhang
AtBAK1/AtSERK3	PGWB17			from Lisha Zhang
AtSERK4	PGWB17	p35s	4 x Myc	from Lisha Zhang
AtSERK5	PGWB17			from Lisha Zhang
SlSEKR3A	PGWB17			from Lei Wang
SlSERK3B	PGWB17			from Lei Wang
StB	PGWB17			
AtBAK1 TM+20aa	PGWB20	p35s	10 x Myc	
BIR2	PB7YWG2.0	p35s	YFP	from Birgit Kemmerling
BIR3	PB7YWG2.0			from Birgit Kemmerling
BIR4	PB7YWG2.0			from Birgit Kemmerling
S1-24	pCAMBIA2300	p35s	GFP	from Katharina Mueller
S19-24	pCAMBIA2300			from Katharina Mueller
AtBAK1-nFLUC	pCAMBIA1300	p35s	3 x HA-nFLUC	from Liping Yu
S15-24-nFLUC	pCAMBIA1300			
BIR3-cFLUC	pCAMBIA1300	p35s	cFLUC	from Liping Yu
AtFLS2-cFLUC	pCAMBIA1300			
S15-24-cFLUC	pCAMBIA1300			
AtBAK1-cFLUC	pCAMBIA1300			

Golden Gate expression construct

construct	backbone	promoter	terminator	tag
AtBAK1-HiBiT	BB10	p35sΩ	nos-T	HiBiT
BIR1	BB10	p35sΩ	nos-T	YFP
BIR1t2	BB10	p35sΩ	nos-T	YFP
BIR2t1	BB10	p35sΩ	nos-T	YFP
EC-AtFLS2	BB10	p35sΩ	nos-T	HA
EC-S15-24	BB10	p35sΩ	nos-T	HA
EC-AtBAK1	BB10	p35sΩ	nos-T	GFP

3.6 Plant transformation and immune response assays

3.6.1 Transient transformation of *Arabidopsis thaliana* mesophyll protoplasts and pFRK1::Luciferase assays

Protoplasts isolation and pFRK1::LUC assay were carried out according to the protocol from (Yoo et al., 2007). Briefly, 40 healthy and fully extended leaves from 5 weeks old *A. thaliana* were sliced into 1 mm straps and submerged in 10 ml enzyme solution (0.4 M mannitol, 20 mM KCl, 20 mM MES pH 5.7, 1.5 % Cellulase R10, 0.4 % Macerozyme R10 were heated at 55 ºC for 10 min and $CaCl_2$, 0.1 % BSA were added after cooled on ice) vacuumed for 30 min in dark and incubated in dark for 3 to 4 hours. 10 ml ice cold W5 solution (2 mM MES pH 5.7, 154 mM NaCl, 125 mM $CaCl_2$, 5 mM KCl) was added in the enzyme solution containing leaf tissue and gently swirling was applied to release protoplasts. Mixed solution containing protoplasts were poured through a 75 µm mesh supported with a funnel into 12 ml round bottom tube (Simport). Protoplasts were sedimented by centrifugation 100 *g* for 2 min and resuspended in 5 ml W5 solution sedimented again by gravity on ice in dark for 30 min. The resuspension and sedimental procedure were repeated another time but in the second time 20 µl of protoplast resuspension was sampled and cell number was counted with a haemocytometer. Cell density was adjusted to 4 x 10^5 cell/ml MMG solution solution (4 mM MES pH 5.7, 0.4 M mannitol, 15 mM $MgCl_2$) before transformation. 30-50 µl (40 µg) of plasmid (prepared from *E. coli* TOP10 or XL1blue with NucleoBond Xtra Maxi EF, Macherey-Nagel) of receptor construct and 30-50 µl (40 µg) of plasmid *pFRK1::Luciferase* reporter construct (Asai et al., 2002) were mixed with 1 ml *A. thaliana* protoplast resuspended in MMG solution in 12 ml round bottom tube. 1.1 ml of PEG solution (0.2 M mannitol, $CaCal_2$ 0.1 M, 40 % PEG 4000) was slowly added into the mixture of plasmids and protoplasts, immediately followed by gently inversion 3-4 times until it was mixed homogeneous and incubated for 5 min at RT. 4.4 ml W5 solution was gently added into the tube and the solution was mixed by inverting the tube 3-4 times again. Protoplasts were sedimented by centrifugation 100 *g* for 2 min and supernatant were decanted. 200 µM of D-luciferin (firefly, PJK) were added to protoplasts post-transformation which were resuspended with W5 solution. 100 µl/well of protoplasts were distributed into 96 well plate and incubated in dark for 12-14 h until measurement. Different peptides were added and luciferase activity was monitored as light emission with a luminometer (Mithras LB 940).

3.6.2 Agrobacterium-mediated transient transformation of *Nicotiana benthamiana*

Agrobacterium tumefaciens GV3101 strain harbouring receptor construct from a single colony was cultivated in LB liquid medium with respective antibiotic in 30 °C shaker, 220 rpm overnight. Agrobacterium was harvested in a 50 ml falcon tube by centrifugation 4500 *g*, 8 min, RT. Infiltration solution containing 10 mM $MgCl_2$ and 150 µM acetosyringone was used to resuspend the bacteria and then incubated with infiltration solution for 1-3 h at OD_{600} = 1.0, RT. *Agrobacterium tumefaciens* C58C1 strain carrying P19 RNA silencing suppressor (Voinnet et al., 2015) was mixed with desired construct 1 : 1, and the final OD_{600} was diluted to 0.1 for each construct. Bacterium were pressure-infiltrated into *N. benthamiana* with 1 ml syringe. Plant leaves were either cut into 3 x 3 mm pieces for ROS assay 24 h post transformation or harvested in liquid N_2 and ground into fine powder 48 h post transformation for protein related assay.

3.6.3 Oxidative burst in *N. benthamiana*

Oxidative burst assays were carried out in *N. benthamiana* as described (Albert et al., 2010b). Cut leaf pieces were floated in petri dish filled with water overnight. Leaves were distributed into 96 well plate containing 20 µM luminol (L-012, Waco) and 2 µg /ml horseradish peroxidase (Applichem) in the way of 1 leaf piece/well. Light emission was measured as RLU with a luminometer (Mithras LB 940) every minute before and after elicitation.

3.7 Molecular interaction assay

3.7.1 Split luciferase assay

N. benthamiana leaves expressing firefly luciferase constructs for 2 days were cut into 3 x 3mm squares floating on water overnight. Leaf pieces were placed into 96-well plate supplied with D-luciferin as described (Zhou et al., 2018) and monitored as RLU with a luminometer (Mithras LB 940) with or without peptide treatment.

3.7.2 Microsomal fraction isolation

Leaves from 6-week-old *A. thaliana fls2 x bak1-4* plants or from *N. benthamiana* expressing AtFLS2 or Sl15-24 or AtBAK1 for 2 days were ground in liquid N_2 to fine powder with mortar and pestle. For obtaining mixed microsomal preparations, equal amounts (~2 g) of

tissues expressing receptor or co-receptor, w/o ~2 g *A. thaliana* leaf material, were mixed and ground in liquid N_2. Leaf powder was suspended in (3 ml/g) cold (4 ºC) microsome extraction buffer (50 mM Tris pH 8 at 4 °C, 0.5 M sucrose, 30 mM $MgCl_2$, 2 mM EDTA, 1 mM PMSF, 0.1 mM ABSF, 2 mM DTT and PPI (40 µl/ml extraction buffer)) and ground for 3-4 min. Cell debris were removed by 2 x centrifugation at 4500 *g* 30 min 4 °C. The final supernatant was filtered through a 20 µm nylon net and microsomes were collected by centrifugation (145,000 *g* at 4 °C for 30 min). Microsomal pellets were resuspended in extraction (160 µl/g powder) and incubated on ice for 20 min w/o 1 µM flg22, followed by three further rounds of collection (42, 000 rpm (rotor RP45A) at 4 °C for 30 min) and resuspension (in extraction buffer w/o 1 µM flg22 or, in the last rounds, in MES buffer (pH 5.7 at 4°C, 150 mM NaCl, 100 mM KCl, 5 mM $MgCl_2$, 2 mM DTT, 40 µl/ml PPI). Microsomes were finally sedimented (42,000 rpm, 20 min, 4 °C), solubilized and used in co-ip with the standard protocols described below.

3.7.3 Immunoprecipitation

Immunoprecipitation protocol was modified from (Chinchilla et al., 2007). 230 mg of *N. benthamiana* frozen leaf powder were incubated with 1.2 ml solubilization buffer (25 mM Tris, pH 8, 150 mM NaCl, 1% Nonidat P-40, 0.5% Deoxycholic acid sodium salt) supplied with 2 mM DTT and 8µl/ml PPI) for 1 h on a rotatory shaker at 4°C. Non-solubilized material was removed by ultracentrifugation (42,000 rpm, 30 min, 4 °C). Samples of the supernatant, solubilisates, were kept as "input". 10 µl of GFP-Trap Agarose/Magnetic Agarose (ChromoTek) were used to immune-absorb GFP-tagged receptor constructs from solubilisate for 45 min at 4 °C on a rotatory shaker. GFP-Trap were quickly washed 2 times with solubilization buffer and 2 times with wash buffer (extraction buffer without detergents). 40µl of 2 x SDS buffer (5% β-ME) was added to boil the GFP-Trap at 95 °C for 10 min.

3.7.4 Affinity column for proteins binding to the ECD of AtBAK1

Ectodomains (ECDs) of AtFLS2 and Sl15-24 c-terminally tagged with HA, and of AtBAK1, c-terminally tagged with GFP, were independently expressed in separate *N. benthamiana* plants for ~ 48 h. Leaves were harvested in liquid N_2 and ground to fine powder. 1.2 ml of MES buffer was used to extract the soluble protein from 230 mg plant material for 1 h at 4 °C. Insoluble material was removed with ultra-centrifugation (42,000 rpm, 20 min, 4 °C). The ECD AtBAK1-GFP was immuno-adsorbed to GFP-Agarose (ChromoTek, 1 h, 4 ºC) and the beads were packed into 1 ml syringe plugged with polyethylene frits to hold the beads. After

prewashing with MES buffer, these columns were used as affinity columns for the ECDs. Aliquots (30 µl) of these ECD preparations were fractionated by running these columns with MES buffer. Fractions, and washed column material extracted by boiling in SDS sample buffer, were analysed for presence of tags in western blots. Affinity absorption assays were performed in the absence of flg22 in all steps or in the presence of 1 µM flg22, added to the ECD preparation of AtFLS2 or Sl15-24 and the MES elution buffer.

3.7.5 SDS-PAGE and Western blotting

For standard assays, 10 µl of samples were loaded on 8 % of separation and 5 % of stacking acrylamide gel, ran at 140 V for 1 h with running buffer (25 mM Tris, 192 mM glycine, 0.1% SDS). Proteins on acrylamide gel were transferred on to nitrocellulose membrane (Amersham) with transfer buffer (48 mM Tris, 39 mM glycine, 20% MeOH) wetted Whatman filter paper at 17 V for 75 min by semi-dry blotting (Bio-Rad). Ponceau staining (10 % acetic acid, 40% MeOH, 0.1% Ponceau-S)was used to monitor the quantity of Rubisco for each sample before blocking the membrane with 5 % milk PBS-T (17 mM NaH_2PO_4, 58 mM Na_2HPO_4, 68 mM NaCl, 0.05% Tween-20) for 30 min at RT. Primary antibody including anti-GFP antibody (1:5,000, TP401, Torrey Pines Biolabs) and anti-Myc antibody (1:5,000, C3956, Sigma-Aldrich) both produced from rabbit diluted in 5% milk PBS-T were added on membranes either incubated for 1h at RT or overnight at 4 °C. After 2 times washing with 10 ml PBS-T, membranes were incubated with anti-rabbit secondary antibody coupled to alkaline phosphatase (1:50,000) in 5% milk PBS-T 40 min at RT, followed by 2 times washing with 10 ml PBS-T and 2 times washing with 10ml assay buffer. 5% of Nitroblock was used to block the nitrocellulose membrane before 2% of CDP-Star (Roche) was applied. Chemiluminoscence was detected via CCD camera (Amersham).

3.7.6 HiBiT blotting

SDS-PAGE and Ponceau staining was done the same way as described above. After Ponceau staining, membranes were washed 2 times 5 min with TBS-T (20 mM Tris, 150 mM NaCl, 0.1 % Tween-20) and followed by 30 min incubation with TBS-T at RT. LgBiT protein in NanoGlo buffer was added to the membrane according to the product manual (Promega) overnight at 4 °C. Substrate furimazine was added before detection with a CCD camera (Amersham).

3.7.7 *In vitro* ligand-receptor binding assay

In vitro ligand-receptor binding assay with crude plant material was performed followed the protocol from Wildhagen et al (2015). Briefly, 300 mg *N. benthamiana* leaf material overexpressing receptor constructs were washed with 1mL binding buffer (25 mM MES, pH 6.0, 150 mM NaCl, 1 mM DTT and 12 µl PPI). Cell debris were collected by centrifugation 13, 000 *g*, 1 min, 4 ºC and resuspended in 1 mL binding buffer. 80µl of the suspension was aliquoted in to 1.5 ml eppendorf tube and supplied with 10 µl of 10 µM unlabelled peptide as competitor for 2min, then 10 µl of 10 nM acridium-labelled-peptide. Those tubes were incubated 20 min on ice in dark, followed by centrifugation for 1 min 13,000 *g* at 4 ºC. Cell debris were collected and washed twice with 1 ml binding buffer by centrifugation and resuspension (13,000 *g*, 1 min, 4 ºC). The final pellet was resuspended in 100 µl of 5 mM citric acid. Light emission (flash of 10 seconds) triggered by the addition of 150 µl of the H_2O_2 solution (20 mM H_2O_2 in 100 mM NaOH) was measured with a single tube luminometer (FB12: Berthold).

4 Results and Discussion

4.1 Molecular characterization of FLS2 receptors when expressed in *A. thaliana* protoplasts

4.1.1 AtFLS2 and SlFLS2 show different sensitivity for flg22 and distinct dependency on AtBAK1

SlFLS2 was observed to be more sensitive to flg22 and less AtBAK1-dependet than AtFLS2 when expressed in *A. thaliana* (Bittel, 2010, Mueller et al., 2012). To corroborate these observations, *AtFLS2* or *SlFLS2*, both genes expressing under the 35S-promoter fused with C-terminal GFP tags, were co-transformed with a *pFRK1::Luciferase* reporter construct into mesophyll protoplasts from *Arabidopsis* mutants lacking FLS2 (*efr* x *fls2* plants) or mutants lacking FLS2 and BAK1 (*fls2* x *bak1-4* plants). Expressing both forms of FLS2 in cells of both types of mutants reconstituted perception of flagellin, as shown by the clear increase in luciferase activity after treatment with 1 µM of flg22 (Figure 4.1.1). In cells with AtBAK1 (Figure 4.1.1A), the same induction of luciferase was observed after treatment with a lower concentration of 10 nM flg22. In cells without AtBAK1 (Figure 4.1.1B), however, a full response with 10 nM flg22 was observed only for cells expressing SlFLS2 while cells expressing AtFLS2 showed only a much-reduced response. Our data suggested that the functionality and sensitivity of SlFLS2, in contrast to AtFLS2 (Mueller et al., 2012), seems not to depend on the presence of AtBAK1.

As a next step we studied the sensitivity of AtFLS2 and SlFLS2 using a more extended concentration range of flg22 (Figure 4.1.2). Interestingly, *A. thaliana* cells expressing the heterologous SlFLS2 showed a ~1000-fold higher sensitivity for flg22 than cells overexpressing the autologous AtFLS2 (EC_{50} values of ~0.2 pM for SlFLS2 and ~ 0.3 nM for AtFLS2, respectively (Figure 4.1.2). More interestingly, the sensitivity of SlFLS2 for flg22 remained high when expressed in cells without AtBAK1 whereas, in contrast, the sensitivity of AtFLS2 to flg22 further dropped > 10-fold in the cells lacking AtBAK1 (EC_{50} ~ values in *fls2* x *bak1-4* cells of ~ 0.3 pM for SlFLS2 and > 3.6 nM for AtFLS2, respectively).

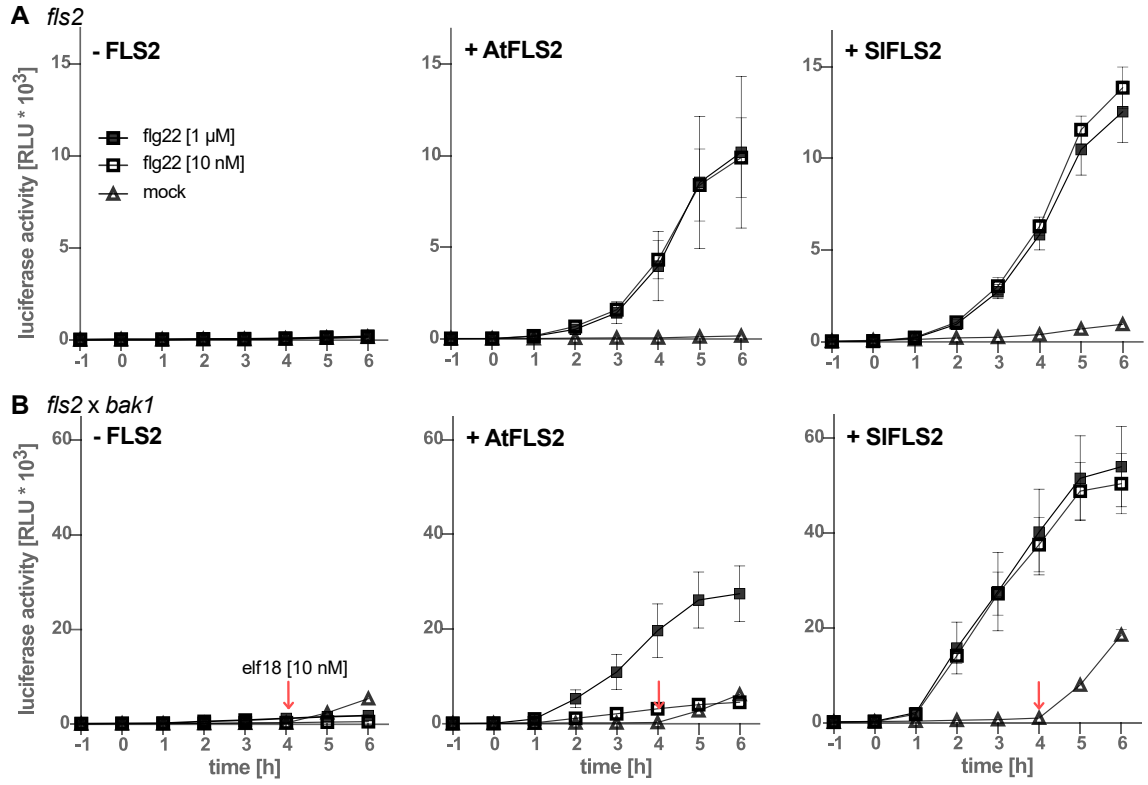

Figure 4.1.1 AtFLS2 and SlFLS2 expressed in *A. thaliana* protoplasts differ in their AtBAK1 dependency

Induction of pFRK1::Luciferase activity in cells co-transformed with *AtFLS2* or *SlFLS2*. Mesophyll protoplasts were prepared from Col-0 *A. thaliana* with A) *efr* x *fls2* or B) *fls2* x *bak1-4* mutant background. At t = 0, cells were treated with flg22 as indicated. Mock treated cells in B) were treated with 10 nM elf18 at t = 4 (red arrows) to assess the general responsiveness of the cells in the absence of AtBAK1. Luciferase activity was measured with a luminometer as RLU. Data points and error bars stand for the mean and SD of 3 replicates. The same pattern of outcome was observed in an independent repetition of the experiment shown.

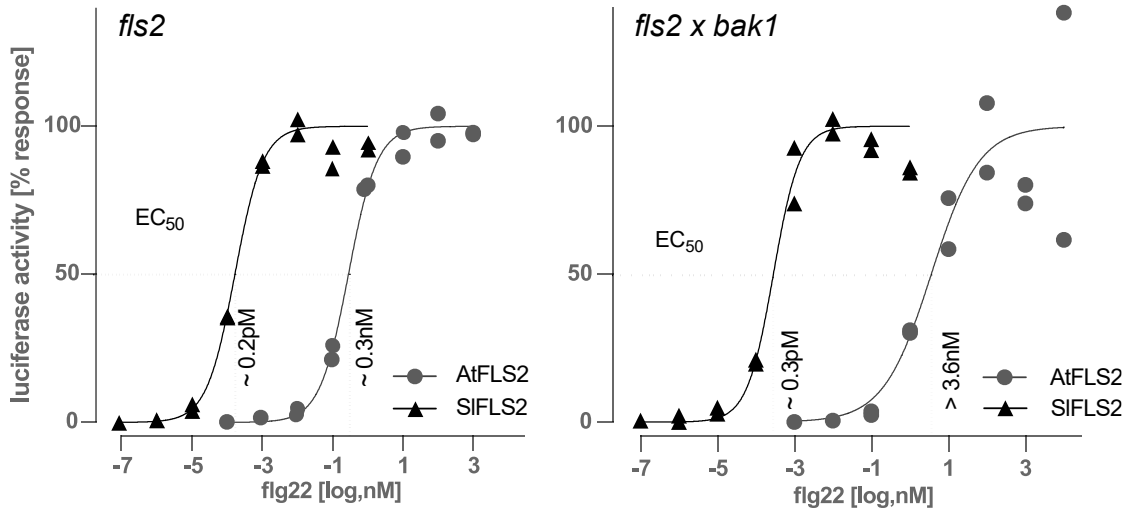

Figure 4.1.2 SlFLS2 shows higher sensitivity of flg22 perception compared to AtFLS2

***p35s::AtFLS2-GFP* or *p35s::SlFLS2-GFP* was co-transformed with a reporter construct *pFRK1::Luciferase* in protoplasts with the *efr* x *fls2* or *fls2* x *bak1-4* mutant background. Values show luciferase activity after 6 h of treatment with different doses of flg22. RLU values were normalized as percentage of maximal response. Non-linear fit was used to calculate the EC_{50} in Graphpad Prism.**

Transformation of protoplasts can vary considerably between individual PEG transformation events. For the receptor genes used in our study, this variation goes along with differences in the maximal amplitude of the luciferase reporter activity reached with saturating amounts of ligand. The successfully transformed protoplasts can be expected to harbour many copies of the plasmid added, resulting in overexpression of the receptors and the exquisite ligand sensitivity often observed. The percentage of transformed cells, however, is not expected to affect the sensitivity to the ligand. In all our experiments (Pascal Bittel, Katharina Mueller and my own ones), SlFLS2 showed a higher sensitivity towards the flg22 ligand and a lower dependency on the presence of AtBAK1 than AtFLS2 when expressed in *A. thaliana*.

4.1.2 Sl15-24 induces ligand-independent but AtBAK1-dependent activation in *A. thaliana* protoplasts

To test whether Sl15-24 is also autoactive in *A. thaliana* protoplasts, we expressed this chimeric receptor in protoplasts derived from mutant plants lacking AtFLS2 (*efr* x *fls2* mutant) or AtFLS2 and AtBAK1(*fls2* x *bak1-4* mutant), respectively (Figure 4.1.3). In

contrast to transformation with AtFLS2, which restored the response to the flg22 ligand as in the experiments described above, the cells expressing *Sl15-24* exhibited constitutive induction of the *pFRK1::Luciferase* gene. Besides, no further induction was observed when these cells were treated by adding either 1µM of Atpep1 or 100 nM of flg22.

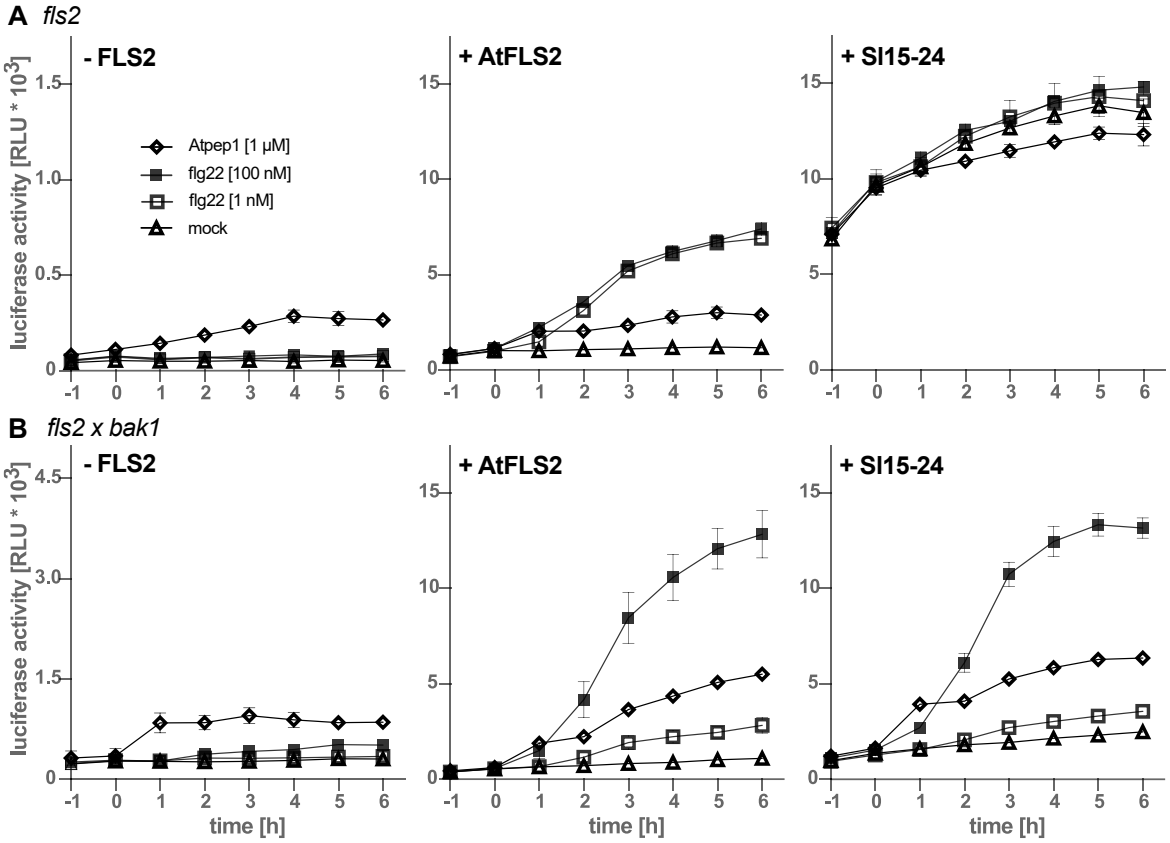

Figure 4.1.3 Autoactivation of Sl15-24 depends on AtBAK1

AtFLS2 Sl15-24 **were co-transformed with** ***pFRK1::Luciferase*** **into protoplast from A)** ***efr*** **x** ***fls2*** **or B)** ***fls2*** **x** ***bak1-4*** **mesophyll cells. Treatments with the peptides indicated were conducted at t = 0. Data points and error bars stand for the mean and SD of 3 replicates. The results shown are representative for n > 3 independent repetitions of experiments.**

This suggested that the immune response triggered by Sl15-24 in the absence of ligand is saturated and no further stimulation via AtFLS2 or PEPR1/2 is possible. Apparently, autoactivity of Sl15-24 is already fully established at the beginning of our standard protoplast assays used to test receptor functionality 12 to 14 h (overnight) after protoplast transformation. We thus measured the luciferase reporter activity in cells transformed with Sl15-24 during this pre-incubation period (Supp. 2). Luciferase activity stayed low in the

absence of AtBAK1, in cells with AtBAK1, however, reporter activity started to increase ~ 6h after transformation and reached a maximum at or some hours before the time transformants are used for induction studies in standard assays. Thus, we used a high luciferase background, together with the lack of response to additional treatments with Atpep1, elf18 or flg22, as criteria for qualifying receptor constructs as “autoactive”.

Interestingly, in cells lacking AtBAK1, the Sl15-24 receptor did not show autoactivity and cells responded to Atpep1, and importantly, also to flg22. Thus, in the absence of AtBAK1, Sl15-24 exhibited characteristics like the authentic AtFLS2 responded to ≥ 1 nM flg22 (Figure 4.1.3 B). To confirm these results, we tested Sl15-24 and AtFLS2 also in the mutant *efr* x *fls2* x *bak1-5* x *serk4* which lacks functional AtBAK1/SERK3 but also AtSERK4. When transformed with AtFLS2, these mutant cells responded to treatment with ≥ 10 nM flg22 (Supp. 3). Importantly, expression of Sl15-24 in these mutant cells did not cause autoactivation but conferred responsiveness to flg22 similar to the one observed with AtFLS2.

4.1.3 Autoactivity of Sl15-24 depends on its functional kinase

In order to test whether autoactivity depends on the kinase output of Sl15-24, we tested a Sl15-24 kinase dead (KDead) version mutated in the active site of the KD. As shown in Figure 4.1.4A, cells expressing the Sl15-24 KDead did not exhibit autoactivation and did not show response to flg22. As control we checked for transformation of reporter construct by treatment with Atpep1 and for accumulation of Sl15-24 kinase dead protein by western blot (Figure 4.1.4B). With these results, we confirmed experiments in *planta* (Figure 1.7.7) that kinase activity is essential for the AtBAK1-dependent but ligand-independent activation observed with Sl15-24.

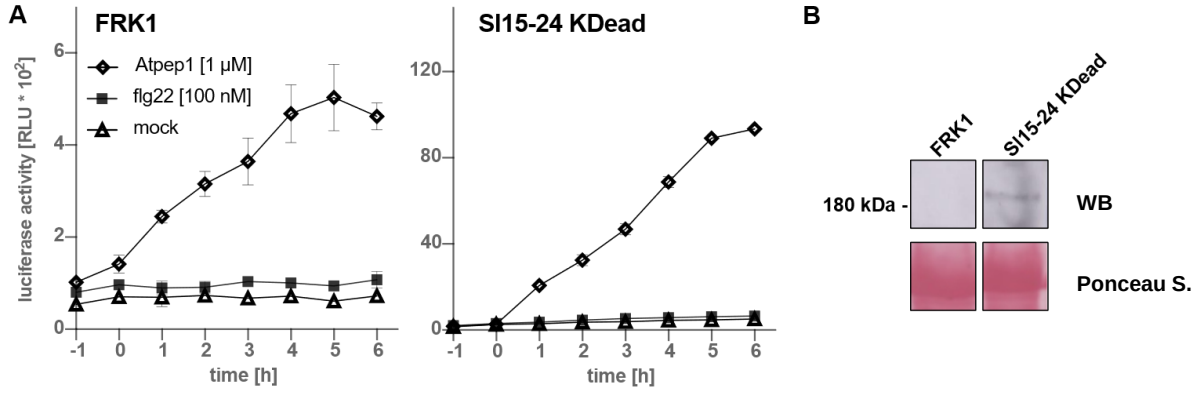

Figure 4.1.4 Autoactivation of Sl15-24 depends on a functional kinase domain

Mesophyll protoplasts of *efr* x *fls2* mutants were transformed with A) the *Luciferase* reporter construct alone or the reporter construct together with the *Sl15-24 KDead* construct. Data points and error bars stand for the mean and SD of 3 replicates. The results shown are representative for n = 3 independent repetitions of experiments. B) Western blot analysis to confirm the presence of *Sl15-24 KDead-GFP* in protoplasts.

4.2 Do Sl15-24 and AtBAK1 interact in the absence of the ligand flg22?

4.2.1 Is Sl15-24 autoactive when expressed in *N. benthamiana*?

It was unclear whether expressing Sl15-24 in *N. benthamiana* also induces autoactivation due to the presence of NbSERKs. To examine this, ROS assay was performed with *N. benthamiana* leaves transiently expressing Sl15-24 or AtFLS2 as control. As illustrated in Figure 4.2.1B, *N. benthamiana* leaves expressing AtFLS2 gained responsiveness to concentration of flg22 as low as 1 pM, a sensitivity never observed in plants with only the endogenous NbFLS2 such as the control transformants with P19 (Figure 4.2.1A). Interestingly, *N. benthamiana* leaves expressing Sl15-24 showed a clearly increased constitutive ROS production in the absence of flg22 which was not observed in leaves expressing AtFLS2 and P19 (Figure 4.2.1 C & D). However, the leaves expressing Sl15-24 were still able to respond to 10 nM of flg22 (Figure 4.2.1 C). Whereas it is not clear whether this response is attributable to Sl15-24 or the endogenous NbFLS2, it indicates that the PTI signalling was not generally saturated by the expression of Sl15-24. These results also indicate that NbSERKs, for example, NbSERK3/BAK1, can only partially substitute for the

function of AtBAK1in autoactivation of Sl15-24. Alternatively, a third factor, present only in *Arabidopsis* might be requested for saturated autoactivation observed in *A. thaliana.*

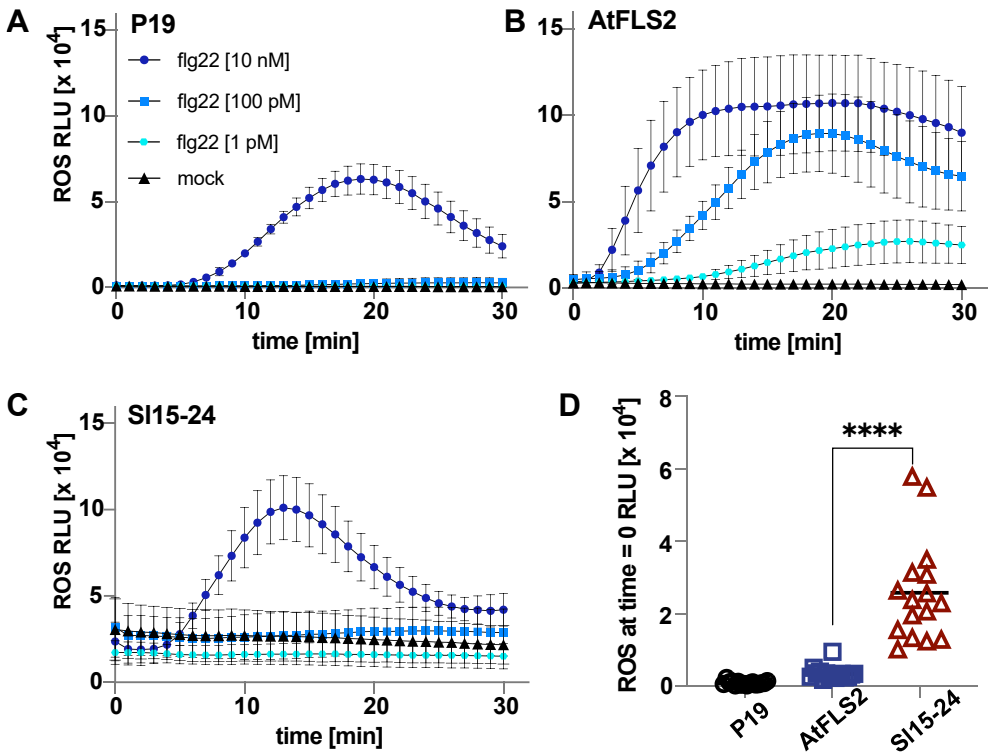

Figure 4.2.1 Sl15-24 is autoactive in *N. benthamiana* but not able to saturate the immune signalling

ROS assay with *N. benthamiana* leaf expressing P19, AtFLS2 and Sl15-24. A)-C) ROS production was monitored as relative light unit (RLU) every minute with a luminometer for 30 mins. Treatments (indicated in A) were done at time = 0. Data points and error bars show the mean and SD of 4 replicates, respectively. D) Background ROS production of *N. benthamiana* leaves expressing P19, AtFLS2 or Sl15-24, respectively, at time = 0 used in A)-B). The black line indicated the mean of n = 16 replicates. The elevated ROS production of *N. benthamiana* leaf expressing Sl15-24 is statistically significant at the $p < 0.0001$ level (T-test). The data shown are representative for n = 3 independent repetitions of the experiments.

4.2.2 Do Sl15-24 and AtBAK1 interact in *N. benthamiana*?

A further attempt was carried out to investigate the interactions of Sl15-24 and AtFLS2 with AtBAK1 in *N. benthamiana* expression system. AtBAK1 was c-terminally labelled with the HiBiT tag in order have a small tag that allows for a more sensitive detection in co-immunoprecipitates than in previous experiments with anti-AtBAK1 antibodies (Figure 1.7.8). Figure 4.2.2 shows an example of such an experiment where a marginal amount of AtBAK1-HiBiT was detected as co-immunoprecipitate of Sl15-24, irrespective of treatment with flg22. In the control experiments, AtBAK1-HiBiT was clearly detectable as co-immunoprecipitate of AtFLS2, but only when leaf tissue was treated with flg22. In total, this type of experiment was repeated 14 times. In all experiments with the reference pair AtFLS2 and AtBAK1, a flg22-dependent appearance of AtBAK1 was observed in the immunoprecipitates of AtFLS2. In contrast, immunoprecipitates from leaves expressing Sl15-24 and AtBAK1 resulted in variable and inconsistent patterns. To sum up the 14 times co-ip experiment with the representative examples illustrated in Figure 4.2.2 and Supp. 5, only in 3 cases a faint ligand-independent interaction of Sl15-24 and AtBAK1 as in Figure 4.2.2 was observed; in 6 cases there was no AtBAK1 detectable in the immunoprecipitates of Sl15-24, irrespective of the treatment with flg22 or water (Supp. 5A); in 3 cases AtBAK1 was detectable in both ligand-dependent and -independent manner in the IPs of Sl15-24 (Supp. 5B); in 2 cases AtBKA1 was only detected in the flg22 supplied immunoprecipitates of Sl15-24 (Supp. 5C).

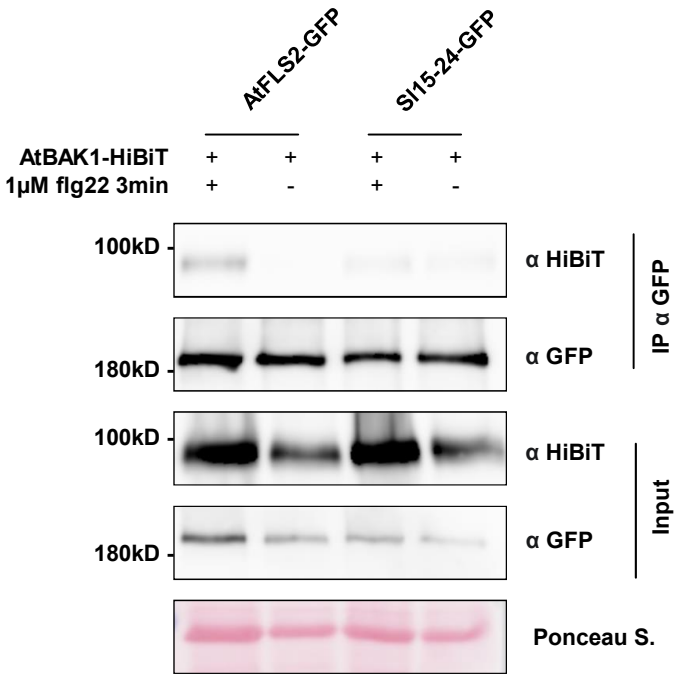

Figure 4.2.2 Do Sl15-24 and AtBAK1 form a ligand-independent complex in *N. benthamiana*?

Immunoprecipitation of extracts from *N. benthamiana* leaves co-expressing FLS2-GFP and AtBAK1-HiBiT. *N. benthamiana* leaves were harvested 3 min after infiltration with 1 µM flg22 or H2O as negative control. GFP-Trap was used to immunoprecipitate the GFP-tagged FLS2 receptor from solubilized leaf extracts. Western blots were developed either with anti-GFP antibody or the HiBiT detection system.

Activated PTI signalling could cause disappearance of the receptor/co-receptor complex via endocytosis and degradation, a process that might lead to the lower amounts of receptor complexes detectable. To avoid this, we performed co-ip experiments with AtFLS2, Sl15-24 and AtBAK1 constructs with truncated KDs, leaving only with 20 amino acids after the TMDs in all three constructs (Figure 4.2.3A). *N. benthamiana* leaves co-expressing these receptor/co-receptor pairs were treated with flg22 or water and used for co-immunoprecipitation as described above for the full-length versions (Figure 4.2.3B). Much like in the experiments with the full-length constructs, a significantly higher amount of AtBAK1TM was found in the immunoprecipitates of AtFLS2TM after treatment with flg22. In contrast, AtBAK1TM in the immunoprecipitates of Sl15-24TM was low and barely detectable, irrespective of the treatment with flg22 or water.

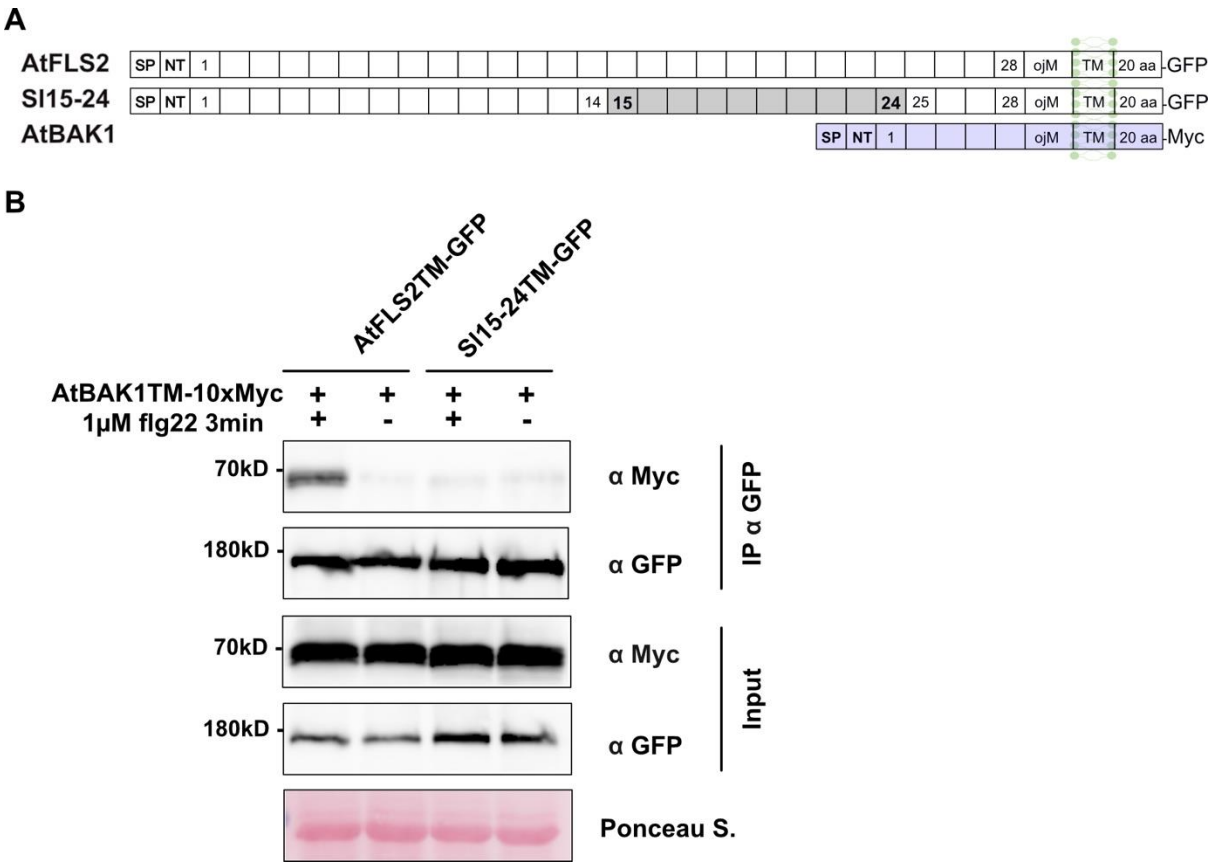

Figure 4.2.3 Kinase truncated forms of Sl15-24 and AtBAK1 do not form a stable complex detectable in immunoprecipitates

Co-immunoprecipitation with extracts from *N. benthamiana* leaves co-expressing AtFLS2TM-GFP or Sl15-24TM-GFP and AtBAK1TM-10xMyc. *N. benthamiana* leaves were harvested 3 min after infiltration with 1 µM flg22 or water as negative control. GFP-Trap was used to immunoprecipitated GFP-tagged AtFLS2 or Sl15-24 kinase truncated from solubilized leaf extracts. Western blots were development either with anti-GFP antibodies or anti-Myc antibodies.

All co-ip results did not provide convincing evidence for physical interaction between Sl15-24TM and AtBAK1TM, at least not when expressed in tissue of *N. benthamiana* and not in a manner that is stable throughout the immunoprecipitation procedure.

4.2.3 Do the ectodomains of Sl15-24 and AtBAK1 interact *in vitro*?

Crystallographic evidence showed that ECDs of AtFLS2 and AtBAK1 can form a complex *in vitro* in the presence of flg22 (Sun et al., 2013a). We thus tried to perform a further interaction

experiment with soluble ECDs. Accordingly, leaf extracts of *benthamiana* co-expressing *ECD-AtFLS2-HA* and *ECD-AtBAK1-GFP* w/o flg22 treatment were used to immunoprecipitate ECD-AtBAK1 via GFP-Trap (Figure 4.2.4) However, although both presumptive interaction partners were present, no complex of ECD-AtFLS2 and ECD-AtBAK1 could be detected even upon flg22 treatment.

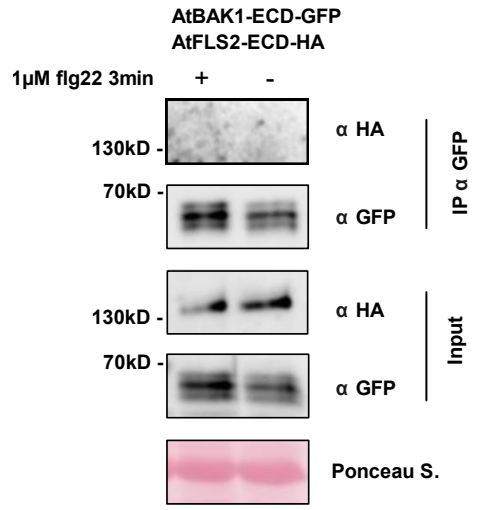

Figure 4.2.4 Ectodomain of AtFLS2 and AtBAK1 did not form a flg22-induced complex *in planta*

Leaf extract of *benthamiana* expressing ECD-AtFLS2-GFP or ECD-Sl15-24-GFP and ECD-AtBAK1-4xMyc w/o flg22 treatment were immune absorbed with GFP-Trap. Ip and crude extract were used for western blots developed with anti-GFP or anti-Myc antibodies, respectively.

One possible explanation might be the interacting partners got further diluted when expressed in *N. benthamiana* apoplast. Thus, the chance of ECD of AtFLS2 and AtBAK1 to interact in the correct orientation is lower than purified proteins.

The other possibility is this might be due to weaker interaction of the ECDs compared to the membrane bound forms. Weaker interaction could lead to separation of the complex partners during the lengthy time of immunoprecipitation. In order to detect also weaker interactions, such as the ones that might also prevail between Sl15-24 and AtBAK1, we used ECD-AtBAK1 insolubilized via its GFP tag to GFP-trap beads as a simple affinity column (Figure 4.2.5A). We expected that in the absence of flg22, ECD-AtFLS2 should have little or no affinity for ECD-AtBKA1 and readily pass through the affinity column (no interaction, Figure

4.2.5B). As a positive control, in the presence of flg22, ECD-AtFLS2 should exhibit a higher affinity for ECD-AtBAK1 and gets retained or delayed on this affinity column (Figure 4.2.5B). For the interaction between Sl15-24 and AtBAK1, we expected that the ECD-Sl15-24 might elute later than the ECD-AtFLS2 in the absence of flg22. However, under the conditions used, ECD-AtFLS2 exhibited no retention on the affinity column regardless of the flg22 supplement (Figure 4.2.5C). Similarly, also ECD-Sl15-24 did not bind to ECD-AtBAK1. In all the cases, close to all of the ECD-AtFLS2 and ECD-Sl15-24 eluted with the flow through in the first two eluting fractions. Subsequent boiling of the GFP-traps in SDS buffer confirmed the presence of ECD-AtBAK1 on the column material but showed no retention of either EC-AtFLS2 or ECD-Sl15-24 (Figure 4.2.5D). A possible explanation of this failure might be the steric hindrance originating from the tags or the binding of the ECD-AtBAK1 to the GFP-trap. Another possibility might be that the TMDs are necessary for stabilizing the complex of flg22-AtFLS2-AtBAK1.

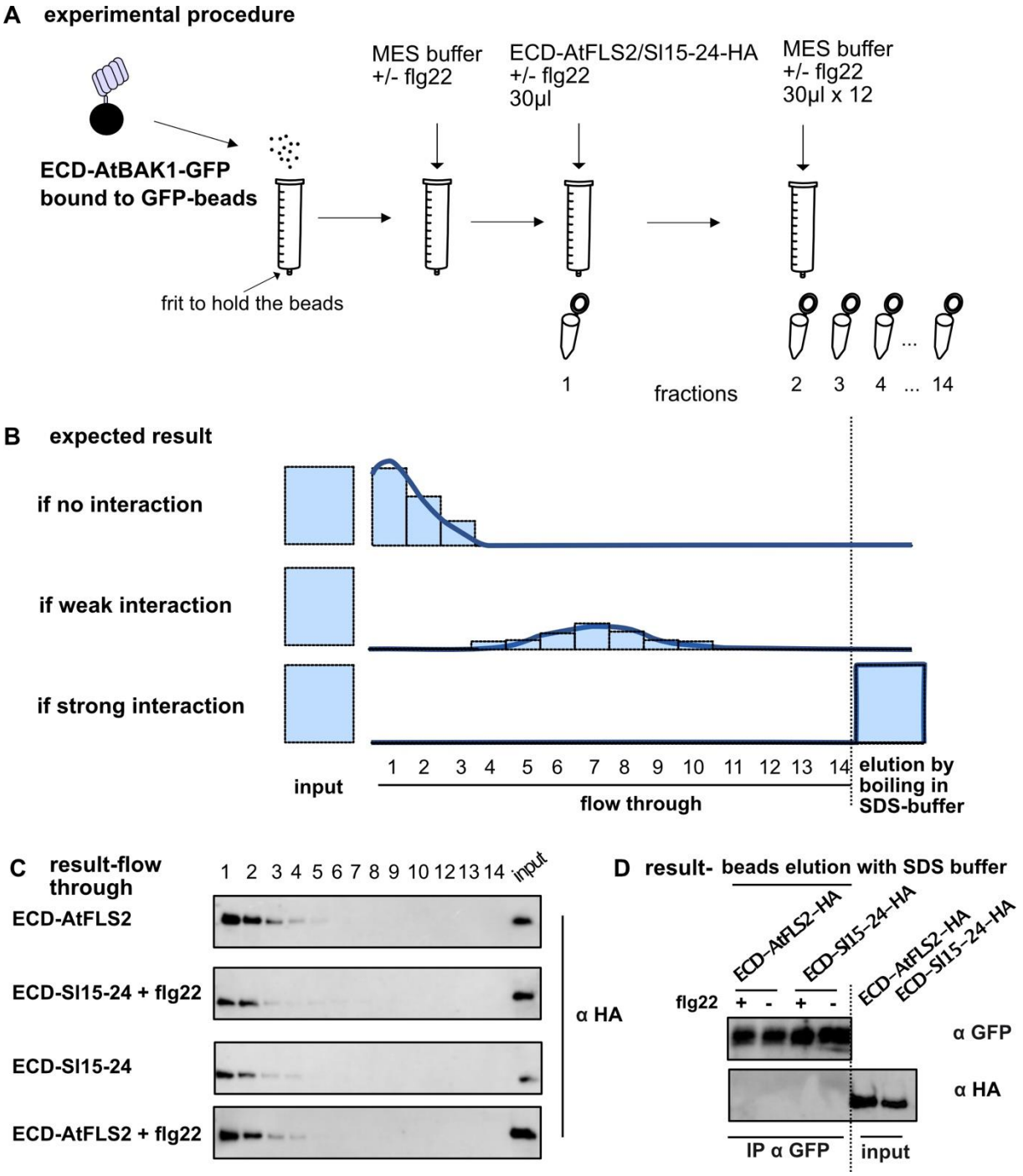

Figure 4.2.5 Do the ectodomains of Sl15-24 and AtBAK1 interact *in vitro*?

A) scheme of experimental procedure. B) scheme of expected results. C) western blot of input and fractions eluting from the affinity columns, developed with anti-HA antibodis. D) western blots of the washed beads (after elution of fraction 14) extracted by boiling in SDS sample buffer. Blots were developed with anti-HA antibodies for detecting ECD-AtFLS2 or -Sl15-24 or with anti-GFP antibodies to confirmed presence of ECD-AtBAK1 on the beads.

4.2.4 Do Sl15-24 and AtBAK1 interact in split luciferase complementation assays?

Besides co-ip experiments, Split luciferase complementation (SPLC) assay was also tried to examine whether Sl15-24 and AtBAK1 interact in a flg22-independent manner. SPLC was first used in mammalian cells to provide evidence for protein-protein interaction (Luker et al., 2004). Subsequently this technique was also applied *in planta* (Chen et al., 2008). For instance, the SPLC was adopted to confirm the interaction of BIK1 and RbohD, an interaction that was previously reported based on co-immunoprecipitation experiments (Li et al., 2014, Zhou et al., 2018). Here, we applied the same methods to examine whether Sl15-24 and AtBAK1 interact in a flg22-independent manner.

AtBAK1 has been reported to constitutively interact with the RLK BIR3 (Imkampe et al., 2017, Hohmann et al., 2020), and this interaction has been observed also in split luciferase assay when the interaction partners were co-coexpressed in *N. benthamiana* (personal communication Liping Yu from Birgit Kemmerling Group). Thus, as a positive control, we also co-expressed AtBAK1-nFLUC and BIR3-cFLUC in *N. benthamiana* leaves. This combination indeed showed high luminescence (>1500 RLU). In contrast, co-expression of AtFLS2-cFLUC and AtBAK1-nFLUC did not result in significant luciferase activity and this also did not change after treatment of the leaf pieces with 100 nM of flg22 (Figure 4.2.6A), (Figure 4.2.6B). Since AtFLS2 and AtBAK1 are known to form a ligand-dependent complex also when expressed in *N. benthamiana* leaves this result might indicated steric problems for the reconstitution of a functional luciferase when attached to the kinase domains of AtFLS2 and AtBAK1.

In a second experiment, I also tried the same SPLC partners in *Arabidopsis* mesophyll cells (Supp. 4 and Figure 4.2.6C). Interestingly, in contrast to the result in *N. benthamiana*, co-expression of AtFLS2-cFLUC and AtBAK1-nFLUC did showed induction of luciferase activity when treated with flg22 but not in the control treatment with elf18, suggesting that the increase of luciferase activity correlated with the ligand-dependent complex formation between AtFLS2 and AtBAK1. However, while ligand-induced complex formation between AtFLS2 and AtBAK1 has been reported to occur within seconds upon flg22 treatment (Schulze et al., 2010), of the increase in luciferase activity occurred only with a lag of about 5 mins. A possible explanation might be that while the complex of AtFLS2 and AtBAK1 forms within seconds upon flg22 treatment, the reconstitution of nFLUC and cFLUC to the active luciferase enzyme occurs much slower and takes much more time. Another problem of this

assay was the high luciferase activity in the absence of flg22 which reached values as high as those in cells expressing the positive control constructs BIR3-cFLUC and AtBAK1-nFLUC. A similar level of luciferase activity was also observed in cells with Sl15-24-cFLUC and AtBAK1-nFLUC (Figure 4.2.6C). However, in contrast to the pair with authentic AtFLS2, the luciferase activity in these cells was not altered after flg22 treatment. Additionally, in an experiment with swapped nFLUC and cFLUC tags the same pattern of luciferase activity was observed.

Overall, the attempts with SPLC in the two transformation systems led to ambiguous results for the ligand dependent interaction of AtFLS2 with AtBAK1. This failure with the reference system also rendered the approach unsuitable for studying the interaction of Sl15-24 and AtBAK1.

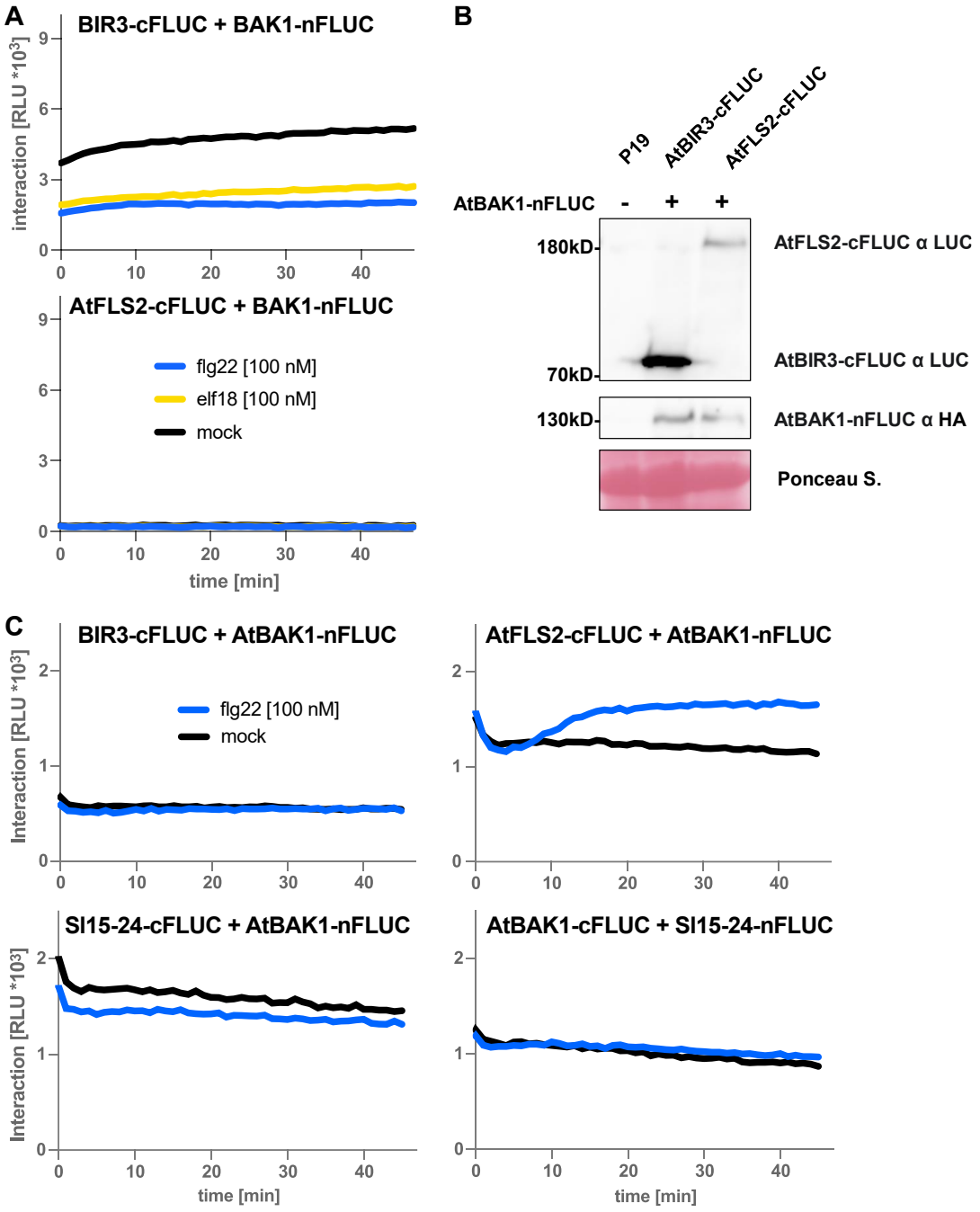

Figure 4.2.6 Split firefly luciferase assay to test for constitutive interaction of Sl15-24 with AtBAK1

Split firefly luciferase assays in A) *N. benthamiana* leaf and B) *A. thaliana* mesophyll protoplast from *fls2* x *bak1-4* mutants. Data points and error bars showed mean of 3 replicates, respectively. The data shown represented for n = 2 independent experiments.

4.3 Molecular characterization of Sl15-24

4.3.1 Sl15-24 and AtBAK1 are both needed to induce autoactivation via double reciprocal approach

Albert and colleagues generated a double reciprocal pair of RLKs with the ectodomain of AtFLS2 fused to the AtBAK1 kinase domain (FtB) and the ectodomain of AtBAK1 fused to the AtFLS2 kinase domain (BtF) (2013a). When co-expressed in *A. thaliana* cells, the combination of these chimeras proved functional as flg22 perception system, demonstrating the heteromeric complex between AtFLS2 and a co-receptor like AtBAK1 is essential for intracellular signal induction (Albert et al., 2013a). We thus wondered whether reciprocal swaps of the kinase domains between Sl15-24 and AtBAK1 would also lead to autoactivity.

Accordingly, a double reciprocal chimeric receptor pair with StB comprising the ECD of Sl15-24 and the KD of AtBAK1 and BtF (identical with BtS) was generated and analysed for its autoactivation activity in *Arabidopsis* mesophyll protoplasts (*fls2* x *bak1-4* background) (Figure 4.3.1A). When individually expressed in these protoplasts, the single chimeric receptors did not cause an autoactivated state with induction of the luciferase reporter. As expected, these cells did not respond to treatment with flg22 but responded to the control stimulus elf18 (Figure 4.3.1B). In contrast, much like with the Sl15-24 expressed in presence of AtBAK1, co-expressing the reciprocal chimeras StB and BtF exhibited ligand-independent constitutive induction of the luciferase reporter activity and no further stimulation occurred after additional treatment with elf18 or flg22. Protein expression of the constructs was confirmed by western blot analysis (Figure 4.3.1C).

These results corroborated the finding that it needs the combination of the protein pair Sl15-24 and AtBAK1 to generate ligand-independent activation. The results with the reciprocal chimeric receptor pair also suggest that this interaction of Sl15-24 and AtBAK1 is sufficient to trigger downstream signalling.

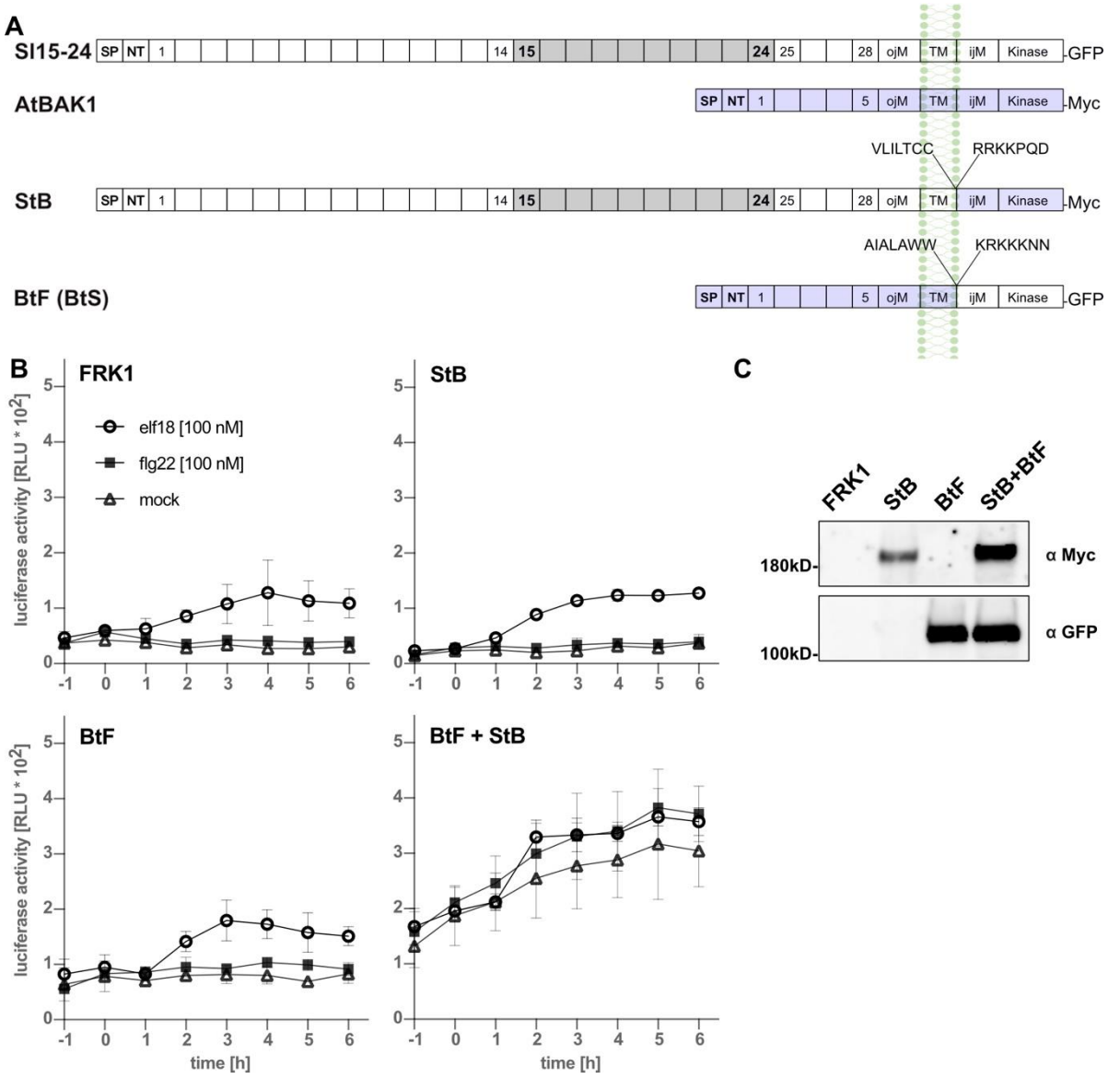

Figure 4.3.1 Autoactivation by a Sl15-24/AtBAK1 pair with reciprocally swapped kinase domains

A) schematic view of double reciprocal chimeras between Sl15-24 and AtBAK1. B) mesophyll protoplast of *fls2* x *bak1-4* mutants were transformed with the luciferase reporter and *StB-Myc* or *BtF-GFP* or the combination of *StB-Myc* + *BtF-GFP*. Data points and error bars stand for the mean and SD of 3 replicates. C) western blots of protoplast used in this assay were developed with anti-GFP antibodies or anti-Myc antibodies. The data here represented for n = 3 independent experiments.

4.3.2 Sl15-24 and AtFLS2 share similar responsiveness in cells lacking AtBAK1

Sl15-24 is a functional FLS2 receptor perceiving flg22 when AtBAK1 was impaired (Figure 1.7.6, Figure 4.1.3, Supp. 3). We next compared the responsiveness of Sl15-24 and AtFLS2 to different concentrations of flg22 in *Arabidopsis fls2* x *bak1-4* protoplasts. Applying flg22 in concentrations from 10 pM to 10µM (Figure 4.3.2) resulted in EC_{50} values of ~ 46 nM for AtFLS2 and ~ 60 nM for Sl15-24, respectively. Thus, in the absence of AtBAK1, AtFLS2 and Sl15-24 exhibited similar responsiveness to flg22. This fits with the equivalent apparent binding affinities for flg22 of both forms of receptor reported by Katharina Mueller (Figure 1.7.6A).

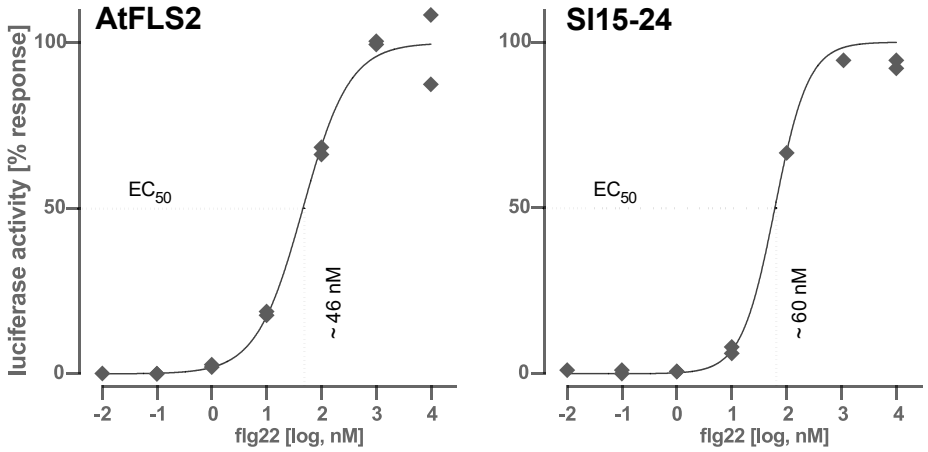

Figure 4.3.2 AtFLS2 and Sl15-24 are functional flg22 receptors in the absence of AtBAK1

flg22-dose-dependent induction of pFRK1::Luciferase reporter activity in *A. thaliana fls2* x *bak1-4* mesophyll cells co-transformed with *AtFLS2* or *Sl15-24*. Y axis values stand for the normalized induction of luciferase activity 6-h-post-flg22-stimulation as percentage (100% = saturation). The experiment was repeated in an independent experiment resulting in similar EC_{50} values of ~40 nM for AtFLS2 and ~110 nM for Sl15-24, respectively.

4.3.3 Sl15-24 is not autoactive in cells overexpressing SERKs other than AtBAK1/AtSERK3

Arabidopsis has five SERKs (Chinchilla et al., 2009, Ma et al., 2016), but autoactivity of Sl15-24 is lost when only in the absence of AtBAK1/AtSERK3. This raised the question whether the endogenous expression level of the other AtSERKs did not reach the threshold to activate Sl15-24. To answer this, we overexpressed the other *AtSERKs* under the 35s promoter together with *Sl15-24* in *A. thaliana fls2* x *bak1-4* protoplasts. As illustrated in Figure 4.3.3A, the protoplasts overexpressing *AtSERK1*, *AtSERK2*, *AtSERK4* or *AtSERK5* in combination

with *Sl15-24* did not show constitutive induction of the luciferase reporter and these cells still responded to flg22 and elf18 treatment.

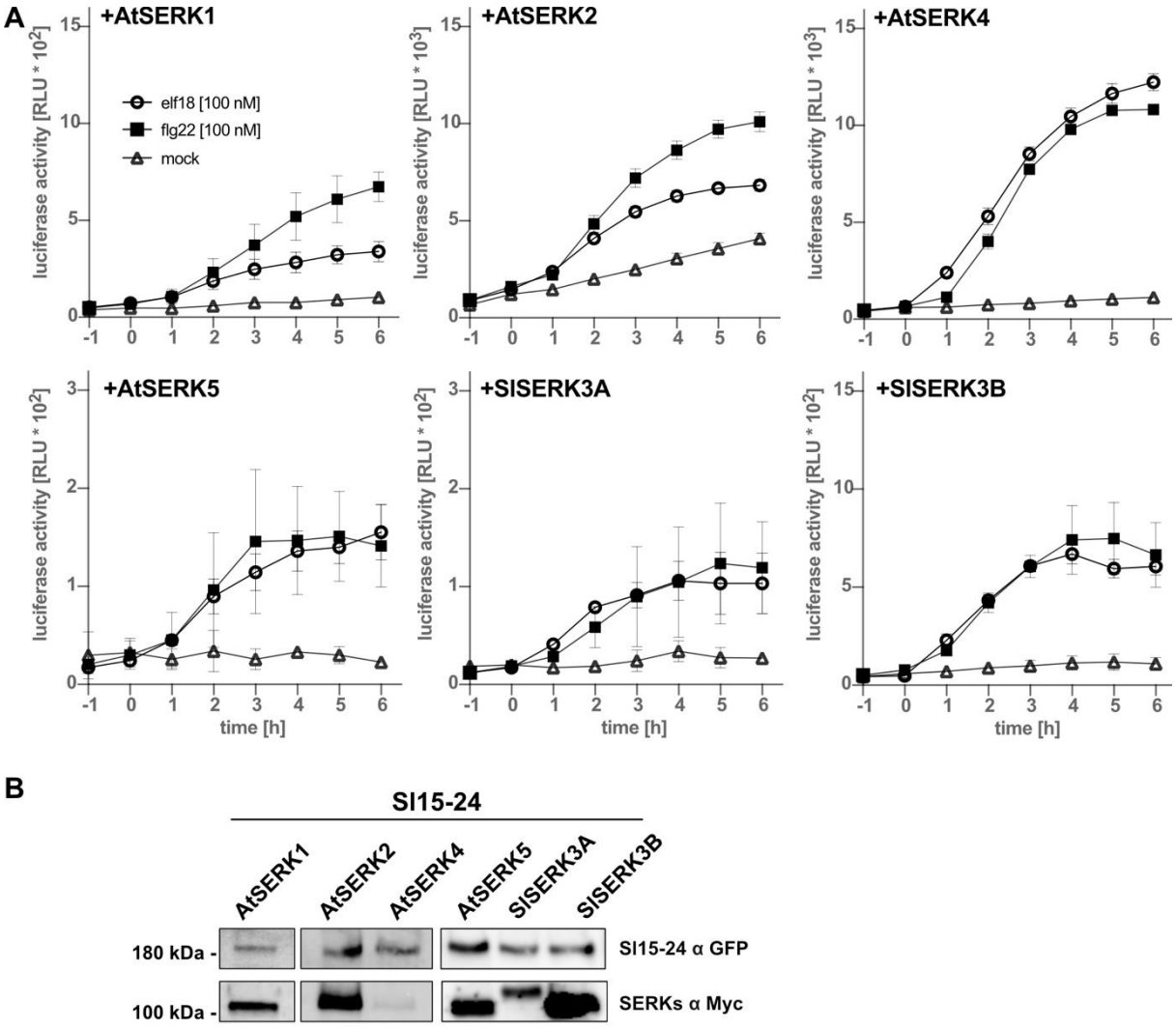

Figure 4.3.3 Autoactivity of Sl15-24 is not caused by overexpression of SERKs other than AtBAK1

A) Induction of pFRK1::Luciferase activity in *Arabidopsis fls2* x *bak1-4* cells. Various *p35s::SERKs-4xMyc* were co-transformed with the reporter construct *pFRK1::Luciferase* and *p35s::Sl15-24-GFP*. Cells were treated with elf18 or flg22 at t = 0, data points and error bars stand for mean and SD of 3 replicates, respectively. Luminescence was measured as RLU with luminometer. B) Protoplasts were collected for western blot, Sl15-24 and SERKs expression were developed with anti GFP antibodies and anti Myc antibodies, respectively. Data shown represented n = 2 independent experiments.

Sl15-24 contains parts of the FLS2 receptor from tomato. Thus, it was interesting to know whether SERK homologs of tomato would also cause autoactivity of the hybrid receptor *Sl15-24.* The AtBAK1/AtSERK3 homologs SlSERK3A and SlSERK3B have been implicated in the activation of SlFLS2 (Peng and Kaloshian, 2014). However, in co-expression assays SlSERK3A and SlSERK3B did not lead to autoactivation of Sl15-24 and cells still responded to flg22 and elf18 (Figure 4.3.3A) Except for AtSERK4 which accumulated only to a reduced amount, all the SERK variants accumulated strongly in the protoplasts used for the experiments (Figure 4.3.3B). These data demonstrated that ligand-independent activation of Sl15-24 in *A. thaliana* strictly depends on AtBAK1 and none of the other SERKs tested, notably also the AtBAK1 homologs SlSERK3A and SlSERK3B from tomato, caused autoactivation of Sl15-24. With respect to the high degree of conservation between AtBAK1 and SlSERK3B (Figure 4.3.4), which includes conservation of the residues T52-V54 relevant for contacting flg22 at G18 and F60, R72, Y96, Y100, R143, F144, R146 involved in interaction with FLS2, respectively (Sun et al., 2013a). Rather surprisingly, the small number of differences between AtBAK1 and SlSERK3B was located on the surface which is not supposed to involve in flg22 or FLS2 interaction.

In order to specify the LRRs or amino acids from AtBAK1 that cause the autoactivity of Sl15-24, it will be interesting to swap the LRR subdomain between AtBAK1and SlSERK3B. However, our preliminary data (Supp. 6) did not give a clear picture but an intermediate autoactivation phenomenon was observed when co-expressed Sl15-24 and chimeric form of SERK3 in protoplasts lacking both FLS2 and AtBAK1, indicating there might be two regions from AtBAK1 needed to induce the autoactivation of Sl15-24. Further swaps will be generated to narrow down the region from AtBAK1 that are needed for the autoactivity of Sl15-24. Alternatively, this intermediate autoactivation might be due to overexpression of the chimeric form of SERK3, according to the report that overexpression of AtBAK1 in *A. thaliana* induce cell death and activate immune signalling (Domínguez-Ferreras et al., 2015).

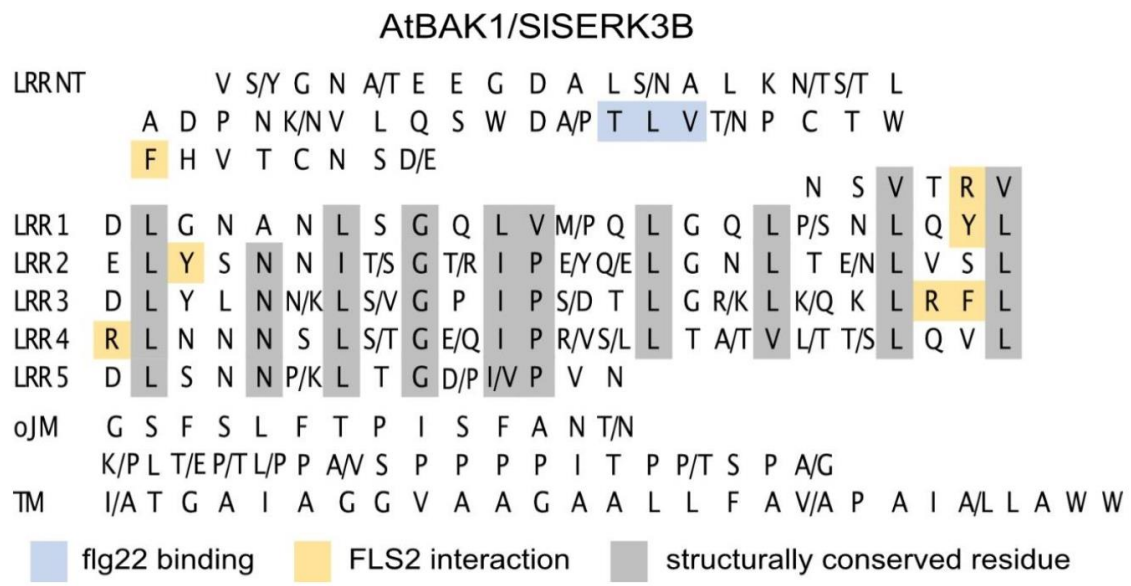

Figure 4.3.4 Amino acid residues for FLS2 binding are conserved between AtBAK1 and SlSERK3B

Comparison of AtBAK1 and SlSERK3B ECD-TM. Non-conserved residues are represented by X/Y.

4.3.4 Sl15-24 autoactivation also occur in the *sobir1* mutant

AtBAK1 overexpression has been reported to induce growth inhibition and cell death in *A. thaliana*, even with a kinase truncated version (Domínguez-Ferreras et al., 2015). In this report, *sobir1* mutant was found to partially rescue the effects of AtBAK1 overexpression. We thus wondered whether Sl15-24 autoactivation might also depend on SOBIR1. Thus, we expressed Sl15-24-GFP in protoplasts of *sobir1-12* mutant of *Arabidopsis* which contain wildtype alleles of AtBAK1. When expressing Sl15-24, these protoplasts lacking SOBIR1 still exhibited constitutive induction of luciferase activity and were not able to further respond to elf18 and flg22 treatment (Figure 4.3.5 right panel). In comparison, *sobir1* cells transformed with the FRK1::Luciferase reporter alone responded normally to treatments with elf18 and flg22 (Figure 4.3.5 left panel).

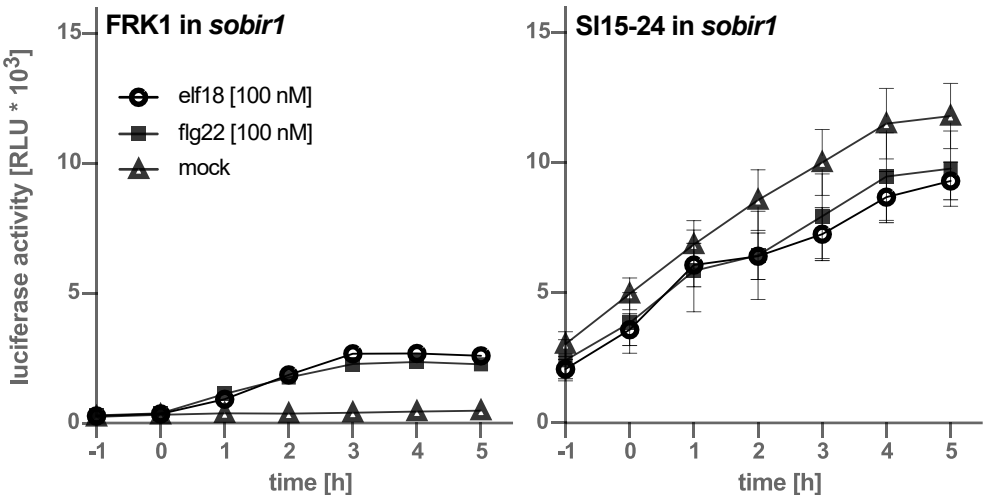

Figure 4.3.5 Sl15-24 autoactivation occurs also in *sobir1*mutant

Mesophyll protoplasts of *sobir1* mutant plants were transformed with pFRK1::Luciferase reporter construct or the reporter construct and *p35s::Sl15-24-GFP*. Elicitors were added at t = 0, and luminescence was monitored as RLU by using a luminometer over 5 hours after treatments. Data points and error bars stand for the mean and SD of 3 replicates. The data shown represents for n = 3 independent experiments.

4.3.5 Sl15-24 autoactivation is suppressed by overexpression of BIR2

The *Arabidopsis* RLK BIR2 was found to act as a negative regulator of AtBAK1, notably suppressing AtFLS2 mediated immune signalling (Ma et al., 2017, Halter et al., 2014a, Halter et al., 2014b). We thus tested whether the autoactivation of Sl15-24 would be abolished or diminished when expressed in protoplasts from plants overexpressing BIR2 (BIR2OX) in a genetic background with wildtype genes encoding AtFLS2 and AtBAK1. BIR2 OX protoplasts, when transformed with the luciferase reporter alone, showed induction of luciferase but only when treated with a very high concentration of 1 µM flg22 (Figure 4.3.6 left panel). In contrast, BIR2OX protoplasts co-transformed with Sl15-24 and the reporter gene proved more sensitive and responded strongly also to 100 nM flg22 (Figure 4.3.6 right panel). Importantly though, Sl15-24 did not cause autoactivation in these BIR2OX protoplasts, despite the presence of wildtype AtBAK1. These results suggested that overexpression of BIR2 could suppress autoactivation of Sl15-24.

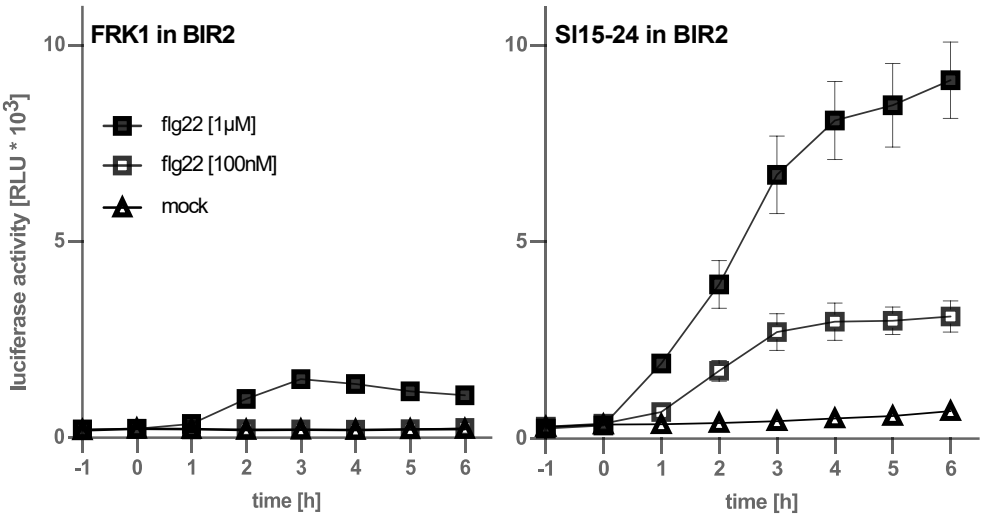

Figure 4.3.6 BIR2 overexpression inhibits the autoactivation of Sl15-24

Mesophyll cells of BIR2 overexpression line were transformed with pFRK1::Luciferase reporter construct or the reporter and *Sl15-24*. Data points and error bars stand for the mean and SD of 3 replicates. The data shown represents for n = 3 independent experiments.

4.3.6 The autoactivity of Sl15-24 is inhibited by overexpression of BIR2, BIR3, BIR4 but not by BIR1

To confirm the inhibitory effect of BIR2 on the autoactivation of Sl15-24, further experiment was performed with overexpression of BIR2 and its homologs BIR1, BIR3 and BIR4 in protoplasts from wildtype plants with AtBAK1 (Figure 4.3.7). The Sl15-24-induced autoactivation of luciferase activity was suppressed by the concomitant overexpression of either BIR2, BIR3 or BIR4 and the protoplasts expressing these genes also responded to the stimulation of elf18 and flg22 (Figure 4.3.7B, E, F, G). In contrast, overexpression of BIR1 did not inhibit the autoactivation of Sl15-24 (Figure 4.3.7C, D and H). These data are in accordance with the observation that BIR2, BIR3, but not BIR1, can negatively regulate the immune pathway mediated by AtFLS2 (Halter et al., 2014b, Liu et al., 2016).

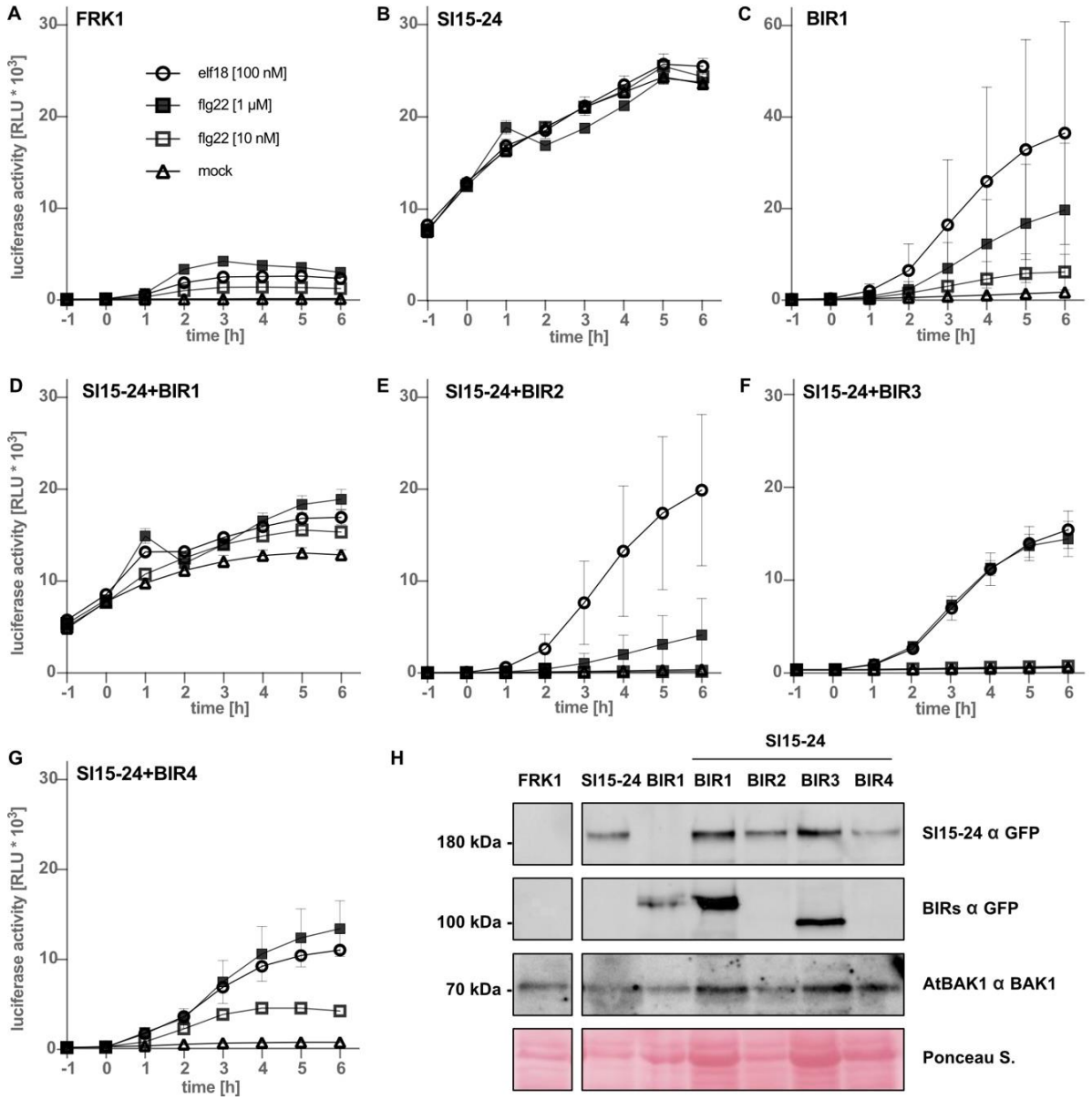

Figure 4.3.7 BIR2, BIR3 and BIR4 but not BIR1 inhibit Sl15-24-caused autoactivation

Mesophyll cells of Col-0 *Arabidopsis* were transformed with A) the reporter construct (*pFRK1::luciferase*) or B) the reporter construct and Sl15-24 or C) the reporter construct and BIR1 or D)-G) the reporter construct and *Sl15-24-GFP* and *BIR-YFP*. Luminescence was measured with luminometer as RLU. Data points and error bars stand for the mean and SD of 3 replicates. Data shown represents for n = 2 independent of experiments. H), protein expression analysis via western blot with anti-GFP antibodies. Endogenous AtBAK1was detected with anti-BAK1 antibodies as control. This experiment was repeated another time with protoplasts from *efr* x *fls2* mutant plants and same trend of results were obtained.

4.3.7 BIR1 with the pseudokinase domain of BIR2 inhibits autoactivation of Sl15-24

All four BIRs share a high conservation of their amino acid sequences. The most distinctive feature is that BIR1 has an active kinase whereas BIR2 to BIR4 are thought to harbour inactive pseudokinases (Ma et al., 2017, Gao et al., 2009, Halter et al., 2014b, Halter et al., 2014a). In order to test whether the type of kinase determines the inhibitory function on the autoactivity of Sl15-24, hybrid BIRs with swaps of their KDs, BIR1 ECD with BIR2 KD (BIR1t2) or BIR2 ECD with BIR1 KD (BIR2t1), respectively, were generated (Figure 4.3.8A). *A. thaliana* cells expressing Sl15-24 and BIR1t2 showed no sign of autoactivation but gained responsiveness to flg22 and also responded to Atpep1 treatment (Figure 4.3.8 B left panel). Cells expressing Sl15-24 and BIR2t1 exhibited saturated luciferase induction with mock treatment already (Figure 4.3.8B right panel). These data suggested that the KD of BIR2, likely the absence of kinase activity, determines the inhibitory function on Sl15-24 autoactivation.

In planta co-ip experiments with full length protein of BIRs and AtBAK1 showed that all the BIRs can constitutively interact with AtBAK1 (Halter et al., 2014b). Interestingly, in yeast two hybrid assays, the KDs of BIR2, BIR3 and BIR4 but not the KD of BIR1 interacted with the KD of AtBAK1 (Halter et al., 2014b), indicating that the pseudokinase domains of BIR2, BIR3 and BIR4 might inhibit the activity of AtBAK1 by interaction. Thus, in future experiments it will be interesting to test whether BIR1 with a dead kinase will be able to inhibit AtBAK1 and prevent the autoactivity of Sl15-24.

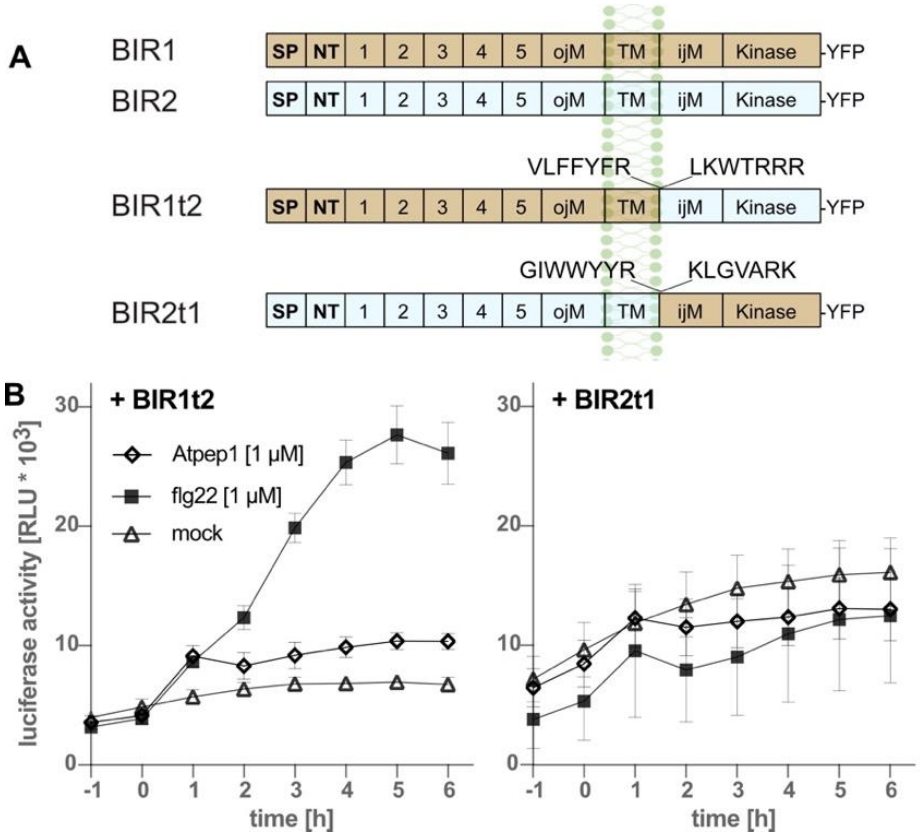

Figure 4.3.8 BIR1 with the kinase domain of BIR2 inhibits the autoactivation of Sl15-24

A) swapping scheme of BIR hybrid between BIR1 and BIR2. B) induction of pFRK1::luciferase activity. Cells of *efr* x *fls2* mutant were co-transformed with *pFRK1::Luciferase* reporter and *p35s::Sl15-24-GFP* and BIR1t2 or BIR2t1 constructs indicated on the figure. Ile directly after TM of BIR1t2 was mutated to a Leu for cloning convenience. Treatments were done at t = 0, data points and error bars show the mean and SD of 3 replicates. This experiment was repeated independently with protoplasts from Col-0 plants and the similar tendency was observed.

4.4 Mapping the subdomains responsible for autoactive forms of FLS2

4.4.1 N663L mutation on LRR24 of Sl15-24 did not inhibit its autoactivity

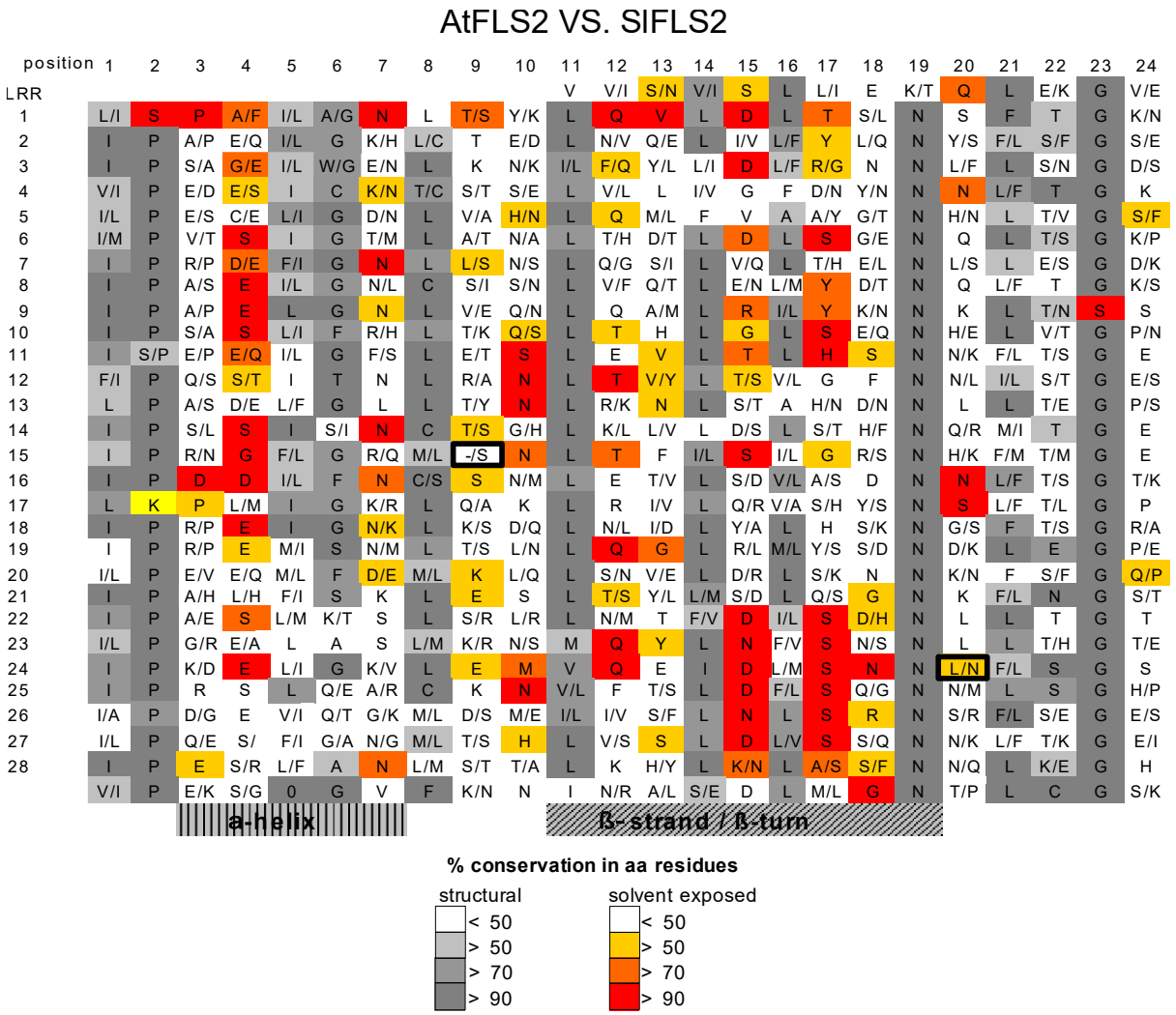

Figure 4.4.1 Amino acid sequence alignment of the ECDs of AtFLS2 and SlFLS2

Conservation alignment of AtFLS2 and SlFLS2. 1-28 LRRs are indicated to the left of the map. Each LRR contains 24 amino acids, the position of each amino acid is indicated on the top. Conservation rate of AtFLS2 and SlFLS2 aa residues among the FLS2 receptors in different (>20) plant species are indicated in different colour. Black frames indicate positions where AtFLS2 has a deletion of on aa and where SlFLS2 has an additionally N-glycosylation site (Modified from Prof. G. Felix).

Many plant LRR-RLKs are highly glycosylated at Asn (N) (NxS/T sites). N-glycosylation of plant PRRs is important for structure stabilization and functionality (Imperiali and O'Connor, 1999, Haweker et al., 2010). Noticeably, SlFLS2 harbours a potential N-glycosylation site 663N on LRR 24 while AtFLS2 has a Leu at this position (Figure 4.4.1). Furthermore, LRR 24 is part of the LRRs 23-26 which were found to directly interact with AtBAK1 in the

crystallographic analysis of the flg22-AtFLS2-AtBAK1 (Sun et al., 2013a). In order to examine whether the potential glycosylation site of SlFLS2 663N contributes to the AtBAK1-dependent autoactivation, we generated the Sl15-24 N663L mutant with the leucine substituting asparagine. Reciprocally, the leucine of AtFLS2 663 position was mutated to a asparagine as a control.

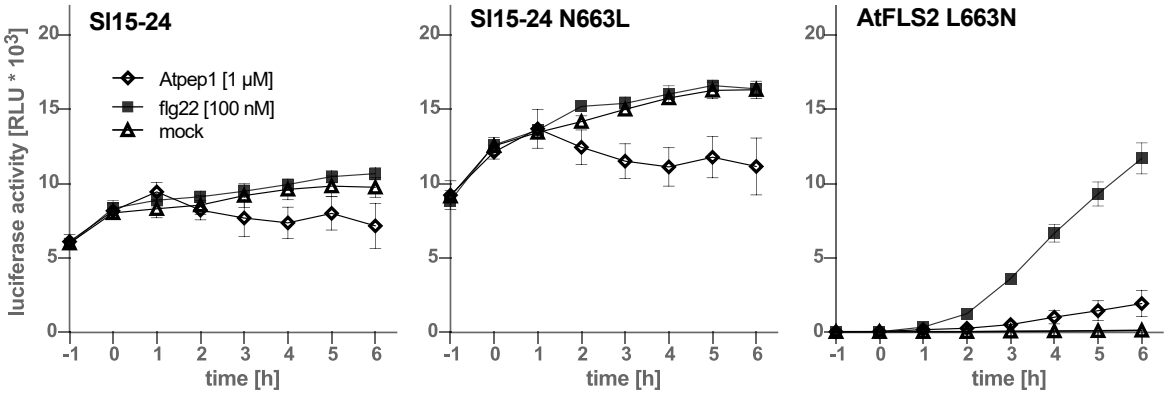

Figure 4.4.2 Potential N-glycosylation site does not determine the autoactivation of Sl15-24 in *efr* x *fls2 A. thaliana*

Induction of pFRK1::Luciferase activity in protoplasts from *Arabidopsis efr* x *fls2* mutant. *Sl15-24* or *Sl15-24 N663L or AtFLS2 L663N* were co-transformed with *pFRK1::Luciferase* into *A. thaliana efr* x *fls2* mesophyll cells. Data point indicates 3 replicates and error bar stands for SD. Data shown represented for n = 2 independent experiments.

However, neither the removal nor the introduction of the N-glycosylation site at this position had an effect on the functionality of Sl15-24 or AtFLS2, respectively (Figure 4.4.2). Thus, the position 663N of SlFLS2 is not the reason for the autoactivity of Sl15-24.

4.4.2 The LRRs 15-24 of SlFLS2 alone are not responsible for ligand-independent activation

SlFLS2 and several chimeric forms like Sl1-24 and Sl1-19 are functional flg22 receptors when expressed in *A. thaliana* that do not show signs of autoactivation in the presence of AtBAK1 (Mueller et al., 2012) (Figure 4.4.3). Thus, the mere presence of LRRs 15-24 from tomato FLS2 is not responsible for autoactivation. Rather, the interplay of LRRs 15-24 from SlFLS2 with elements of AtFLS2 seems to cause this phenomenon. Such a novel interplay might be caused at the swap sites that could change the backbones of the LRR structure. However, the functional non-autoactive chimeras Sl1-24 and Sl19-24 have the same swap site

AtLRR 24/ SlLRR 25 as Sl15-24, indicating this swap site is less possible to be the reason for autoactivation.

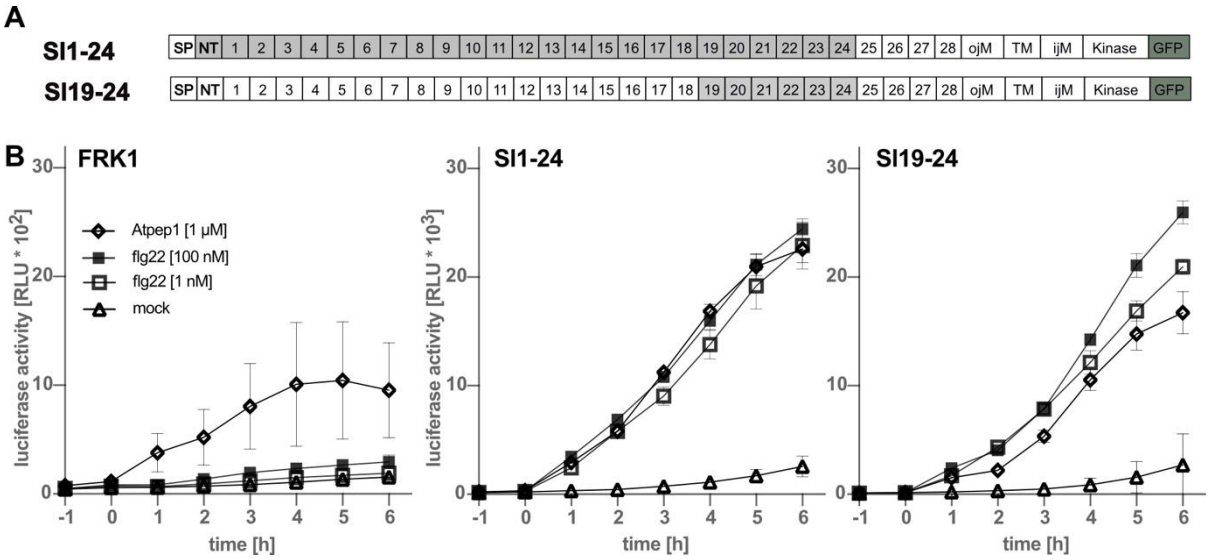

Figure 4.4.3 Sl1-24 and Sl19-24 do not show autoactivity

***Sl1-24* was co-transformed with the reporter construct *pFRK1::Luciferase.* Luciferase induction was monitored with a luminometer as RLU. Data points stand for the mean of 3 replicates and the error bars showed the standard deviation.**

In contrast, the swap site at AtLRR 14/SlLRR 15 was not present in any of the chimeras tested so far. Also, at LRR 15, AtFLS2 has one amino acid less than SlFLS2 (Figure 4.4.1). To question whether the additional one amino acid and/or the swap site at 14/15 LRR are causing autoactivation of Sl15-24, chimeras Sl15-16 and Sl15-19 were generated (Figure 4.4.4A). *A. thaliana* protoplasts from *efr* x *fls2* mutants expressing *Sl15-16* or *Sl15-19* showed no increased background of the reporter luciferase activity and these cells were clearly responsive to flg22 and Atpep1 (Figure 4.4.4B). These results suggested that the swap site at LRR 14/15 and the difference of one residue in LRR 15 do not cause the autoactivity of Sl15-24.

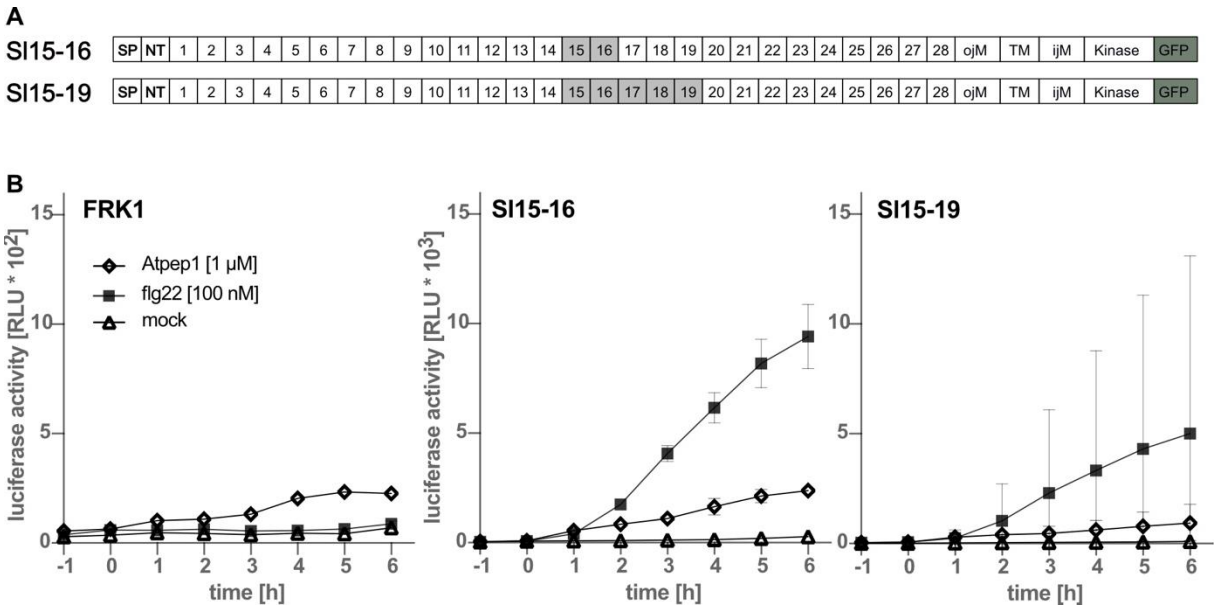

Figure 4.4.4 Sl15-16 and Sl15-19 do not induce AtBAK1-dependent autoactivation

A) schematic view of hybrid FLS2 receptors. B) Induction of pFRK1::Luciferase activity. Cells from *efr* x *fls2 A. thaliana* were co-transformed with *pFRK1::Luciferase* and *Sl15-16 or Sl15-19*. Treatments were done at t = 0, luciferase activity was measured for 6 hours after elicitor addition. Data points and error bars show the mean and SD of 3 replicates. The data shown represents for 3 independent experiments.

4.4.3 Sl16-24, Sl17-24 and Sl18-24 hybrids show Sl15-24-like AtBAK1-dependent autoactivation

To define the parts of SlFLS2 that cause autoactivity when introduced in AtFLS2, we generated and tested more chimeric FLS2 receptors, with different ranges of LRRs from SlFLS2 introduced into AtFLS2 (Figure 4.4.5A). For example, in *A. thaliana* protoplasts from *efr* x *fls2* plants with functional AtBAK1the chimeric receptors *Sl16-24*, *Sl17-24* or *Sl18-24* exhibited constitutively elevated levels of the luciferase reporter activity (Figure 4.4.5B) but showed an additional small response to flg22. However, compared to the response in cells lacking AtBAK1this additional flg22-dependent induction was marginal. Autoactivity of these chimeras was reproducible and also evident when monitored during the first hours after transformation (Supp. 7). However, *Sl16-24* and *Sl17-24* caused a stronger induction over this period than *Sl18-24*, indicating that shortening the domain originating from SlFLS2 might lead to a gradual reduction of autoactivity. Indeed, further shortening, as in the construct *Sl19-*

24, resulted in a functional FLS2 receptor that exhibited no signs of autoactivity (Figure 4.4.3B). In a second test with expression in *N. benthamiana* leaves, *Sl16-24*, *Sl17-24* or *Sl18-24*, but not *Sl19-24*, also showed high ROS production in the absence of ligand (Supp. 8). These results narrowed the ECD part required for Sl15-24-like autoactivation to the LRRs 18-24 from SlFLS2. In a further experiment, as expected, BIR2OX can suppress the autoactivation of Sl16-24, Sl17-24 or Sl18-24 (Supp. 9).

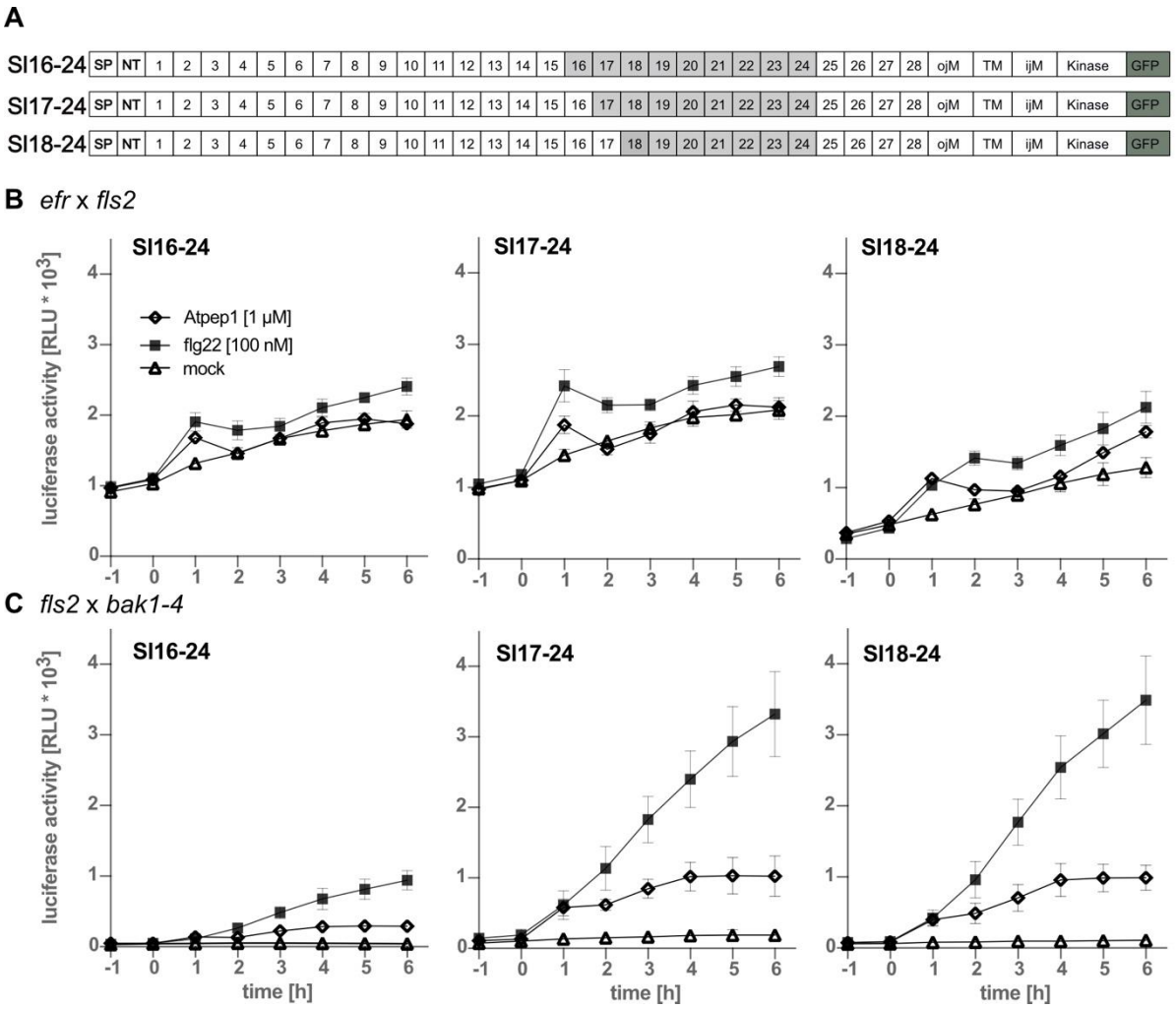

Figure 4.4.5 Sl16-24, Sl17-24 and Sl18-24 show Sl15-24-like AtBAK1-dependent autoactivation

A) schematic representation of hybrid FLS2 receptors. Induction of pFRK1::Luciferase activity in *A. thaliana* B) *efr* x *fls2* and C) *fls2* x *bak1-4*. Protoplast were co-transformed with *pFRK1::Luciferase* and *p35s::Sl16-24/17-24/18-24-GFP*. Data points and error bars show the mean and SD of 3 replicates. Data shown are representatives for three independent repetitions of the experiments.

4.4.4 LRR18-24 from SlFLS2 cannot be further shortened to induce autoactivity

Next, it was interesting to know whether all of the LRRs 18-24 originating from SlFLS2 contribute to the autoactivity of hybrid FLS2 receptors. For this we generated and tested a further series of chimeric receptors (Figure 4.4.6A, Supp. 10A). However, none of these constructs, including Sl18-24, Sl18-23, Sl18, Sl24 or Sl18&24, did show constitutive

induction of luciferase and all of these constructs restored responsiveness to flg22 treatment (Figure 4.4.6B, Supp. 10B). These data demonstrated that, rather than due to a single residue or a single LRR, several features in the LRRs 18-24 of SLFLS2 are required for the ligand-independent activation that occurs when embedded in the ECD of AtFLS2.

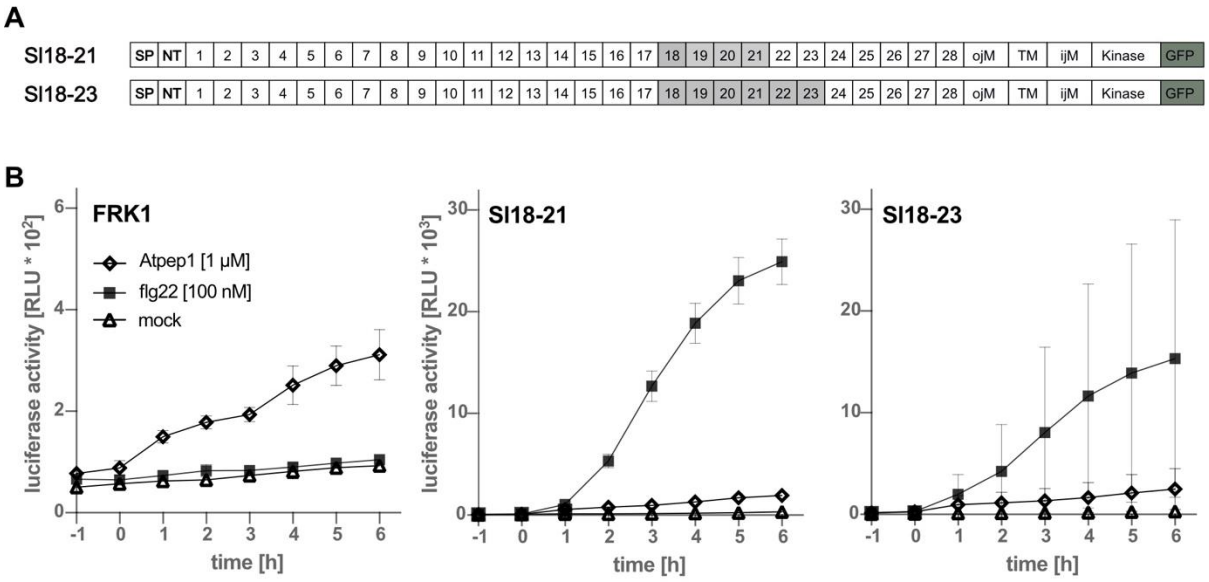

Figure 4.4.6 LRR18-21 and Sl18-23 do not induce autoactivation

A) schematic view of hybrid FLS2 receptors. B) Induction of pFRK1::Luciferase activity in cells of *Arabidopsis efr* x *fls2* mutant. Protoplasts were co-transformed with reporter gene *pFRK1::Luciferase* and *Sl18-21 or Sl18-23*. Data points and error bars show the mean and SD of 3 replicates. In another independent repetition, the same result was observed.

4.4.5 LRR7-14 from *A. thaliana* is essential for the AtBAK1-dependent autoactivation

As a following step, we investigated which LRRs from AtFLS2 were critical for the AtBAK1-dependent autoactivation of Sl15-24. To do this, LRRs in AtFLS2 were further replaced with LRRs of SlFLS2. Exchanging also the LRRs 1-6, as in the construct Sl1-6/15-24 (Figure 4.4.7A), did not prevent the autoactivity associated with the exchange of the LRRs 15-24 alone when expressed in protoplasts from *efr* x *fls2* (Figure 4.4.7B). As shown for Sl1-6/15-24, this autoactivation was dependent on the presence of AtBAK1 (Figure 4.4.7B), could be inhibited by co-expression of BIR2 (Supp. 11) and also occurred in *N. benthamiana* as

evident by the increase levels of ROS in the absence of the flg22 ligand (Supp. 12). However, the control chimeric construct Sl1-6 (Figure 4.4.7A), tested to exclude the possibility that LRRs 1-6 of SLFLS2 alone can lead to autoactivation, did not show any sign of autoactivity (Supp. 12) but restored flg22 responsiveness to cells lacking FLS2 (Figure 4.4.7B). From these results we concluded that for AtBAK1-dependent autoactivation, a combination of the LRRs 7-14 from AtFLS2 and the LRRs 18-24 of SlFLS2 is required.

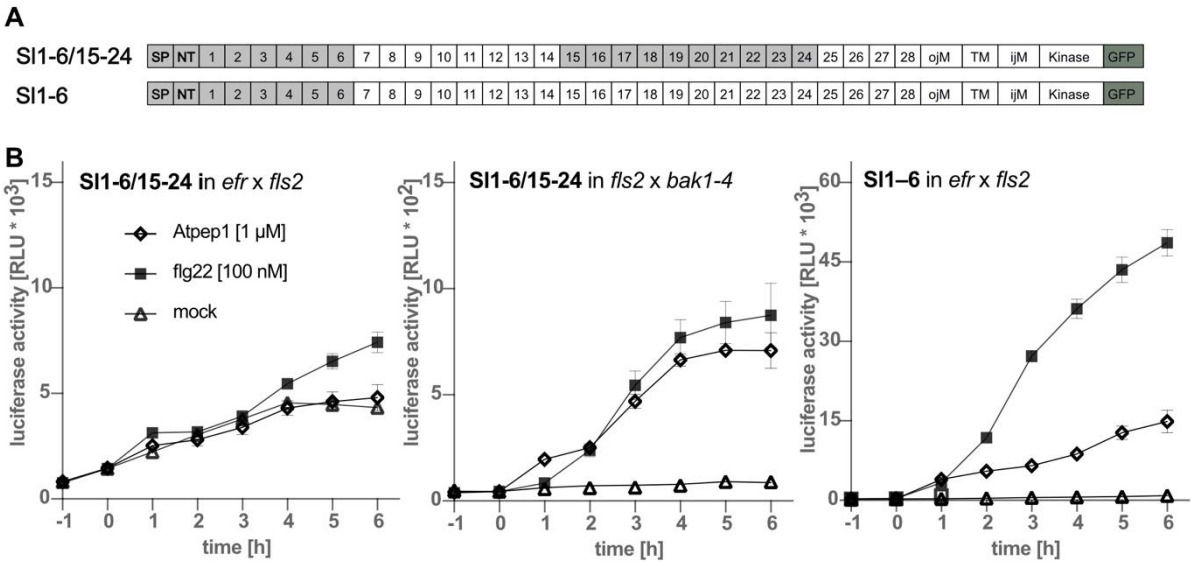

Figure 4.4.7 AtBAK1-dependent autoactivation occurs with LRRs 1-6 from AtFLS2 or SlFLS2 in combination of LRRs 15-24 from SlFLS2 in *A. thaliana*

A) schematic view of hybrid FLS2 receptors. B) Induction of pFRK1::Luciferase activity in *A. thaliana.* Protoplast were co-transformed with *pFRK1::Luciferase* and *p35s::hybrid FLS2-GFP*. Data points and error bars show the mean and SD of 3 replicates. Data shown represented for n = 2 independent experiments.

4.4.6 The reciprocal version of Sl15-24, At15-24, has a functional binding site for flg22 but does not induce response output

The particular combination of LRRs from AtFLS2 and SlFLS2 in Sl15-24 leads to ligand-independent but AtBAK1-dependent activation of signalling. We thus wondered about the

characteristics of the reciprocal swap with the LRR 15-24 from AtFLS2 embedded in the SlFLS2 (Figure 4.4.8A). When expressed in protoplasts from plant lacking FLS2 (*efr* x *fls2*), *At15-24* did not cause autoactivation and, strikingly, did not reconstitute flagellin perception (Figure 4.4.8B). These cells responded to Atpep1 treatment with increased luciferase activity, indicating successful transformation of the reporter gene. The cells also expressed At15-24, as confirmed by the presence of this protein on western blots (Figure 4.4.8 C).

As a next step, we were curious to know whether At15-24 harbours a functional flg22 binding site. For this, *At15-24* and *SlFLS2* as a positive control were expressed in *N. benthamiana* leaf tissues were used in competitive binding assays with acridium-labelled-flg22 (acri-flg22) and unlabelled flg22 or the unrelated control peptide Atpep1, respectively (Figure 4.4.8 D). Total binding of acri-flg22 to the preparations from leaves expressing either construct were at least three times higher than in control leaves transformed only with no FLS2 construct (P19 control), indicating that binding by endogenous NbFLS2 reaches only marginal values. The binding of acri-flg22 to the preparations with At15-24 and SlFLS2 was not competed by an excess of the unrelated peptide Atpep1 but by an excess of unlabelled flg22, demonstrating specific flg22 binding for At15-24 as for SlFLS2. Thus, despite binding of flg22 (and flg15), At15-24 cannot activate downstream signalling and induction of the reporter luciferase. This might be explained by a failure to get activated by AtBAK1 (or the other SERKs). In further studies it will be interesting to see whether (and how) the combination of LRRs from AtFLS2 and SlFLS2 in At15-24 prevents activation by AtBAK1 while the reciprocal combination in Sl15-24 leads to constitutive activation by AtBAK1.

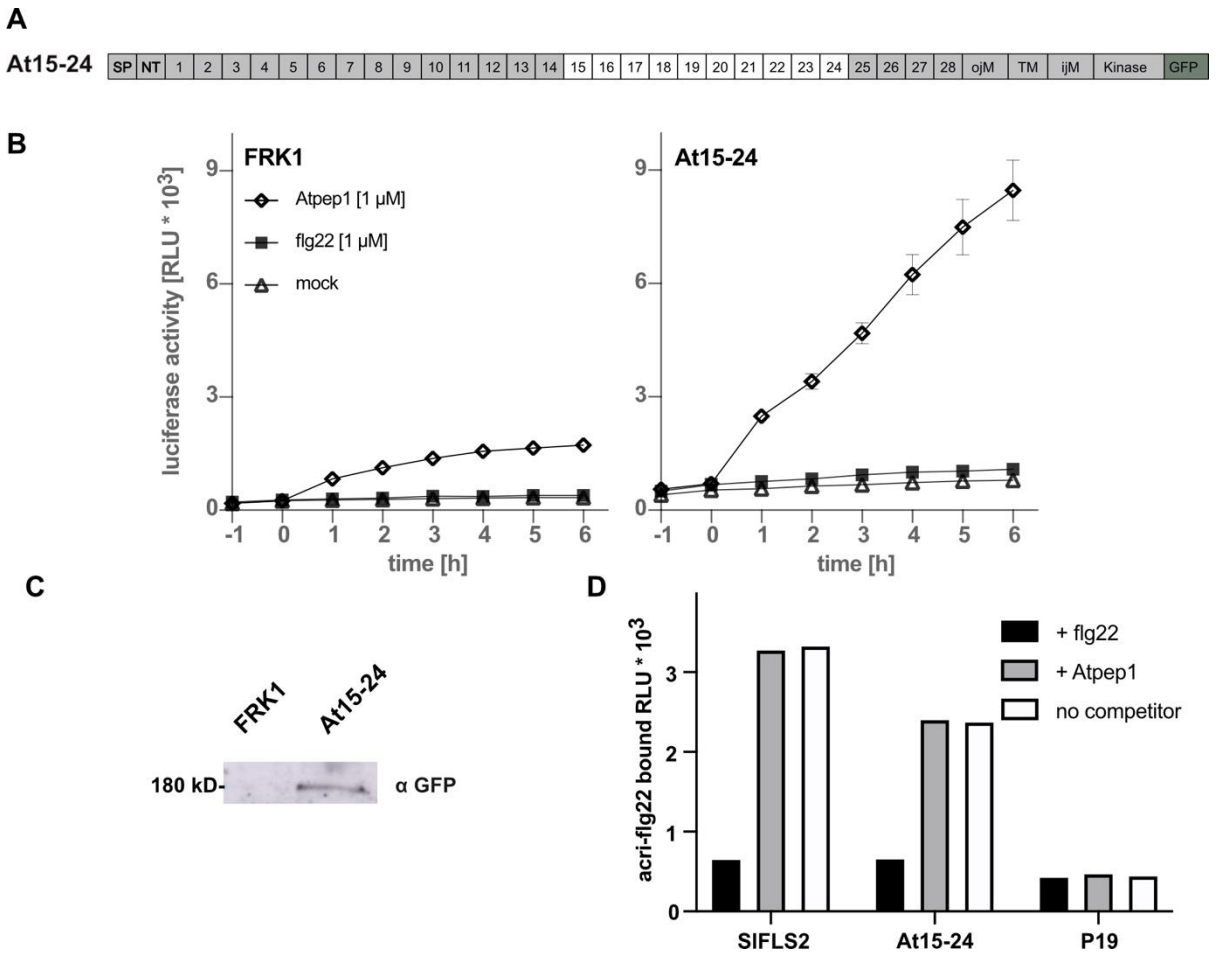

Figure 4.4.8 At15-24 has a functional ligand-binding site but does not induce downstream signalling

A) schematic representation of At15-24. B) Protoplasts from *efr* x *fls2 Arabidopsis* were co-transformed with reporter construct *pFRK1::Luciferase* or reporter construct and *p35s::At15-24-GFP*. Data points and error bars show the mean and SD of 3 replicates. C) western blot of protein expression analysis of protoplasts developed with anti-GFP antibodies. D) acridium-labelled-flg22 binding assay with cell debris of *N. benthamiana* leaf expressing SlFLS2, At15-24 or only P19. 10 nM of acri-flg22 were used for binding and 10 µM of unlabelled-flg22 as competitor, 10 µM of Atpep1 were used as an unspecific competitor. Each bar shows the integral over the first 10 s of light emission. Only one replicate was use for the binding assay, but 3 independent experiments were performed, and similar results were obtained.

4.4.7 Mapping reveals that the LRRs 7-14 from AtFLS2 and LRRs 18-24 from SlFLS2 are essential for the ligand-independent autoactivation

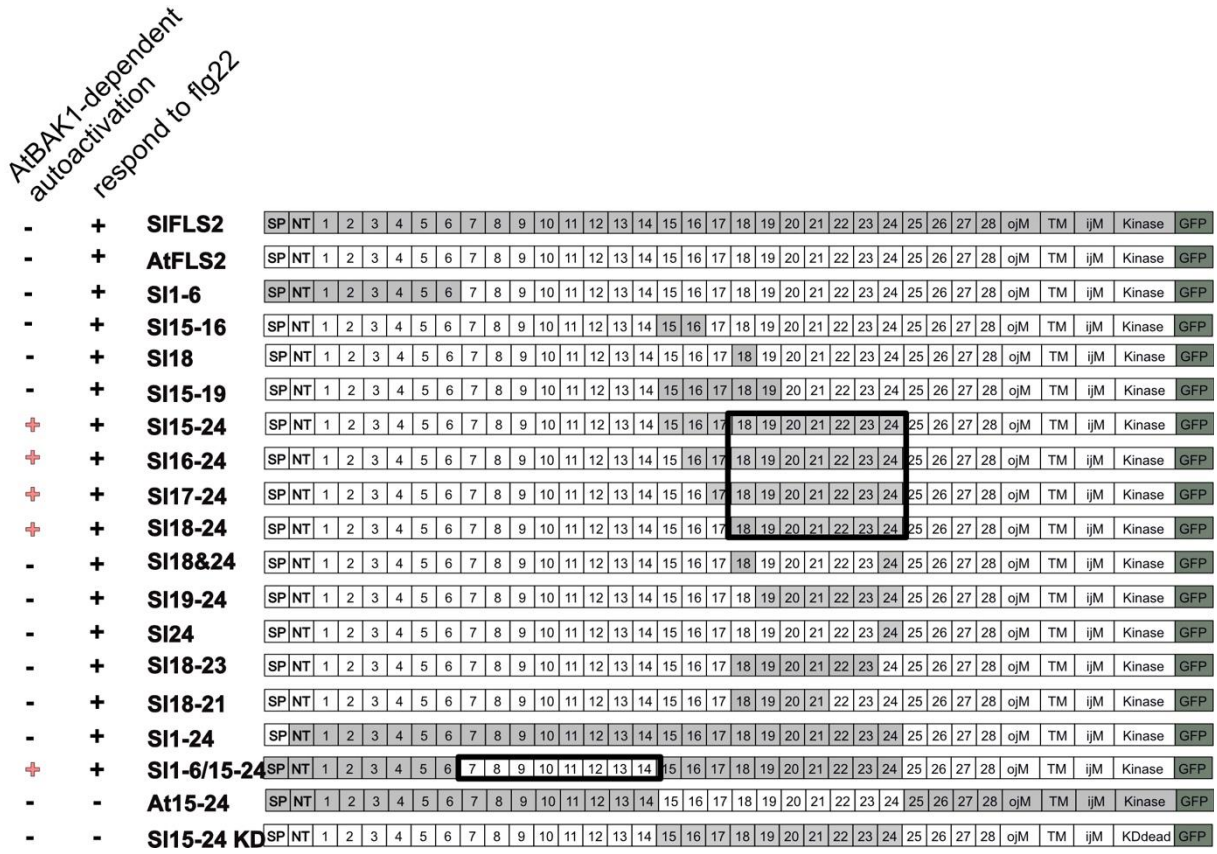

Figure 4.4.9 Schematic view of chimeric FLS2 receptors

Domain swapping scheme of FLS2 receptors. Gray boxes stand for portion from SlFLS2 and white boxes stand for AtFLS2. The important LRRs 18-24 from SlFLS2 and 7-14 AtFLS2 were squared in bold black line.

To summarise our mapping (Figure 4.4.9), we narrowed down the regions needed for flg22-independent but AtBAK1-dependent activation of chimeric FLS2 receptor to the combination of AtFLS2 LRRs 7-14 and SlFLS2 LRRs 18-24. The autoactive chimeras including Sl15-24, Sl16-24, Sl17-24, Sl18-24 and Sl1-6/15-24 all exhibited AtBAK1-dependent autoactivity when expressed in *A. thaliana* protoplasts, and this autoactivity can be suppressed by BIR2OX, also ROS production in *N. benthamiana* leaf tissue expressing these constructs was elevated without stimulus.

5 General Discussion and Conclusion

5.1 Is there direct interaction of Sl15-24 and AtBAK1 in the absence of ligand?

In this work, we started out from the observation that the ligand-independent activation of Sl15-24 depends strictly on the presence of functional AtBAK1. This led to the hypothesis that, much like in the process of ligand-dependent activation of AtFLS2, Sl15-24 gets activated by direct interaction with AtBAK1 in the absence of ligand. Reciprocal exchange of the kinase domains of AtBAK1 and AtFLS2 has previously been used to demonstrate that the flg22-dependent signal output indeed requires the formation of a heteromeric complex between AtFLS2 and AtBAK1 (Albert et al., 2013b). Similarly, swapping the cytoplasmic kinase domains between Sl15-24 and AtBAK1, resulted in ligand-independent activation, but only when both chimeric partners were concomitantly present in the cells (Figure 4.3.1). These findings further suggest a direct interaction between Sl15-24 and AtBAK1.

Flg22 binding to AtFLS2 leads to rapid formation of a heteromeric complex with the co-receptor AtBAK1, a complex that is stable throughout procedures of membrane solubilization and immunoprecipitation (Chinchilla et al., 2007). However, in many attempts, we could not detect a complex of similar stability between Sl15-24 and AtBAK1 in the absence of flg22. In the following two possible explanations are discussed that may explain the failure to detect a Sl15-24/AtBAK1 complex.

A first possibility is that stable interaction does occur but involves only a minor subfraction of the Sl15-24 present. A small subfraction might be difficult to detect in assays performed but sufficient to result in the autoimmune effects observed. Indeed, a full response output of FLS2 was reported in tomato cells under conditions where only a small percentage (< 5 %) of the FLS2 receptors present were occupied by the flg22 ligand (Meindl et al., 2000). Similarly, in a case study with mathematical modelling of root growth inhibition by BRI1, it was predicted that the endogenous level of BL activates only 1 % of BRI1 and a saturated response output required approximately 5 % of active BRI1 (Bücherl et al., 2013, van Esse et al., 2012). These two studies suggested the presence of functional “spare receptors” that increase the sensitivity of the perception systems. Furthermore, these results indicate that maximal signal output is limited by a “bottleneck” downstream of ligand binding receptor sites. Thus, it is still

conceivable that a minority of the Sl15-24 forms a stable complex with AtBAK1 and causes a persistent activation of immune responses. However, how could such a subfraction originate? Is there a random process leading to misfolding a small fraction of either Sl15-24 or AtBAK1 that allows for this specific interaction? Or is there an additional, limited, plant component that specifically glues together Sl15-24 and AtBAK1 as a substitute ligand? At present, we cannot rule out completely the "minor fraction hypothesis". However, our experiments did not provide any evidence to support this hypothesis. Rather, our results indicate that the majority of Sl15-24 behaves different from SlFLS2 and AtFLS2 in the presence of AtBAK1.

A second possibility is that ligand-independent interaction of Sl15-24 and AtBAK1 occurs but in a much less stable manner than in ligand-induced complex formation of AtFLS2 and AtBAK1. In the ligand activation process, the binding of the ECD of AtBAK1 to the ECD of AtFLS2 brings the two cytoplasmic KDs in close contact, thus allowing transphosphorylation and activation of downstream signalling. So far, however, the physiological role of forming a stable complex for signal transduction is not clear since kinase activation by transphosphorylation may proceed very quickly. The stability of the complex could, contrarily, rather serve as a signal for inactivation of the immune activation by internalisation of the complex (Silke et al., 2006). Thus, even a very weak and transient interaction of AtBAK1 with Sl15-24 might activate immune responses, since the receptors and co-receptors likely aren't recycled as usual, the transient activation could occur repeatedly.

Physiological and structural analysis have demonstrated that flg22 binds to AtFLS2 as a first step that forms a new surface to which AtBAK1 then binds as a second step in receptor activation (Sun et al., 2013a). Such an activation process implies that AtBAK1 must continually probe AtFLS2 for the presence or absence of a bound ligand. We propose a model whereby AtBAK11 scans FLS2 by approaching it via an "entry" domain and leaving it via an "exit" domain (Figure 5.1.1B). In this scanning process the co-receptor gets close to the receptor, but the interaction is transient and not sufficient to activate cytoplasmic signalling. Once the flg22 ligand binds to FLS2 receptor, it stops AtBAK1 from leaving which prolongs the scanning time of AtBAK1 on FLS2, finally leads to transphosphorylation and receptor activation (Figure 5.1.1C). While functioning according to the same mechanism, AtFLS2 and SlFLS2 might differ with respect to whether the speed of scanning is limited more at the "entry" or the "exit" domain. The combination of the LRRs 7-11 from AtFLS2 and the LRRs 18-24 from SlFLS2 in the autoactive FLS2 receptors might thus represent an inadvertent combination of "entry" and "exit" domains that both allow only for slow scanning by

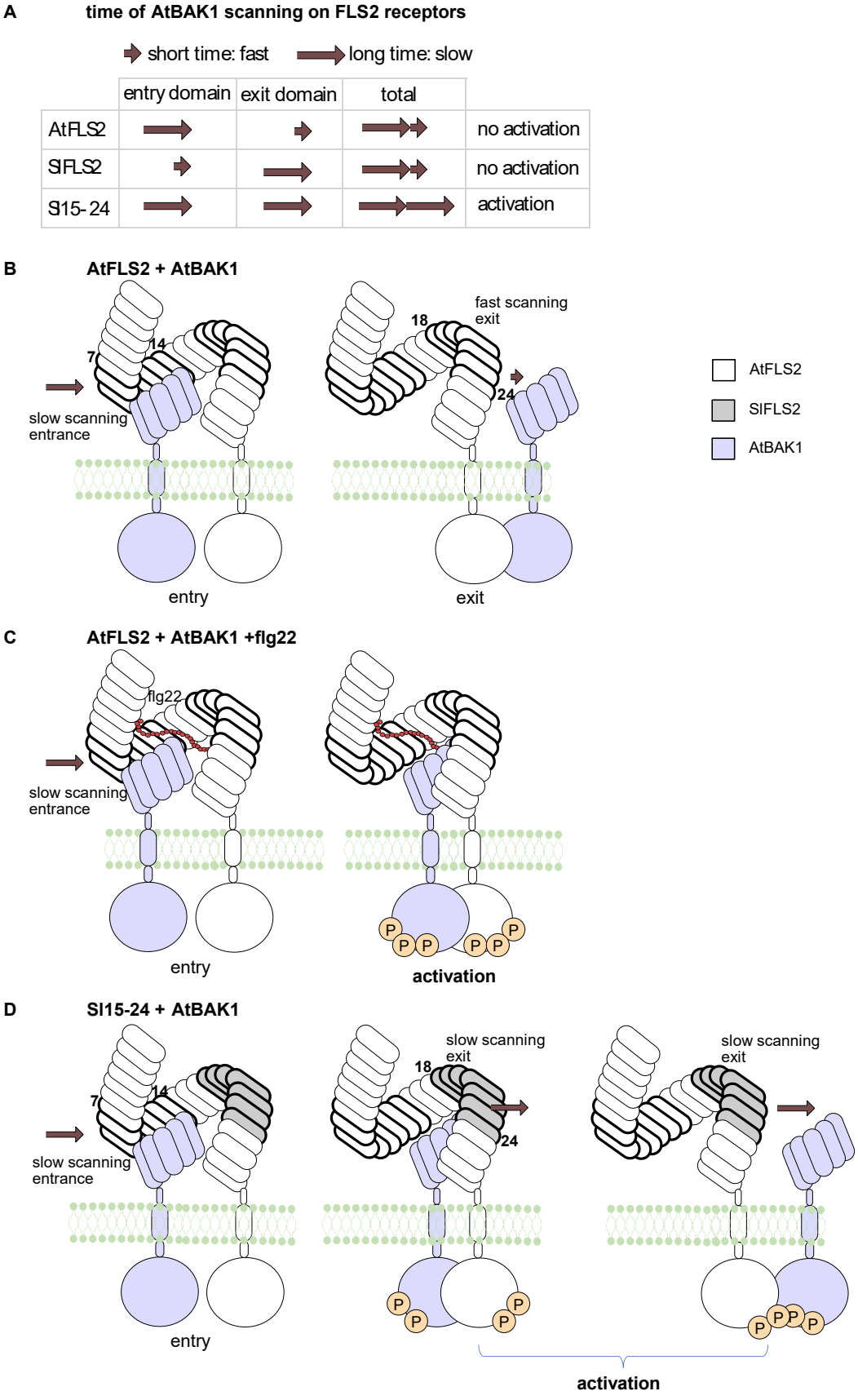

Figure 5.1.1 Hypothetical model for a scanning mechanism of SERK co-receptors on FLS2

In adapted receptor/co-receptor systems SERK co-receptors like AtBAK1 probe for the presence of the flg22 ligand on the LRR domain of FLS2 by approaching the receptor and scanning through an "entry" domain, for instance, represented by the LRRs7-14, and, in the absence of ligand, leaving FLS2 through an "exit" domain, represented by the LRRs 18-24 of Sl15-24. A) table of time length AtBAK1 needs to scan FLS2, represented with arrows. B) In the absence of ligand, the interaction time of the SERK with AtFLS2 or SlFLS2 is not sufficient for receptor activation. AtFLS2 and SlFLS2 might differ with respect to the speed of scanning, one with rate limiting scanning of the entry site, the other on the exit site, respectively. C) In the presence of the flg22 ligand, AtBAK1 gets stopped by sticking tightly to the ligand and LRRs 18-20 and LRRs 23-26 of AtFLS2. This brings the cytoplasmic kinase domains in close proximity and allows for the intracellular transphosphorylation necessary for activation of signal output. D) Swaps of the corresponding domains, such as in the chimeric receptor Sl15-24, might thus combine two domains that can get scanned by AtBAK1 only slowly. This slowdown might allow for sufficient length of interaction between AtBAK1 and Sl15-24 to activate cytoplasmic signalling.

AtBAK1, thus leading to a significantly longer interaction of the co-receptor with the idle receptor (Figure 5.1.1A & D). This longer interaction period might be sufficient for activation of chimeric FLS2 receptors by AtBAK1 without stable interaction.

Moreover, according to the scanning hypothesis, the reciprocal chimera At15-24 binds flg22 like SlFLS2 but shows no functional signal output could mean that in this chimera, an inefficient entry domain got combined with an inefficient exit domain, thus abolishing functional interaction even in the presence of ligand on the receptor.

Besides, the preferential interaction of AtFLS2 with AtBAK1 over the other SERKs might also be explained by a scanning model with the different SERKs exhibiting different affinities for the "entry" or "exit" domains. In cells lacking AtBAK1, the Sl15-24 chimera resembles functional AtFLS2 in ligand binding activities and low sensitivity. The total scanning time of the other AtSERKs on Sl15-24 or AtBAK1 is shorter than AtBAK1 which might be insufficient to activate cytoplasmic signalling.

In summary, we propose a scanning model which explains the dynamic interaction of AtFLS2 and AtBAK1 including the new findings based on AtFLS2 and SlFLS2 chimeras. Notably, this model accounts for the fact the LRRs 15-24 from SlFLS2 do not provoke activation by AtBAK1 in the context of their native protein. For spontaneous activation to occur, rather, LRRs 15-24 from SlFLS2 must be combined with LRRs from AtFLS2. This evidence

strongly indicates that AtBAK1 interacts somehow with the LRRs 7-14 of AtFLS2 in addition to the LRRs 18-20 and LRRs 23-26 where AtBAK1 stably interacts in the ligand-activated complex, as nicely shown by the crystallographic analysis of Sun et al. (2013a).

6 References

ALBERT, I., BOHM, H., ALBERT, M., FEILER, C. E., IMKAMPE, J., WALLMEROTH, N., BRANCATO, C., RAAYMAKERS, T. M., OOME, S., ZHANG, H. Q., KROL, E., GREFEN, C., GUST, A. A., CHAI, J. J., HEDRICH, R., VAN DEN ACKERVEKEN, G. & NURNBERGER, T. 2015. An RLP23-SOBIR1-BAK1 complex mediates NLP-triggered immunity. *Nature Plants,* 1.

ALBERT, I., HUA, C., NURNBERGER, T., PRUITT, R. N. & ZHANG, L. 2020. Surface Sensor Systems in Plant Immunity. *Plant Physiol,* 182**,** 1582-1596.

ALBERT, M., JEHLE, A. K., FURST, U., CHINCHILLA, D., BOLLER, T. & FELIX, G. 2013a. A Two-Hybrid-Receptor Assay Demonstrates Heteromer Formation as Switch-On for Plant Immune Receptors. *Plant Physiology,* 163**,** 1504-1509.

ALBERT, M., JEHLE, A. K., FÜRST, U., CHINCHILLA, D., BOLLER, T. & FELIX, G. 2013b. A two-hybrid-receptor assay demonstrates heteromer formation as switch-on for plant immune receptors. *Plant Physiology,* 163**,** 1504-1509.

ALBERT, M., JEHLE, A. K., LIPSCHIS, M., MUELLER, K., ZENG, Y. & FELIX, G. 2010a. Regulation of cell behaviour by plant receptor kinases: Pattern recognition receptors as prototypical models. *European Journal of Cell Biology,* 89**,** 200-207.

ALBERT, M., JEHLE, A. K., MUELLER, K., EISELE, C., LIPSCHIS, M. & FELIX, G. 2010b. Arabidopsis thaliana pattern recognition receptors for bacterial elongation factor tu and flagellin can be combined to form functional chimeric receptors. *Journal of Biological Chemistry,* 285**,** 19035-19042.

APEL, K. & HIRT, H. 2004. REACTIVE OXYGEN SPECIES: Metabolism, Oxidative Stress, and Signal Transduction. *Annual Review of Plant Biology,* 55**,** 373-399.

ASAI, T., TENA, G., PLOTNIKOVA, J., WILLMANN, M. R., CHIU, W. L., GOMEZ-GOMEZ, L., BOLLER, T., AUSUBEL, F. M. & SHEEN, J. 2002. MAP kinase signalling cascade in Arabidopsis innate immunity. *Nature,* 415**,** 977-83.

BAR, M., SHARFMAN, M., RON, M. & AVNI, A. 2010. BAK1 is required for the attenuation of ethylene-inducing xylanase (Eix)-induced defense responses by the decoy receptor LeEix1. *Plant Journal,* 63**,** 791-800.

BAUER, Z., GÓMEZ-GÓMEZ, L., BOLLER, T. & FELIX, G. 2001. Sensitivity of Different Ecotypes and Mutants of Arabidopsis thaliana toward the Bacterial Elicitor Flagellin Correlates with the Presence of Receptor-binding Sites. *Journal of Biological Chemistry,* 276**,** 45669-45676.

BINDER, A., LAMBERT, J., MORBITZER, R., POPP, C., OTT, T., LAHAYE, T. & PARNISKE, M. 2014. A modular plasmid assembly kit for multigene expression, gene silencing and silencing rescue in plants. *PLoS ONE,* 9.

BITTEL, P. 2010. Innate immunity mediated by the flagellin receptor FLS2 in Arabidopsis and tomato : A molecular approach to characterize ligand binding and function , using receptor chimeras.

BLAUM, B. S., MAZZOTTA, S., NOLDEKE, E. R., HALTER, T., MADLUNG, J., KEMMERLING, B. & STEHLE, T. 2014. Structure of the pseudokinase domain of BIR2, a regulator of BAK1-mediated immune signaling in Arabidopsis. *J Struct Biol,* 186**,** 112-21.

BOHM, H., ALBERT, I., FAN, L., REINHARD, A. & NURNBERGER, T. 2014. Immune receptor complexes at the plant cell surface. *Current Opinion in Plant Biology,* 20**,** 47-54.

BOLLER, T. & FELIX, G. 2009. A Renaissance of Elicitors: Perception of Microbe-Associated Molecular Patterns and Danger Signals by Pattern-Recognition Receptors. *Annual Review of Plant Biology,* 60**,** 379-406.

BRUTUS, A., SICILIA, F., MACONE, A., CERVONE, F. & DE LORENZO, G. 2010. A domain swap approach reveals a role of the plant wall-associated kinase 1 (WAK1) as a receptor of oligogalacturonides. *Proceedings of the National Academy of Sciences of the United States of America,* 107**,** 9452-9457.

BÜCHERL, C. A., ESSE, G. W. V., KRUIS, A., LUCHTENBERG, J., WESTPHAL, A. H., AKER, J., HOEK, A. V., ALBRECHT, C., BORST, J. W., VRIES, S. C. D., E, G. W. & V, S. C. 2013. Visualization of BRI1 and BAK1 (SERK3) Membrane Receptor Heterooligomers during. *Plant physiology,* 162**,** 1911-1925.

CAO, Y. R., LIANG, Y., TANAKA, K., NGUYEN, C. T., JEDRZEJCZAK, R. P., JOACHIMIAK, A. & STACEY, G. 2014. The kinase LYK5 is a major chitin receptor in Arabidopsis and forms a chitin-induced complex with related kinase CERK1. *Elife,* 3.

CHEN, H., ZOU, Y., SHANG, Y., LIN, H., WANG, Y., CAI, R., TANG, X. & ZHOU, J. M. 2008. Firefly luciferase complementation imaging assay for protein-protein interactions in plants. *Plant Physiol,* 146**,** 368-76.

CHINCHILLA, D., BAUER, Z., REGENASS, M., BOLLER, T. & FELIX, G. 2006. The Arabidopsis receptor kinase FLS2 binds flg22 and determines the specificity of flagellin perception. *Plant Cell,* 18**,** 465-476.

CHINCHILLA, D., SHAN, L., HE, P., DE VRIES, S. & KEMMERLING, B. 2009. One for all: the receptor-associated kinase BAK1. *Trends in Plant Science,* 14**,** 535-541.

CHINCHILLA, D., ZIPFEL, C., ROBATZEK, S., KEMMERLING, B., NÜRNBERGER, T., JONES, J. D. G., FELIX, G. & BOLLER, T. 2007. A flagellin-induced complex of the receptor FLS2 and BAK1 initiates plant defence. *Nature,* 448**,** 497-500.

COUTO, D. & ZIPFEL, C. 2016. Regulation of pattern recognition receptor signalling in plants. *Nature Reviews Immunology,* 16**,** 537-552.

CUI, H., TSUDA, K. & PARKER, J. E. 2015. Effector-Triggered Immunity: From Pathogen Perception to Robust Defense. *Annual Review of Plant Biology,* 66**,** 487-511.

DANGL, J. L., HORVATH, D. M. & STASKAWICH, B. J. 2013. Pivoting the Plant Immune System. *Science,* 341**,** 745-751.

DEGER, A. G., SCHERZER, S., NUHKAT, M., KEDZIERSKA, J., KOLLIST, H., BROSCHE, M., UNYAYAR, S., BOUDSOCQ, M., HEDRICH, R. & ROELFSEMA, M. R. G. 2015. Guard cell SLAC1-type anion channels mediate flagellin-induced stomatal closure. *New Phytologist,* 208**,** 162-173.

DOMÍNGUEZ-FERRERAS, A., KISS-PAPP, M., JEHLE, A. K., FELIX, G. & CHINCHILLA, D. 2015. An overdose of the arabidopsis coreceptor BRASSINOSTEROID INSENSITIVE1-ASSOCIATED RECEPTOR KINASE1 or its ectodomain causes autoimmunity in a SUPPRESSOR OF BIR1-1-dependent manner. *Plant Physiology,* 168**,** 1106-1121.

DUNNING, F. M., SUN, W., JANSEN, K. L., HELFT, L. & BENT, A. F. 2007. Identification and mutational analysis of Arabidopsis FLS2 leucine-rich repeat domain residues that contribute to flagellin perception. *Plant Cell,* 19**,** 3297-3313.

FELIX, G., DURAN, J. D., VOLKO, S. & BOLLER, T. 1999. Plants have a sensitive perception system for the most conserved domain of bacterial flagellin. *Plant Journal,* 18**,** 265-276.

FUERST, U., ZENG, Y., ALBERT, M., WITTE, A. K., FLIEGMANN, J. & FELIX, G. 2020. Perception of Agrobacterium tumefaciens flagellin by FLS2(XL) confers resistance to crown gall disease. *Nature Plants,* 6**,** 22-+.

GAO, M., WANG, X., WANG, D., XU, F., DING, X., ZHANG, Z., BI, D., CHENG, Y. T., CHEN, S., LI, X. & ZHANG, Y. 2009. Regulation of cell death and innate immunity by two receptor-like kinases in Arabidopsis. *Cell Host Microbe,* 6**,** 34-44.

GÓMEZ-GÓMEZ, L., BAUER, Z., BOLLER, T., THE, S., CELL, P., MAY, N., GMEZ-GMEZ, L., BAUER, Z. & BOLLERAB, T. 2001. Both the Extracellular Leucine-Rich Repeat Domain and the Kinase Activity of FLS2 Are Required for Flagellin Binding and Signaling in Arabidopsis *Plant Cell,* 13**,** 1155-1163.

GÓMEZ-GÓMEZ, L. & BOLLER, T. 2000. FLS2: An LRR receptor-like kinase involved in the perception of the bacterial elicitor flagellin in Arabidopsis. *Molecular Cell,* 5**,** 1003-1011.

GOU, X., YIN, H., HE, K., DU, J., YI, J., XU, S., LIN, H., CLOUSE, S. D. & LI, J. 2012. Genetic evidence for an indispensable role of somatic embryogenesis receptor kinases in brassinosteroid signaling. *PLoS Genet,* 8**,** e1002452.

GOU, X. P. & LI, J. 2020. Paired Receptor and Coreceptor Kinases Perceive Extracellular Signals to Control Plant Development(1)([OPEN]). *Plant Physiology,* 182**,** 1667-1681.

GUST, A. A., BISWAS, R., LENZ, H. D., RAUHUT, T., RANF, S., KEMMERLING, B., GOTZ, F., GLAWISCHNIG, E., LEE, J., FELIX, G. & NURNBERGER, T. 2007. Bacteria-derived peptidoglycans constitute pathogen-associated molecular patterns triggering innate immunity in Arabidopsis. *Journal of Biological Chemistry,* 282**,** 32338-32348.

GUST, A. A. & FELIX, G. 2014. Receptor like proteins associate with SOBIR1-type of adaptors to form bimolecular receptor kinases. *Current Opinion in Plant Biology,* 21**,** 104-111.

HALTER, T., IMKAMPE, J., BLAUM, B. S., STEHLE, T. & KEMMERLING, B. 2014a. BIR2 affects complex formation of BAK1 with ligand binding receptors in plant defense. *Plant Signal Behav,* 9.

HALTER, T., IMKAMPE, J., MAZZOTTA, S., WIERZBA, M., POSTEL, S., BUCHERL, C., KIEFER, C., STAHL, M., CHINCHILLA, D., WANG, X., NURNBERGER, T., ZIPFEL, C., CLOUSE, S., BORST, J. W., BOEREN, S., DE VRIES, S. C., TAX, F. & KEMMERLING, B. 2014b. The leucine-rich repeat receptor kinase BIR2 is a negative regulator of BAK1 in plant immunity. *Curr Biol,* 24**,** 134-143.

HAWEKER, H., RIPS, S., KOIWA, H., SALOMON, S., SAIJO, Y., CHINCHILLA, D., ROBATZEK, S. & VON SCHAEWEN, A. 2010. Pattern Recognition Receptors Require N-Glycosylation to Mediate Plant Immunity. *Journal of Biological Chemistry,* 285**,** 4629-4636.

HAYAFUNE, M., BERISIO, R., MARCHETTI, R., SILIPO, A., KAYAMA, M., DESAKI, Y., ARIMA, S., SQUEGLIA, F., RUGGIERO, A., TOKUYASU, K., MOLINARO, A., KAKU, H. & SHIBUYA, N. 2014. Chitin-induced activation of immune signaling by the rice receptor CEBiP relies on a unique sandwich-type dimerization. *Proceedings of the National Academy of Sciences of the United States of America,* 111**,** E404-E413.

HE, K., GOU, X., YUAN, T., LIN, H., ASAMI, T., YOSHIDA, S., RUSSELL, S. D. & LI, J. 2007. BAK1 and BKK1 regulate brassinosteroid-dependent growth and brassinosteroid-independent cell-death pathways. *Curr Biol,* 17**,** 1109-15.

HE, Z. H., WANG, Z. Y., LI, J. M., ZHU, Q., LAMB, C., RONALD, P. & CHORY, J. 2000. Perception of brassinosteroids by the extracellular domain of the receptor kinase BRI1. *Science,* 288**,** 2360-2363.

HECHT, V., VIELLE-CALZADA, J. P., HARTOG, M. V., SCHMIDT, E. D. L., BOUTILIER, K., GROSSNIKLAUS, U. & DE VRIES, S. C. 2001. The Arabidopsis SOMATIC EMBRYOGENESIS RECEPTOR KINASE 1 gene is expressed in developing ovules and embryos and enhances embryogenic competence in culture. *Plant Physiology,* 127**,** 803-816.

HOHMANN, U., RAMAKRISHNA, P., WANG, K., LORENZO-ORTS, L., NICOLET, J., HENSCHEN, A., BARBERON, M., BAYER, M. & HOTHORN, M. 2020. Constitutive Activation of Leucine-Rich Repeat Receptor Kinase Signaling Pathways by BAK1-INTERACTING RECEPTOR-LIKE KINASE3 Chimera([OPEN]). *Plant Cell,* 32**,** 3311-3323.

HUFFAKER, A., PEARCE, G. & RYAN, C. A. 2006. An endogenous peptide signal in Arabidopsis activates components of the innate immune response. *Proceedings of the National Academy of Sciences of the United States of America,* 103**,** 10098-10103.

IMKAMPE, J., HALTER, T., HUANG, S., SCHULZE, S., MAZZOTTA, S., SCHMIDT, N., MANSTRETTA, R., POSTEL, S., WIERZBA, M., YANG, Y., VAN DONGEN, W., STAHL, M., ZIPFEL, C., GOSHE, M. B., CLOUSE, S., DE VRIES, S. C., TAX, F., WANG, X. & KEMMERLING, B. 2017. The Arabidopsis Leucine-Rich Repeat Receptor Kinase BIR3 Negatively Regulates BAK1 Receptor Complex Formation and Stabilizes BAK1. *Plant Cell,* 29**,** 2285-2303.

IMPERIALI, B. & O'CONNOR, S. E. 1999. Effect of N-linked glycosylation on glycopeptide and glycoprotein structure. *Current Opinion in Chemical Biology,* 3**,** 643-649.

JEHLE, A. K., LIPSCHIS, M., ALBERT, M., FALLAHZADEH-MAMAGHANI, V., FÜRST, U., MUELLER, K. & FELIX, G. 2013. The receptor-like protein ReMAX of Arabidopsis detects the microbe-associated molecular pattern eMax from Xanthomonas. *Plant Cell,* 25**,** 2330-2340.

JEWORUTZKI, E., ROELFSEMA, M. R. G., ANSCHUTZ, U., KROL, E., ELZENGA, J. T. M., FELIX, G., BOLLER, T., HEDRICH, R. & BECKER, D. 2010a. Early signaling through the Arabidopsis pattern recognition receptors FLS2 and EFR involves Ca2+-associated opening of plasma membrane anion channels. *Plant Journal,* 62**,** 367-378.

JEWORUTZKI, E., ROELFSEMA, M. R. G., ANSCHÜTZ, U., KROL, E., ELZENGA, J. T. M., FELIX, G., BOLLER, T., HEDRICH, R. & BECKER, D. 2010b. Early signaling through the arabidopsis pattern recognition receptors FLS2 and EFR involves Ca2+-associated opening of plasma membrane anion channels. *Plant Journal,* 62**,** 367-378.

JONES, J. & DANGL, J. 2006. The plant immune system. *Nature,* 444**,** 323-329.

KAKU, H., NISHIZAWA, Y., ISHII-MINAMI, N., AKIMOTO-TOMIYAMA, C., DOHMAE, N., TAKIO, K., MINAMI, E. & SHIBUYA, N. 2006. Plant cells recognize chitin fragments for defense signaling through a plasma membrane receptor. *Proceedings of the National Academy of Sciences of the United States of America,* 103**,** 11086-11091.

KEMMERLING, B., SCHWEDT, A., RODRIGUEZ, P., MAZZOTTA, S., FRANK, M., QAMAR, S. A., MENGISTE, T., BETSUYAKU, S., PARKER, J. E., MUSSIG, C., THOMMA, B. P., ALBRECHT, C., DE VRIES, S. C., HIRT, H. & NURNBERGER, T. 2007. The BRI1-associated kinase 1, BAK1, has a brassinolide-independent role in plant cell-death control. *Curr Biol,* 17**,** 1116-22.

KRUIJT, M., KIP, D. J., JOOSTEN, M. H. A. J., BRANDWAGT, B. F. & DE WIT, P. J. G. M. 2005. The Cf-4 and Cf-9 resistance genes against Cladosporium fulvum are conserved in wild tomato species. *Molecular Plant-Microbe Interactions,* 18**,** 1011-1021.

KUNZE, G., ZIPFEL, C., ROBATZEK, S., NIEHAUS, K., BOLLER, T. & FELIX, G. 2004. The N terminus of bacterial elongation factor Tu elicits innate immunity in Arabidopsis plants. *Plant Cell,* 16**,** 3496-507.

LEWIS, M. W., LESLIE, M. E., FULCHER, E. H., DARNIELLE, L., HEALY, P. N., YOUN, J. Y. & LILJEGREN, S. J. 2010. The SERK1 receptor-like kinase regulates organ separation in Arabidopsis flowers. *Plant Journal,* 62**,** 817-828.

LI, J., WEN, J., LEASE, K. A., DOKE, J. T., TAX, F. E. & WALKER, J. C. 2002. BAK1, an Arabidopsis LRR receptor-like protein kinase, interacts with BRI1 and modulates brassinosteroid signaling. *Cell,* 110**,** 213-222.

LI, L., LI, M., YU, L. P., ZHOU, Z. Y., LIANG, X. X., LIU, Z. X., CAI, G. H., GAO, L. Y., ZHANG, X. J., WANG, Y. C., CHEN, S. & ZHOU, J. M. 2014. The FLS2-Associated Kinase BIK1 Directly Phosphorylates the NADPH Oxidase RbohD to Control Plant Immunity. *Cell Host & Microbe,* 15**,** 329-338.

LIN, W. W., LI, B., LU, D. P., CHEN, S. X., ZHU, N., HE, P. & SHAN, L. B. 2014. Tyrosine phosphorylation of protein kinase complex BAK1/BIK1 mediates Arabidopsis innate immunity. *Proceedings of the National Academy of Sciences of the United States of America,* 111**,** 3632-3637.

LIU, H. T. & NAISMITH, J. H. 2008. An efficient one-step site-directed deletion, insertion, single and multiple-site plasmid mutagenesis protocol. *Bmc Biotechnology,* 8.

LIU, T. T., LIU, Z. X., SONG, C. J., HU, Y. F., HAN, Z. F., SHE, J., FAN, F. F., WANG, J. W., JIN, C. W., CHANG, J. B., ZHOU, J. M. & CHAI, J. J. 2012. Chitin-Induced Dimerization Activates a Plant Immune Receptor. *Science,* 336**,** 1160-1164.

LIU, Y., HUANG, X., LI, M., HE, P. & ZHANG, Y. 2016. Loss-of-function of Arabidopsis receptor-like kinase BIR1 activates cell death and defense responses mediated by BAK1 and SOBIR1. *New Phytologist,* 212**,** 637-645.

LOLLE, S., STEVENS, D. & COAKER, G. 2020. Plant NLR-triggered immunity: from receptor activation to downstream signaling. *Current Opinion in Immunology,* 62**,** 99-105.

LU, D. P., WU, S. J., GAO, X. Q., ZHANG, Y. L., SHAN, L. B. & HE, P. 2010. A receptor-like cytoplasmic kinase, BIK1, associates with a flagellin receptor complex to initiate plant innate immunity. *Proceedings of the National Academy of Sciences of the United States of America,* 107**,** 496-501.

LUKER, K. E., SMITH, M. C., LUKER, G. D., GAMMON, S. T., PIWNICA-WORMS, H. & PIWNICA-WORMS, D. 2004. Kinetics of regulated protein-protein interactions revealed with firefly luciferase complementation imaging in cells and living animals. *Proc Natl Acad Sci U S A,* 101**,** 12288-93.

LUNA, E., PASTOR, V., ROBERT, J., FLORS, V., MAUCH-MANI, B. & TON, J. 2011. Callose Deposition: A Multifaceted Plant Defense Response. *Molecular Plant-Microbe Interactions,* 24**,** 183-193.

MA, C., LIU, Y., BAI, B., HAN, Z., TANG, J., ZHANG, H., YAGHMAIEAN, H., ZHANG, Y. & CHAI, J. 2017. Structural basis for BIR1-mediated negative regulation of plant immunity. *Cell Res,* 27**,** 1521-1524.

MA, X., XU, G., HE, P. & SHAN, L. 2016. SERKing Coreceptors for Receptors. *Trends Plant Sci,* 21**,** 1017-1033.

MEINDL, T., BOLLER, T. & FELIX, G. 2000. The bacterial elicitor flagellin activates its receptor in tomato cells according to the address-message concept. *Plant Cell,* 12**,** 1783-1794.

MERSMANN, S., BOURDAIS, G., RIETZ, S. & ROBATZEK, S. 2010. Ethylene Signaling Regulates Accumulation of the FLS2 Receptor and Is Required for the Oxidative Burst Contributing to Plant Immunity. *Plant Physiology,* 154**,** 391-400.

MUELLER, K. 2011. Molecular characterization of the flg22-interaction with FLS2.

MUELLER, K., BITTEL, P., CHINCHILL, D., JEHLE, A. K., ALBERT, M., BOLLER, T. & FELIX, G. 2012. Chimeric FLS2 receptors reveal the basis for differential flagellin perception in arabidopsis and tomato. *Plant Cell,* 24**,** 2213-2224.

NAM, K. H. & LI, J. 2002. BRI1/BAK1, a receptor kinase pair mediating brassinosteroid signaling. *Cell,* 110**,** 203-212.

NEKRASOV, V., LI, J., BATOUX, M., ROUX, M., CHU, Z. H., LACOMBE, S., ROUGON, A., BITTEL, P., KISS-PAPP, M., CHINCHILLA, D., VAN ESSE, H. P., JORDA, L., SCHWESSINGER, B., NICAISE, V., THOMMA, B. P., MOLINA, A., JONES, J. D. & ZIPFEL, C. 2009. Control of the pattern-recognition receptor EFR by an ER protein complex in plant immunity. *EMBO J,* 28**,** 3428-38.

NGOU, B. P. M., AHN, H.-K., DING, P. & JONES, J. D. G. 2021. Mutual potentiation of plant immunity by cell-surface and intracellular receptors. *Nature*.

NOGUCHI, T., FUJIOKA, S., CHOE, S., TAKATSUTO, S., YOSHIDA, S., YUAN, H., FELDMANN, K. A. & TAX, F. E. 1999. Brassinosteroid-insensitive dwarf mutants of Arabidopsis accumulate brassinosteroids. *Plant Physiol,* 121**,** 743-52.

NÜHSE, T. S., PECK, S. C., HIRT, H. & BOLLER, T. 2000. Microbial elicitors induce activation and dual phosphorylation of the Arabidopsis thaliana MAPK 6. *Journal of Biological Chemistry,* 275**,** 7521-7526.

PENG, H. C. & KALOSHIAN, I. 2014. The Tomato Leucine-Rich Repeat Receptor-Like Kinases SlSERK3A and SlSERK3B Have Overlapping Functions in Bacterial and Nematode Innate Immunity. *Plos One,* 9.

PRUITT, R. N., LOCCI, F., WANKE, F., ZHANG, L. S., SAILE, S. C., JOE, A., KARELINA, D., HUA, C. L., FROHLICH, K., WAN, W. L., HU, M. J., RAO, S. F., STOLZE, S. C., HARZEN, A., GUST, A. A., HARTER, K., JOOSTEN, M. H. A. J., THOMMA, B. P. H. J., ZHOU, J. M., DANGL, J. L., WEIGEL, D., NAKAGAMI, H., OECKING, C., EL KASMI, F., PARKER, J. E. & NURNBERGER, T. 2021. The EDS1-PAD4-ADR1 node mediates Arabidopsis pattern-triggered immunity. *Nature,* 598**,** 495-+.

RANF, S., GRIMMER, J., POSCHL, Y., PECHER, P., CHINCHILLA, D., SCHEEL, D. & LEE, J. 2012. Defense-Related Calcium Signaling Mutants Uncovered via a Quantitative High-Throughput Screen in Arabidopsis thaliana. *Molecular Plant,* 5**,** 115-130.

ROBATZEK, S., BITTEL, P., CHINCHILLA, D., KÖCHNER, P., FELIX, G., SHIU, S. H. & BOLLER, T. 2007. Molecular identification and characterization of the tomato flagellin receptor LeFLS2, an orthologue of Arabidopsis FLS2 exhibiting characteristically different perception specificities. *Plant Molecular Biology,* 64**,** 539-547.

RON, M. & AVNI, A. 2004. The receptor for the fungal elicitor ethylene-inducing xylanase is a member of a resistance-like gene family in tomato. *Plant Cell,* 16**,** 1604-1615.

ROUX, M., SCHWESSINGER, B., ALBRECHT, C., CHINCHILLA, D., JONES, A., HOLTON, N., MALINOVSKY, F. G., TOR, M., DE VRIES, S. & ZIPFEL, C. 2011. The Arabidopsis Leucine-Rich Repeat Receptor-Like Kinases BAK1/SERK3 and BKK1/SERK4 Are Required for Innate Immunity to Hemibiotrophic and Biotrophic Pathogens. *Plant Cell,* 23**,** 2440-2455.

RUSSINOVA, E., BORST, J. W., KWAAITAAL, M., CANO-DELGADO, A., YIN, Y., CHORY, J. & DE VRIES, S. C. 2004. Heterodimerization and endocytosis of Arabidopsis brassinosteroid receptors BRI1 and AtSERK3 (BAK1). *Plant Cell,* 16**,** 3216-29.

SCHULZE, B., MENTZEL, T., JEHLE, A. K., MUELLER, K., BEELER, S., BOLLER, T., FELIX, G. & CHINCHILLA, D. 2010. Rapid heteromerization and phosphorylation of ligand-activated plant transmembrane receptors and their associated kinase BAK1. *Journal of Biological Chemistry,* 285**,** 9444-9451.

SCHWESSINGER, B., ROUX, M., KADOTA, Y., NTOUKAKIS, V., SKLENAR, J., JONES, A. & ZIPFEL, C. 2011. Phosphorylation-dependent differential regulation of plant growth, cell death, and innate immunity by the regulatory receptor-like kinase BAK1. *PLoS Genet,* 7**,** e1002046.

SCHWYZER, R. 1977. ACTH: a short introductory review. *Ann N Y Acad Sci,* 297**,** 3-26.

SHIU, S. H. & BLEECKER, A. B. 2001a. Plant receptor-like kinase gene family: diversity, function, and signaling. *Science's STKE : signal transduction knowledge environment,* 2001.

SHIU, S. H. & BLEECKER, A. B. 2001b. Plant receptor-like kinase gene family: diversity, function, and signaling. *Sci STKE,* 2001**,** re22.

SHIU, S. H. & BLEECKER, A. B. 2003. Expansion of the receptor-like kinase/Pelle gene family and receptor-like proteins in Arabidopsis. *Plant Physiology,* 132**,** 530-543.

SILKE, R., DELPHINE, C. & THOMAS, B. 2006. Ligand-induced endocytosis of the pattern recognition receptor FLS2 in Arabidopsis. *Genes & development*, 537-542.

SONG, W., FORDERER, A., YU, D. & CHAI, J. 2021. Structural biology of plant defence. *New Phytol*, 229, 692-711.

SUN, Y., LI, L., MACHO, A. P., HAN, Z., HU, Z., ZIPFEL, C., ZHOU, J. M. & CHAI, J. 2013a. Structural Basis for flg22-Induced Activation of the Arabidopsis FLS2-BAK1 Immune Complex Yadong. 342, 624-629.

SUN, Y. D., HAN, Z. F., TANG, J., HU, Z. H., CHAI, C. L., ZHOU, B. & CHAI, J. J. 2013b. Structure reveals that BAK1 as a co-receptor recognizes the BRI1-bound brassinolide. *Cell Research*, 23, 1326-1329.

TANG, J., HAN, Z., SUN, Y., ZHANG, H., GONG, X. & CHAI, J. 2015. Structural basis for recognition of an endogenous peptide by the plant receptor kinase PEPR1. *Cell Res*, 25, 110-20.

THOR, K. & PEITER, E. 2014. Cytosolic calcium signals elicited by the pathogen-associated molecular pattern flg22 in stomatal guard cells are of an oscillatory nature. *New Phytologist*, 204, 873-881.

VAN DER BURGH, A. M., POSTMA, J., ROBATZEK, S. & JOOSTEN, M. H. A. J. 2019. Kinase activity of SOBIR1 and BAK1 is required for immune signalling. *Molecular Plant Pathology*, 20, 410-422.

VAN DER HOORN, R. A. L., ROTH, R. & DE WIT, P. J. G. 2001. Identification of distinct specificity determinants in resistance protein Cf-4 allows construction of a Cf-9 mutant that confers recognition of avirulence protein AVR4. *Plant Cell*, 13, 273-285.

VAN DER HOORN, R. A. L., WULFF, B. B. H., RIVAS, S., DURRANT, M. C., VAN DER PLOEG, A., DE WIT, P. J. G. M. & JONES, J. D. G. 2005. Structure-function analysis of Cf-9, a receptor-like protein with extracytoplasmic leucine-rich repeats. *Plant Cell*, 17, 1000-1015.

VAN ESSE, G. W., VAN MOURIK, S., STIGTER, H., TEN HOVE, C. A., MOLENAAR, J. & DE VRIES, S. C. 2012. A Mathematical Model for BRASSINOSTEROID INSENSITIVE1-Mediated Signaling in Root Growth and Hypocotyl Elongation. *Plant Physiology*, 160, 523-532.

VETTER, M. M., KRONHOLM, I., HE, F., HAWEKER, H., REYMOND, M., BERGELSON, J., ROBATZEK, S. & DE MEAUX, J. 2012. Flagellin Perception Varies Quantitatively in Arabidopsis thaliana and Its Relatives. *Molecular Biology and Evolution*, 29, 1655-1667.

VOINNET, O., RIVAS, S., MESTRE, P. & BAULCOMBE, D. 2015. An enhanced transient expression system in plants based on suppression of gene silencing by the p19 protein of tomato bushy stunt virus (Retraction of Vol 33, Pg 949, 2003). *Plant Journal*, 84, 846-846.

WANG, J., LI, H., HAN, Z., ZHANG, H., WANG, T., LIN, G., CHANG, J., YANG, W. & CHAI, J. 2015. Allosteric receptor activation by the plant peptide hormone phytosulfokine. *Nature*, 525, 265-8.

WANG, L., EINIG, E., ALMEIDA-TRAPP, M., ALBERT, M., FLIEGMANN, J., MITHOFER, A., KALBACHER, H. & FELIX, G. 2018. The systemin receptor SYR1 enhances resistance of tomato against herbivorous insects. *Nature Plants*, 4, 152-156.

WANG, X., KOTA, U., HE, K., BLACKBURN, K., LI, J., GOSHE, M. B., HUBER, S. C. & CLOUSE, S. D. 2008. Sequential Transphosphorylation of the BRI1/BAK1 Receptor Kinase Complex Impacts Early Events in Brassinosteroid Signaling. *Developmental Cell*, 15, 220-235.

WENDEHENNE, D., LAMOTTE, O., FRACHISSE, J. M., BARBIER-BRYGOO, H. & PUGIN, A. 2002. Nitrate efflux is an essential component of the cryptogein signaling pathway leading to defense responses and hypersensitive cell death in tobacco. *Plant Cell,* 14**,** 1937-1951.

WILDHAGEN, M., BUTENKO, M. A., AALEN, R. B., FELIX, G. & ALBERT, M. 2015. A chemiluminescence based receptor-ligand binding assay using peptide ligands with an acridinium ester label. *Bio-protocol,* 5**,** e1422-e1422.

WU, W. Z., WU, Y. J., GAO, Y., LI, M. Z., YIN, H. J., LV, M. H., ZHAO, J. X., LI, J. & HE, K. 2015. Somatic embryogenesis receptor-like kinase 5 in the ecotype Landsberg erecta of Arabidopsis is a functional RD LRR-RLK in regulating brassinosteroid signaling and cell death control. *Frontiers in Plant Science,* 6.

WULFF, B. B. H., THOMAS, C. M., SMOKER, M., GRANT, M. & JONES, J. D. G. 2001. Domain swapping and gene shuffling identify sequences required for induction of an Avr-dependent hypersensitive response by the tomato Cf-4 and Cf-9 proteins. *Plant Cell,* 13**,** 255-272.

YAMADA, K., YAMASHITA-YAMADA, M., HIRASE, T., FUJIWARA, T., TSUDA, K., HIRUMA, K. & SAIJO, Y. 2016. Danger peptide receptor signaling in plants ensures basal immunity upon pathogen-induced depletion of BAK1. *Embo Journal,* 35**,** 46-61.

YAMAGUCHI, Y., HUFFAKER, A., BRYAN, A. C., TAX, F. E. & RYAN, C. A. 2010. PEPR2 Is a Second Receptor for the Pep1 and Pep2 Peptides and Contributes to Defense Responses in Arabidopsis. *Plant Cell,* 22**,** 508-522.

YOO, S. D., CHO, Y. H. & SHEEN, J. 2007. Arabidopsis mesophyll protoplasts: a versatile cell system for transient gene expression analysis. *Nat Protoc,* 2**,** 1565-72.

YU, X., FENG, B., HE, P. & SHAN, L. 2017. From Chaos to Harmony: Responses and Signaling upon Microbial Pattern Recognition Xiao. *Annu Rev Phytopathol.,* 55**,** 109-137.

YUAN, M., JIANG, Z., BI, G., NOMURA, K., LIU, M., WANG, Y., CAI, B., ZHOU, J.-M., HE, S. Y. & XIN, X.-F. 2021a. Pattern-recognition receptors are required for NLR-mediated plant immunity. *Nature*.

YUAN, M., NGOU, B. P. M., DING, P. & XIN, X. F. 2021b. PTI-ETI crosstalk: an integrative view of plant immunity. *Curr Opin Plant Biol,* 62**,** 102030.

ZHOU, Z., BI, G. & ZHOU, J. M. 2018. Luciferase Complementation Assay for Protein-Protein Interactions in Plants. *Curr Protoc Plant Biol,* 3**,** 42-50.

ZIPFEL, C. 2014. Plant pattern-recognition receptors. *Trends in Immunology,* 35**,** 345-351.

ZIPFEL, C. & FELIX, G. 2005. Plants and animals: A different taste for microbes? *Current Opinion in Plant Biology,* 8**,** 353-360.

ZIPFEL, C., KUNZE, G., CHINCHILLA, D., CANIARD, A., JONES, J. D. G., BOLLER, T. & FELIX, G. 2006. Perception of the bacterial PAMP EF-Tu by the receptor EFR restricts Agrobacterium-mediated transformation. *Cell,* 125**,** 749-760.

ZIPFEL, C. & OLDROYD, G. E. D. 2017. Plant signalling in symbiosis and immunity. *Nature,* 543**,** 328-336.

ZIPFEL, C. & ROBATZEK, S. 2010. Pathogen-associated molecular pattern-triggered immunity: Veni, vidi...? *Plant Physiology,* 154**,** 551-554.

ZIPFEL, C., ROBATZEK, S., NAVARRO, L., OAKELEY, E. J., JONES, J. D. G., FELIX, G. & BOLLER, T. 2004. Bacterial disease resistance in Arabidopsis through flagellin perception. *Nature,* 428**,** 764-767.

Supplementary

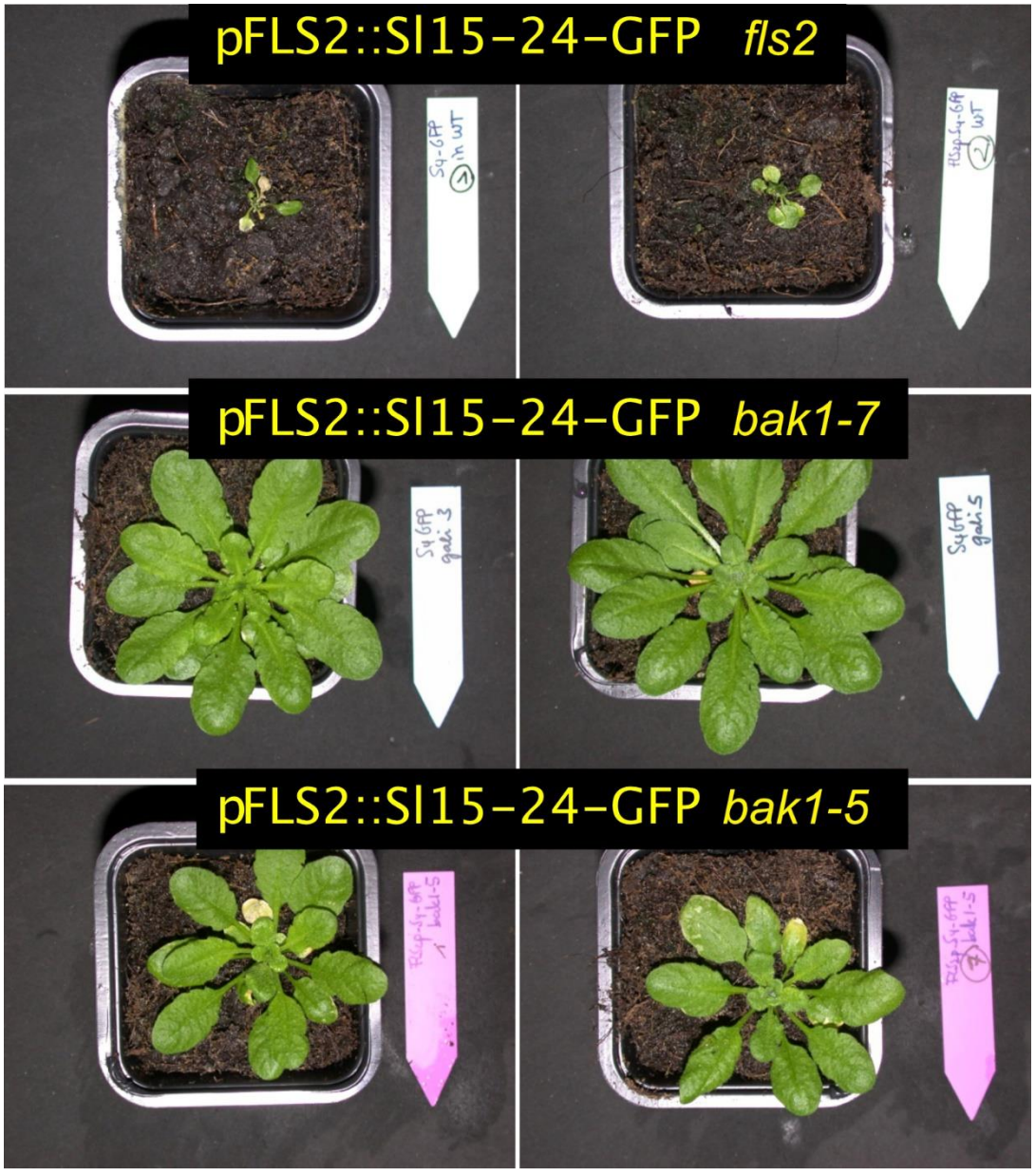

Supp. 1 Sl15-24 under endogenous AtFLS2 induced dwarfism is AtBAK1 dependent

Sl15-24-GFP construct under the endogenous AtFLS2 promoter was transformed via flora dipping in *fls2, bak1-7 or bak1-5* mutant *Arabidopsis.* Pictures were photographed 8 weeks after germination.

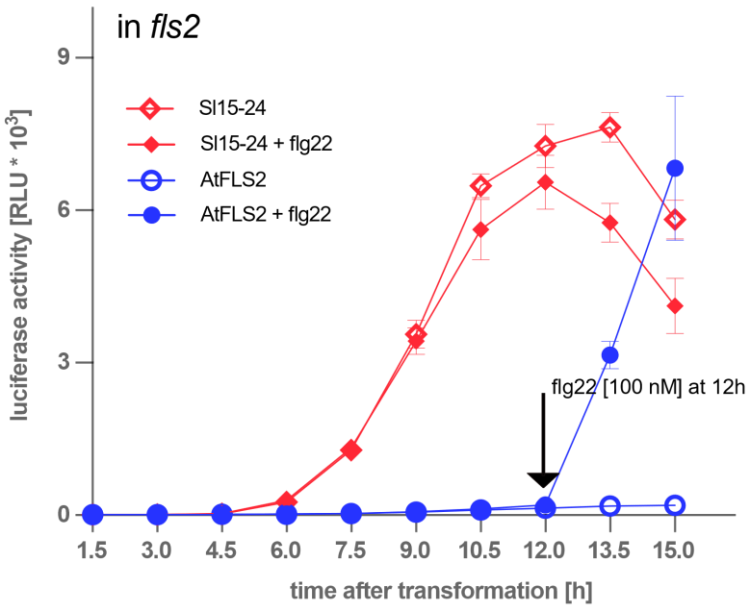

Supp. 2 autoactivation started at around 4.5 h post-transfection

Induction of pFRK1::Luciferase activity. *Sl15-24 or AtFLS2* were co-transformed with *pFRK1::Luciferase* into *A. thaliana efr x fls2* cells. Points and bars show means and standard deviations of 3 replicates. Luminescence was measured with the plate staying inside the luminometer all the time which might lead to a temperature somewhat higher than RT. Where indicated (black arrow), 100 nM of flg22 was added at 12 h post-transfection.

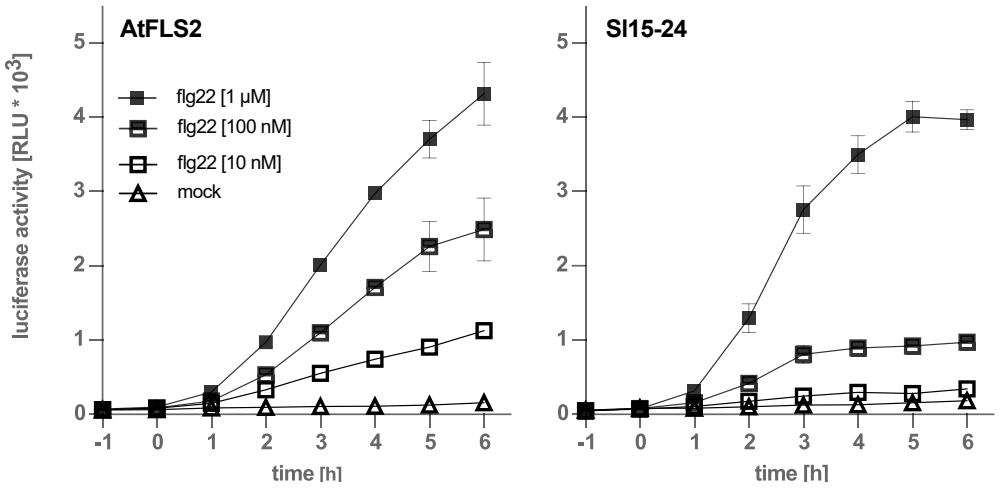

Supp. 3 Sl15-24 did not show autoactivation but respond to flg22 in *efr* x *fls2* x *bak1-5* x *serk4* cells

Mesophyll cells from *Arabidopsis* (*efr* x *fls2* x *bak1-5* x *serk4*) were transformed with a reporter construct *pFRK1::Luciferase* and *p35s::AtFLS2-GFP* or *p35s::Sl15-24-GFP*. Elicitors were added at t = 0, luciferase activity was monitored with a luminometer as RLU. Data points and error bars represented the mean and standard deviation of 3 replicates. The data represents for n = 2 experiments.

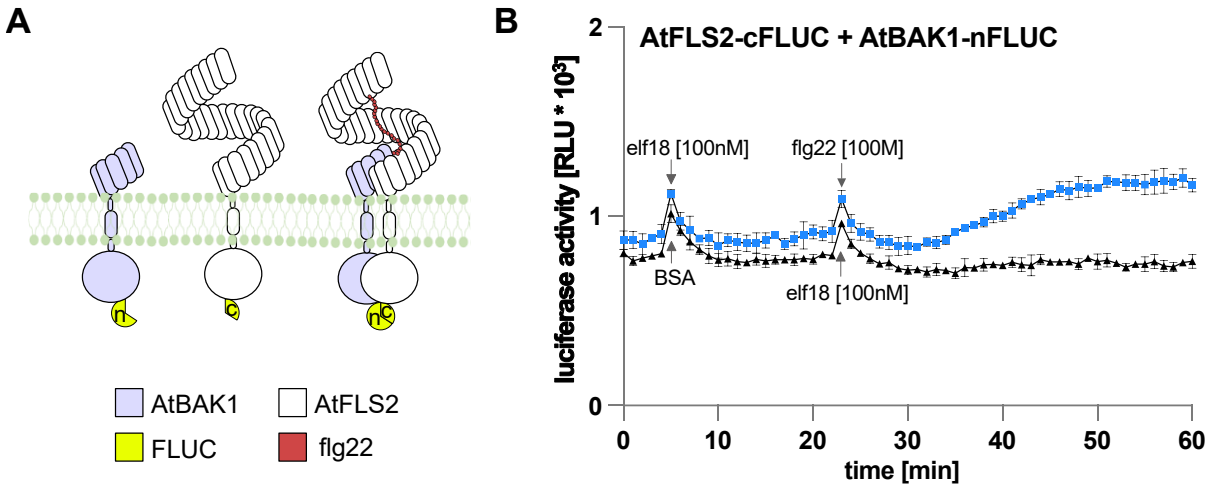

Supp. 4 AtFLS2 and AtBAK1 undergo specific flg22 induced interaction in *A. thaliana* cells

A) scheme of AtBAK1-cFLUC and AtFLS2-nFLUC upon flg22 perception. B) split firefly luciferase assay in *fls2* x *bak1-4 A. thaliana* mesophyll protoplasts. Luciferase activity was monitored as RLU with a luminometer. Data point and error bars show mean and SD of 3 replicates, respectively. Blue data points stand for the luciferase activity of cells treated with 100 nM elf18 followed by 100 nM flg22. Black data points present the luciferase activity of the cells treated with BSA followed by 100 nM of elf18.

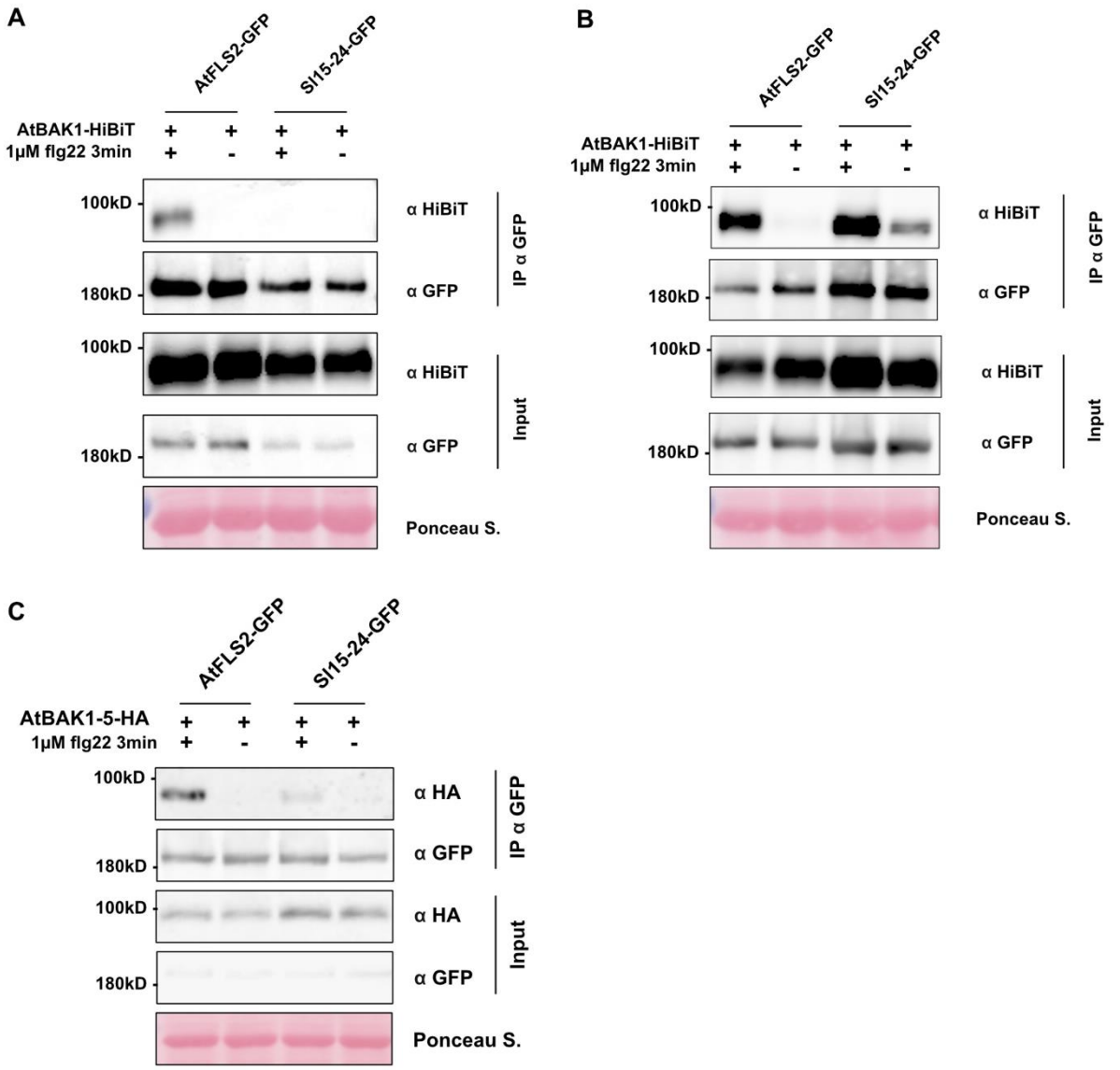

Supp. 5 Sl15-24 does not interact with AtBAK1 in a ligand-independent manner?

coimmunoprecipitation with extract from *N. benthamiana* leaves co-expressing FLS2-GFP and AtBAK1-HiBiT or AtBAK1-5-HA. *Bentamiana* leaves were harvested 3 min after infiltration with 1µM flg22 or water. GFP-tagged FLS2 receptors were immunoprecipitated with GFP-Trap from solubilized leaf extract. Western blots were developed either with anti-GFP antibodies or anti-HA antibodies or via HiBiT detection.

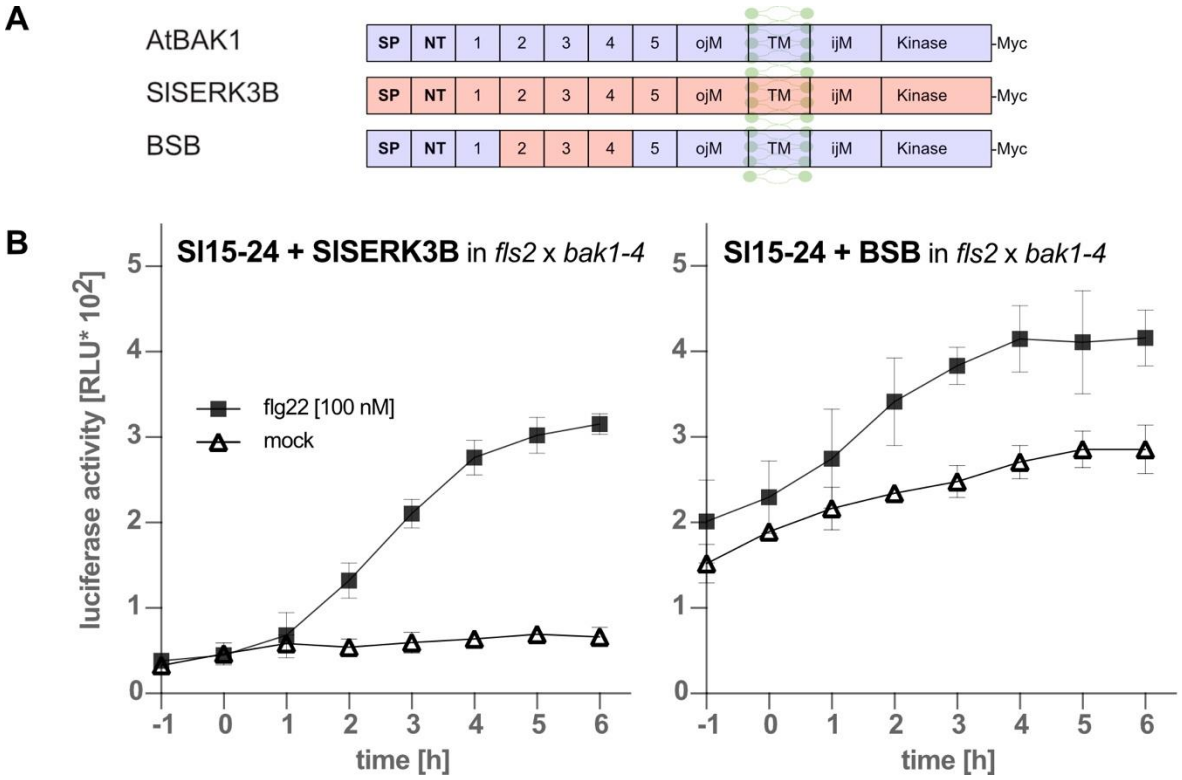

Supp. 6 BSB Chimeric SERK3 between AtBAK1 and SlSERK3B might partially induce the autoactivity of Sl15-24

A) schematic representation of hybrid SERK3 between AtBAK1 and SlSERK3B. B) pFRK1::Luciferase induction in cells from *fls2* x *bak1-4* plant expressing with luciferase reporter gene and Sl15-24 and SlSERK3B or BSB. Luminescence was shown as Y axis measured with a luminometer as RLU. Data points and error bars represent the mean and SD of 3 replicates. This experiment was only done 1 time.

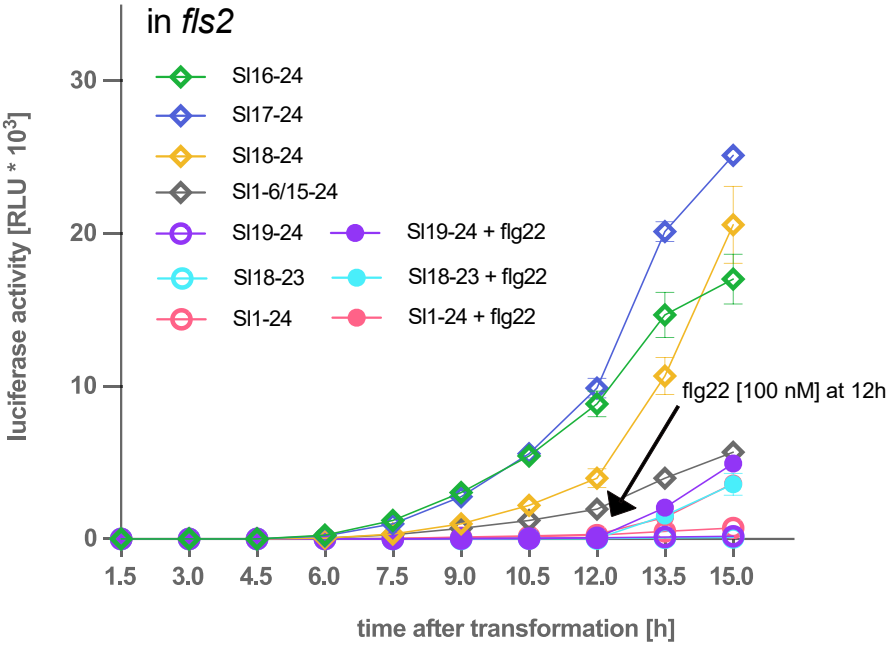

Supp. 7 pFRK1::Luciferase induced without treatment in *fls2* cells expressing Sl15-24-likes

Induction of pFRK1::Luciferase activity. Chimeric *FLS2* were co-transformed with *pFRK1::Luciferase* into *A. thaliana efr x fls2* cells. Each data point shows the mean of 3 replicates. Error bars show SD of the 3 replicates. Luminescence was measured with a luminol meter every 1.5 h automatically with the plate staying inside the luminometer all the time. 100 nM of flg22 was added at 12 h post-transfection, where indicated with black arrow.

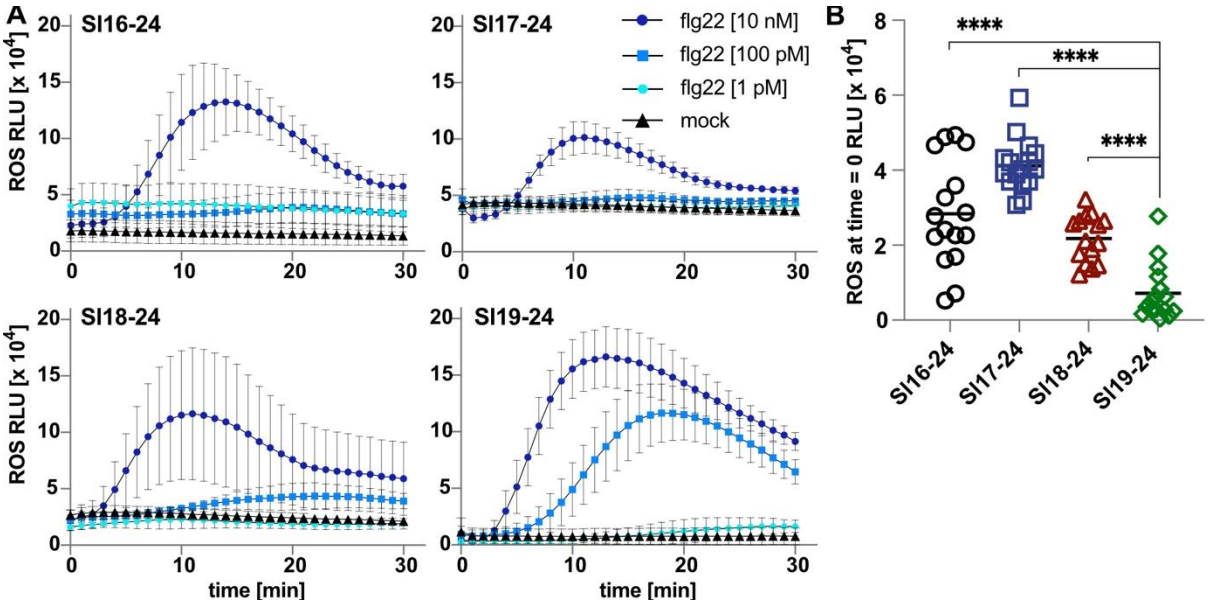

Supp. 8 Sl16-24, Sl17-24 and Sl18-24 are auto active in *N. benthamiana* but in a non-saturated way

ROS assay in *N. benthamiana* leaf expressing chimeric *FLS2* receptors. A) Luminescence was monitored every minute with a luminometer as RLU. Treatments were done as indicated on the graph. Data point and error bars stand for mean and SD of 4 replicates, respectively. B) ROS production of background value (time = 0) of n = 16 *N. benthamiana* leaf material expressing constructs indicated on the figure. The ROS elevation induced by expressing Sl16-24, Sl17-24 or Sl18-24 is statistically significant at the $p < 0.0001$ level, respectively.

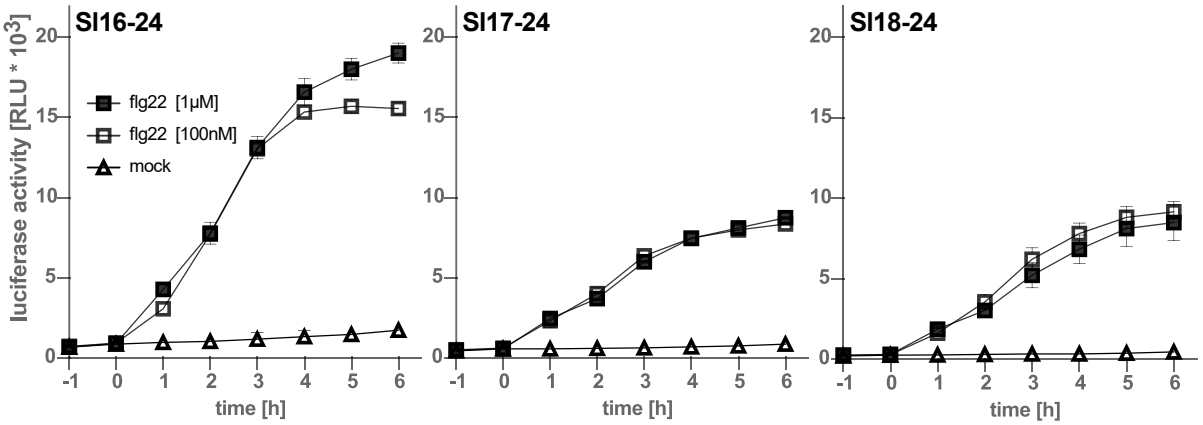

Supp. 9 BIR2OX suppress autoactivation of Sl16-24, Sl17-24 and Sl18-24

pFRK1::Luciferase induction in protoplasts from *A. thaliana* BIR2 overexpression line. Chimeric *FLS2* constructs were co-transformed luciferase reporter. Luciferase activity was measured as RLU with a luminometer. Data points and error bars shows mean an SD of 3 replicates.

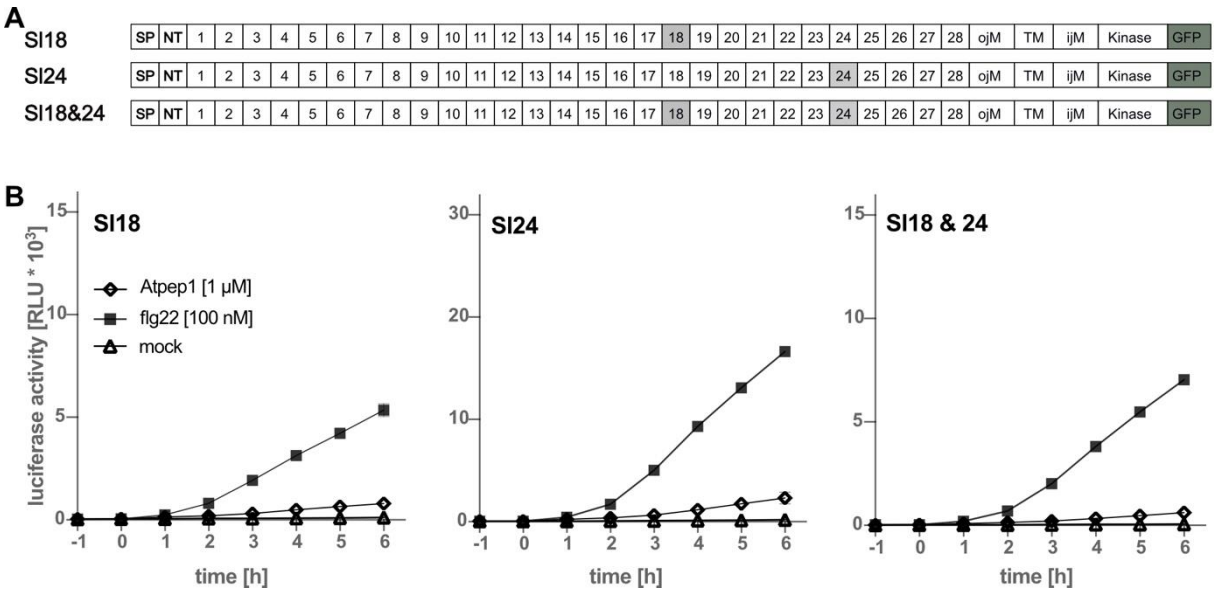

Supp. 10 Sl18, Sl24 or the combination Sl18 & 24 do not induce autoactivation in *A. thaliana*

A) schematic view of chimeric FLS2 receptors. B) induction of *pFRK1::Luciferase* in cells from *efr* x *fls2 Arabidopsis* plants. Cells co-express *Sl18, Sl24 or Sl18 & 24* with luciferase report construct were examined with luminometer. Data points and error bars stand for mean and SD of n = 3 of replicates, respectively. The experiment was repeated for another time and the same trend was observed.

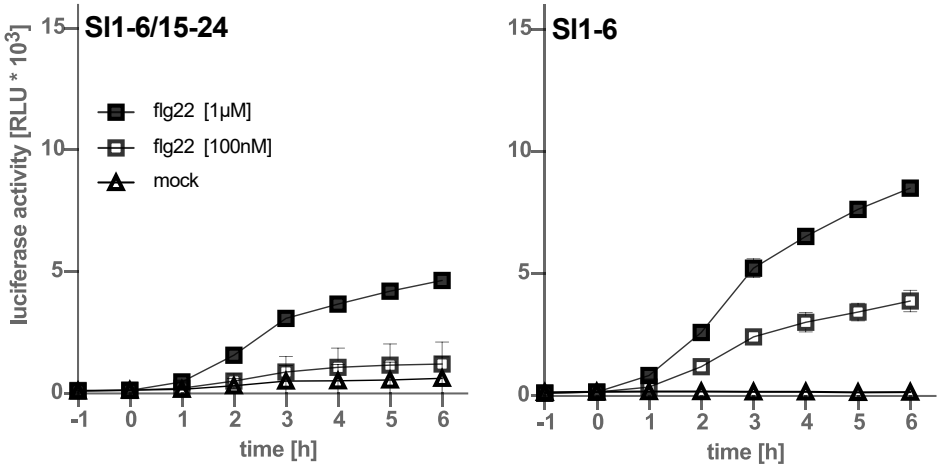

Supp. 11 BIR2 OX inhibited Sl1-6/15-24 induced autoactivation

pFRK1::Luciferase induction in *A. thaliana* protoplasts from BIR2 overexpression plants. Chimeric *FLS2* receptors were co-transformed with luciferase reporter. Luciferase activity was measured as RLU with a luminometer. Data points and error bars shows mean an SD of 3 replicates. Data shown represented for n = 3 independent experiments.

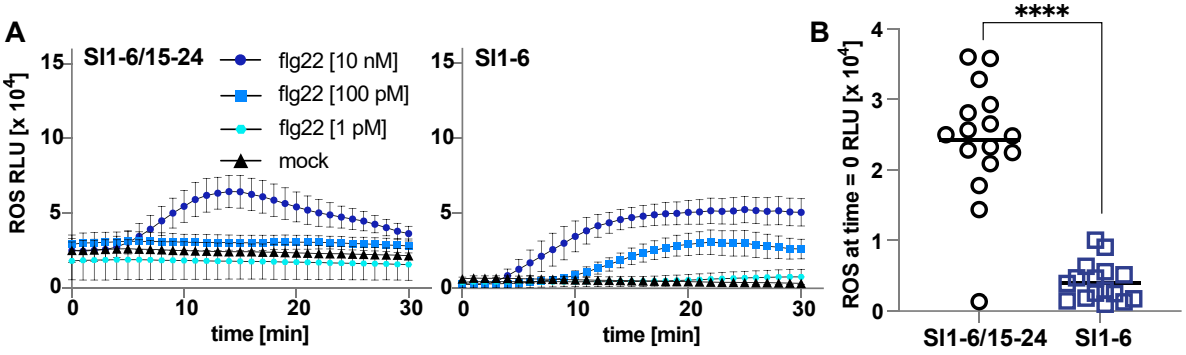

Supp. 12 Sl1-6/15-24 showed constitutive ROS production in *N. benthamiana*

ROS assay in *N. benthamiana* leaf expressing Sl1-6/15-24 and Sl1-6. A) Luminescence was monitored every minute with a luminometer as RLU. Data point and error bars stand for mean and SD of 4 replicates, respectively. B) Background value (time = 0) of ROS production for each replicate was shown as a single data point. Black lines indicated means of n = 16 replicates. The background ROS production of *N. benthamiana* leaf expressing Sl1-6/15-24 is significantly higher than that expressing Sl1-6, $p < 0.0001$ (T-test).

Primer list

Primer name	sequences	aim of using
AtFLS2 LRR15.2 Rev	TAACTGCCCCAACCCATTCGGGATCTCGCCAG TCATT	Sl15-16 overlapping-gateway cloning
SlFLS2 LRR15.3 Fw	AATGACTGGCGAGATCCCGAATGGGTTGGGGC AGTTAT	Sl15-16 overlapping-gateway cloning
SlFLS2 LRR16.23 Rev	CTTCCCAATTAATGGCTTGAGTCCGCTGAAAT TGTTATCAC	Sl15-16 overlapping-gateway cloning
AtFLS2 LRR 16.24 Fw	GTGATAACAATTTCAGCGGAACTCTCAAGCCA TTAATTG	Sl15-16 overlapping-gateway cloning
AtFLS2-16LRR Rev	GCCAATCATTGGTTTGAGAGTTCCTGTTTAAGT TGTTATCTGCC	Sl17-24 overlapping-gateway cloning
Sl15-24 17LRR- Fw	GGCAGATAACAACTTAACAGGAACTCTCAAAC CAATGATTGGC	Sl17-24 overlapping-gateway cloning
Sl15-24 -19LRR Rev	GCTTCATATCAAACATTTCTTCAGGAATTCAC CTTCTAGCTTGTTG	Sl15-19 overlapping-gateway cloning
AtFLS2 20LRR- Fw	CAACAAGCTAGAAGGTGAAATTCCTGAAGAAA TGTTTGATATGAAGC	Sl15-19 overlapping-gateway cloning
AtFLS2 -15LRR Rev	GAACTGTTGAAGAGATCATCAGGAATTTCACC GGTGAAATGATTCCTC	Sl16-24 overlapping-gateway cloning
Sl15-24 16LRR- Fw	GAGGAATCATTTCACCGGTGAAATTCCTGATG ATCTCTTCAACAGTTC	Sl16-24 overlapping-gateway cloning
AtFLS2-17LRR Rev	GTTTACCAATCTCTGGTGGGATCGGTCCAGTG AGAGAGTTATATG	Sl18-24 overlapping-gateway cloning
Sl15-24 18LRR-Fw	CATATAACTCTCTCACTGGACCGATCCCACCA GAGATTGGTAAAC	Sl18-24 overlapping-gateway cloning
Sl18-21 Rev	ACTTAAGGCTTGCAGGGATTGTGCCATTAAGC TTATTTC	Sl18-21 overlapping-gateway cloning
AtFLS2 22LRR- Fw	GAAATAAGCTTAATGGCACAATCCCTGCAAGC CTTAAGT	Sl18-21 overlapping-gateway cloning
BAK1 Ecto Rev	TCCAGTAATTCTATTACTCCCTGC	BAK1 soluble ECD gateway cloning
GG-Sl15-24tm Fw	TTATGGTCTCACACCATGAAGTTACTCTCAAA GACCT	AtFLS2 golden gate(BsaI)-gateway cloning

Primer name	sequences	aim of using
GG-BAK1kin Rev	TTATGGTCTCTCCTTTCTTGGACCCGAGGGGT ATTC	BAK1 golden gate(BSaI) cloning
ggAtFLS2 -3LRR Rev	TTATGGTCTCCATCACCGGACAACAAATTATT TC	Sl4-6/15-24 golden gate(BSaI)-gateway cloning
ggSlFLS2 4LRR- Fw	TTATGGTCTCATGATATACCTGATAGTATATG CAACTG	Sl4-6/15-24 golden gate(BSaI)-gateway cloning
ggSlFLS2 -6LRR Rev	TTATGGTCTCTGTATAGGTCCAGATAACTGGT T	Sl4-6/15-24 golden gate(BSaI)-gateway cloning
ggAtFLS2 7LRR- Fw	TTATGGTCTCAATACCGAGAGATTTTGGAAAT CTC	Sl4-6/15-24 golden gate(BSaI)-gateway cloning
ggSlFLS2 Fw	TTATGGTCTCACACCATGATGATGTTAAAGAC AGTTG	SlFLS2 golden gate(BSaI)-gateway cloning
ggSlFLS2 Rev	TTATGGTCTCTCCTTATCTTTTACCAAATGAG AAGGCA	SlFLS2 golden gate(BSaI)-gateway cloning
ggAtFLS2 17LRR Rev	TTATGGTCTCCCGGTCCAGTGAGAGAGTT	Sl18-23 golden gate(BSaI)-gateway cloning
ggSlFLS2 18LRR Fw	TTATGGTCTCAACCGATCCCACCAGAGATTGG TA	Sl18-23 golden gate(BSaI)-gateway cloning
ggSlFLS2 23LRR Rev	TTATGGTCTCCCTCTCCGTGCAACAAGTT	Sl18-23 golden gate(BSaI)-gateway cloning
ggAtFLS2 24LRR Fw	TTATGGTCTCAAGAGATCCCAAAGGAGCTTGG A	Sl18-23 golden gate(BSaI)-gateway cloning
AtFLS2 TM+20aa Rev	ATCCGGTAATGAGGACTCT	AtFLS2 ECD + TM + 20aa gateway cloning
BAK1 TM+20aa Rev	AACTTCTGGGTCCTCTTCAG	BAK1 ECD + TM + 20aa gateway cloning
AtFLS2 Ecto Rev	TCTGGTTCTCTTCGAGAAG	AtFLS2 soluble ECD gateway cloning
SlFLS2 14LRR Rev	TTATGGTCTCTAGATCCTTCCAGGAGGT	At15-24 golden gate(BSaI)-gateway cloning
AtFLS2 15LRR Fw	TTATGGTCTCAATCTATCCCGCGGGGT	At15-24 golden gate(BSaI)-gateway cloning

Primer name	sequences	aim of using
AtFLS2 24LRR Rev	TTATGGTCTCTGAATAGACCCAGAAAAGAGATTGTTTG	At15-24 golden gate(BSaI)-gateway cloning
S1FLS2 25LRR Fw	TTATGGTCTCAATTCCCAGATCCCTAGAACG	At15-24 golden gate(BSaI)-gateway cloning
ggS1FLS2 18LRR Rev	TTATGGTCTCTGGCACCTGAGAAACTGTT	S118 golden gate(BSaI)-gateway cloning
ggAtFLS2 19LRR Fw	TTATGGTCTCATGCCATCCCGAGAGAGATGTCG	S118 golden gate(BSaI)-gateway cloning
ggS1FLS2 24LRR Rev	TTATGGTCTCCACTGCCTGACAGATTATTATTTGA	S124 golden gate(BSaI)-gateway cloning
ggAtFLS2 25LRR Fw	TTATGGTCTCACAGTATTCCAAGATCTTTACAGGCC	S124 golden gate(BSaI)-gateway cloning
AtFLS2 24LRR 663L-N Fw	CAAACAATAACTTTTCTGGGTCTATTCCAAGATCTTT	Mutagenisis AtFLS2 663 Leucine to Asparagine
AtFLS2 24LRR 663L-N Rev	CCAGAAAAGTTATTGTTTGAAAGGTCGATTTCTTG	Mutagenisis AtFLS2 663 Leucine to Asparagine
S115-24 24LRR 663N-L Fw	CAAATAATCTTCTGTCAGGCAGCATTCCAAGATCTTT	Mutagenisis S115-24 663 Asparagine to Leucine
S115-24 24LRR 663N-L Rev	CCTGACAGAAGATTATTTGACATGTCAATCTCTTGAACC	Mutagenisis S115-24 663 Asparagine to Leucine
BIR3 ~1640bp sequencing	GGACACGATGAGGAGATATT	sequencing pcambia 1300 luc vector
BAK1 ~1700bp sequencing	GAAGGAGATGGTTTAGCTG	sequencing pcambia 1300 luc vector
BIR3 ~150bp Rev	GAAGAGTTTGGGAAAGACC	sequencing pcambia 1300 luc vector
BAK1 ~150bp Rev	GAGTAGCATCCCAACTTTG	sequencing pcambia 1300 luc vector
FlucC -200bp Fw	GCCGTTGTTGTTTTGGAG	sequencing pcambia 1300 luc vector
FlucN -650bp Fw	GATTCTCGCATGCCAGAG	sequencing pcambia 1300 luc vector

Primer name	sequences	aim of using
pcambia 1300 LUC seq Fw	CCTTCGCAAGACCCTTCC	Primer on Pcambia 1300 LUC vector to sequence through
pcambia 1300 cLUC seq Rev	GTAGCCATCCATCCTTGT	Primer on Pcambia 1300 cLUC vector to sequence through
pcambia 1300 nLUC seq Rev	GGACGCGTACGAGATCTG	Primer on Pcambia 1300 nLUC HA vector to sequence through
ggBIR2 B- Fw	TTATGGTCTCATCTGAACAATGAAAGAGATCG GCTCAAAAC	BIR2t1 golden gate(BSaI)cloning
ggBIR2 TM Rev	TTATGGTCTCCTACGATAATACCACCCAAATCC CAAAAGC	BIR2t1 golden gate(BSaI)cloning
ggBIR1 KD Fw	TTATGGTCTCACGTAAATTGGGTGCTGTTC	BIR2t1 golden gate(BSaI)cloning
ggBIR1 -D Rev	TTATGGTCTCTCCTTACGAGCAACTATGAGCT C	BIR2t1 golden gate(BSaI)cloning
ggBIR1 B- Fw	TTATGGTCTCATCTGAACAATGATGATGGGTA GGTTAGTTTTTG	BIR1t2 golden gate(BSaI)cloning
ggBIR1 TM Rev	TTATGGTCTCCTACGGAAATAGAAGAACAAAA CAACC	BIR1t2 golden gate(BSaI)cloning
ggBIR2 KD Fw	TTATGGTCTCGCGTATTAAGTGGACAAGGAGA CGAAG	BIR1t2 golden gate(BSaI)cloning
ggBIR2 kinase Rev -D	TTATGGTCTCTCCTTCACTTTCTCGTTCTCTTGC	BIR1t2 golden gate(BSaI)cloning
BAK1 C408Y Fw	ACATGATCATTACGACCCAAAGATTATTCATC G	mutagenesis *bak1-5* cysteine 408 to tyrosine
BAK1 C408Y Rev	TGGGTCGTAATGATCATGTAAATACGCAAG	mutagenesis *bak1-5* cysteine 408 to tyrosine

ECD amino acid sequences of chimeric FLS2 receptors:

SI15-24

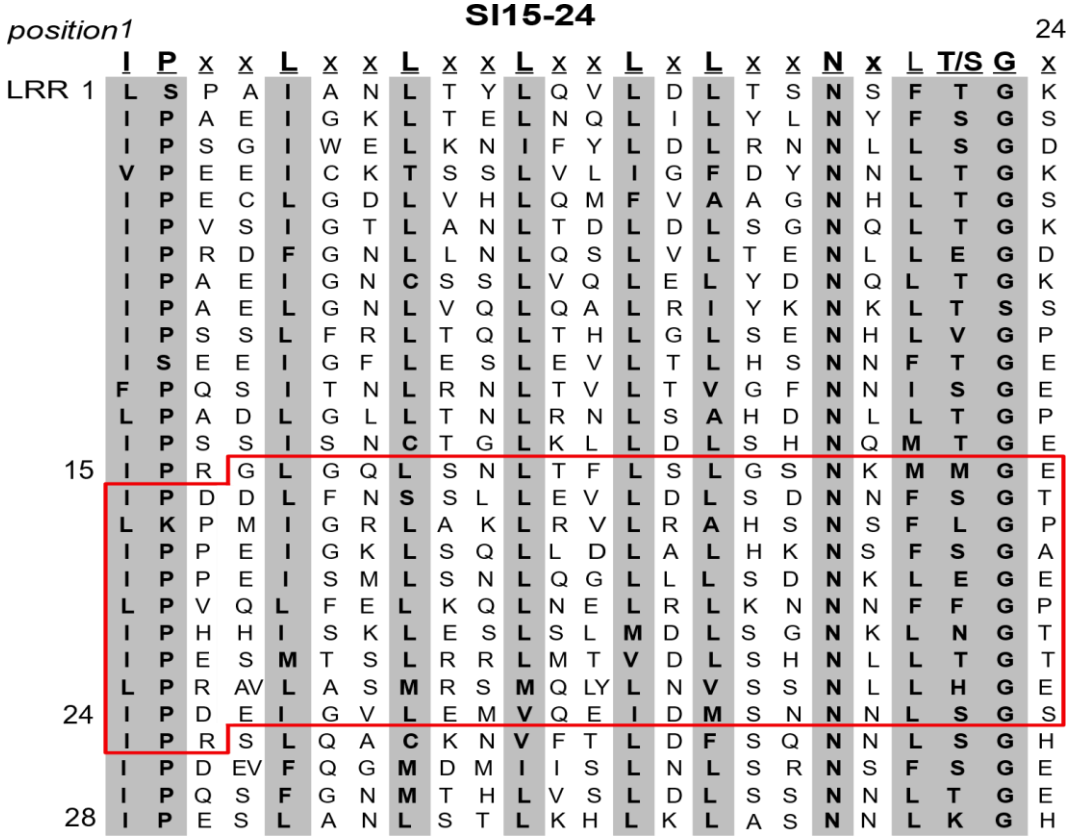

SI16-24

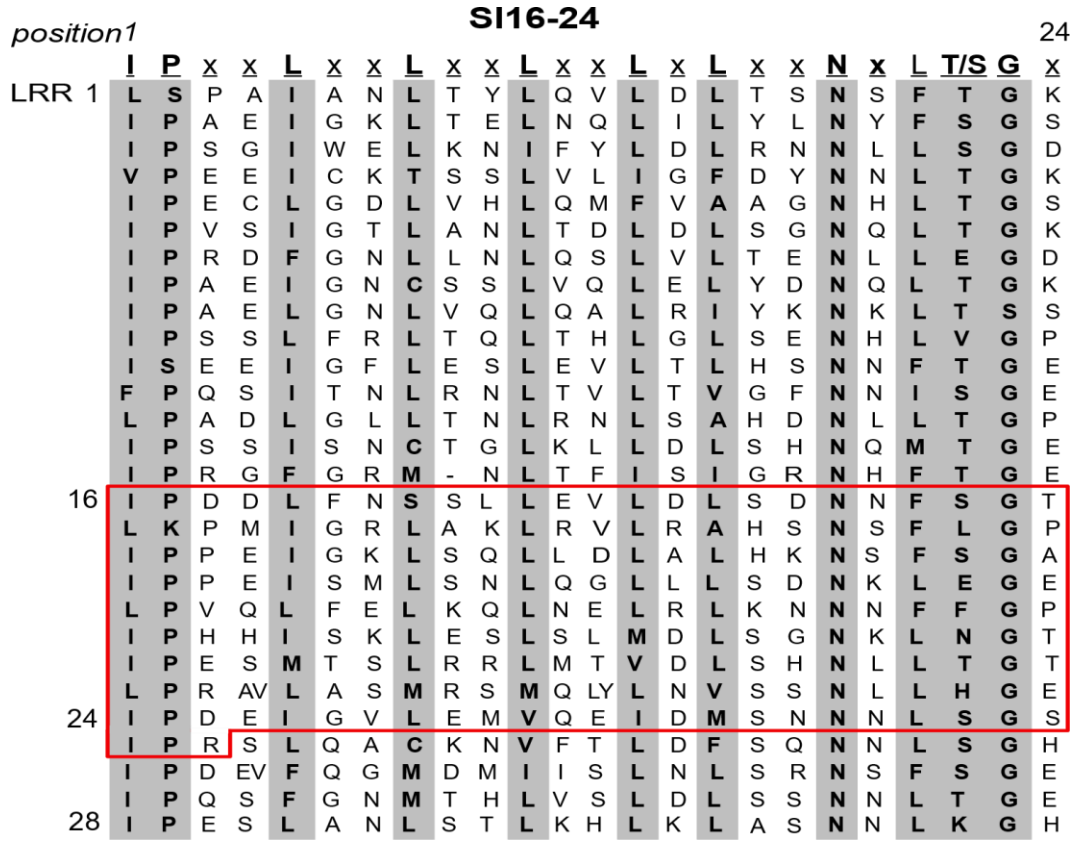

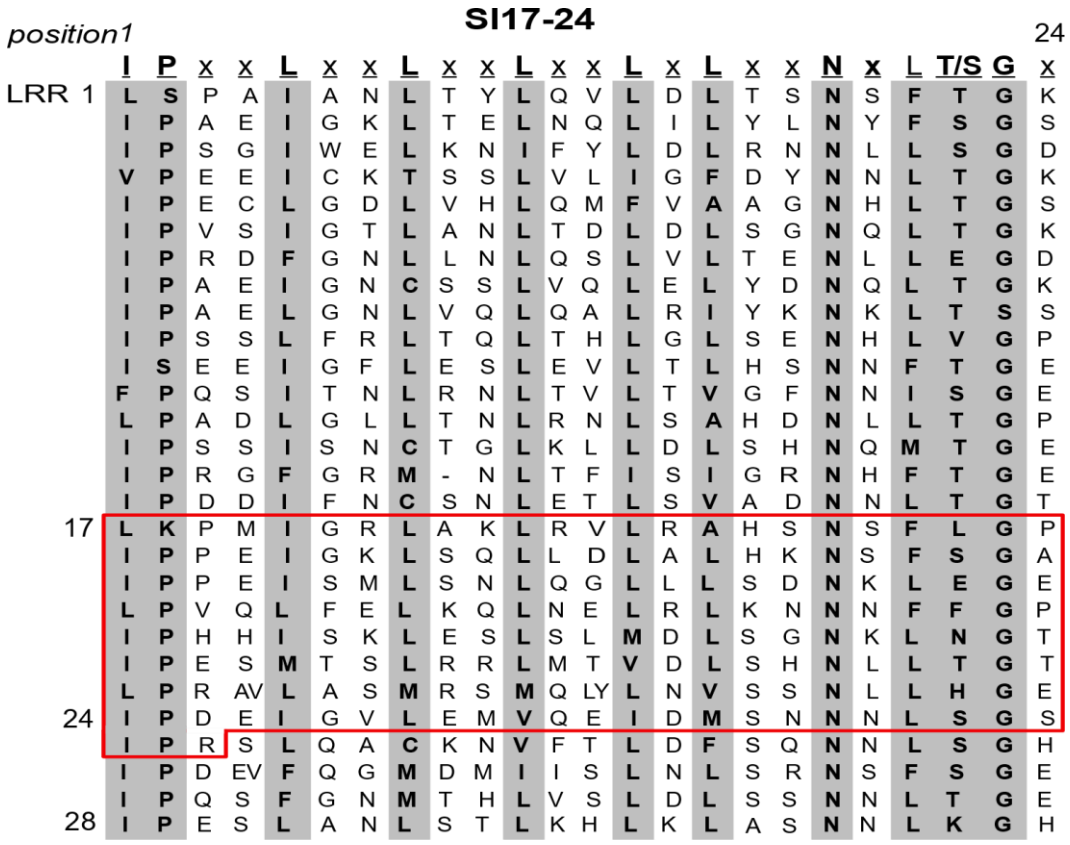
SI17-24
position1
24
I P x x L x x L x x L x x L x L x x N x L T/S G x
LRR 1
L S P A I A N L T Y L Q V L D L T S N S F T G K
I P A E I G K L T E L N Q L I L Y L N Y F S G S
I P S G I W E L K N I F Y L D L R N N L L S G D
V P E E I C K T S S L V L I G F D Y N N L T G K
I P E C L G D L V H L Q M F V A A G N H L T G S
I P V S I G T L A N L T D L D L S G N Q L T G K
I P R D F G N L L N L Q S L V L T E N L L E G D
I P A E I G N C S S L V Q L E L Y D N Q L T G K
I P A E L G N L V Q L Q A L R I Y K N K L T S S
I P S S L F R L T Q L T H L G L S E N H L V G P
I S E E I G F L E S L E V L T L H S N N F T G E
F P Q S I T N L R N L T V L T V G F N N I S G E
L P A D L G L L T N L R N L S A H D N L L T G P
I P S S I S N C T G L K L L D L S H N Q M T G E
I P R G F G R M - N L T F I S I G R N H F T G E
I P D D I F N C S N L E T L S V A D N N L T G T
17
L K P M I G R L A K L R V L R A H S N S F L G P
I P P E I G K L S Q L L D L A L H K N S F S G A
I P P E I S M L S N L Q G L L L S D N K L E G E
L P V Q L F E L K Q L N E L R L K N N N F F G P
I P H H I S K L E S L S L M D L S G N K L N G T
I P E S M T S L R R L M T V D L S H N L L T G T
L P R AV L A S M R S M Q LY L N V S S N L L H G E
24
I P D E I G V L E M V Q E I D M S N N N L S G S
I P R S L Q A C K N V F T L D F S Q N N L S G H
I P D EV F Q G M D M I I S L N L S R N S F S G E
I P Q S F G N M T H L V S L D L S S N N L T G E
28
I P E S L A N L S T L K H L L K L A S N N L K G H

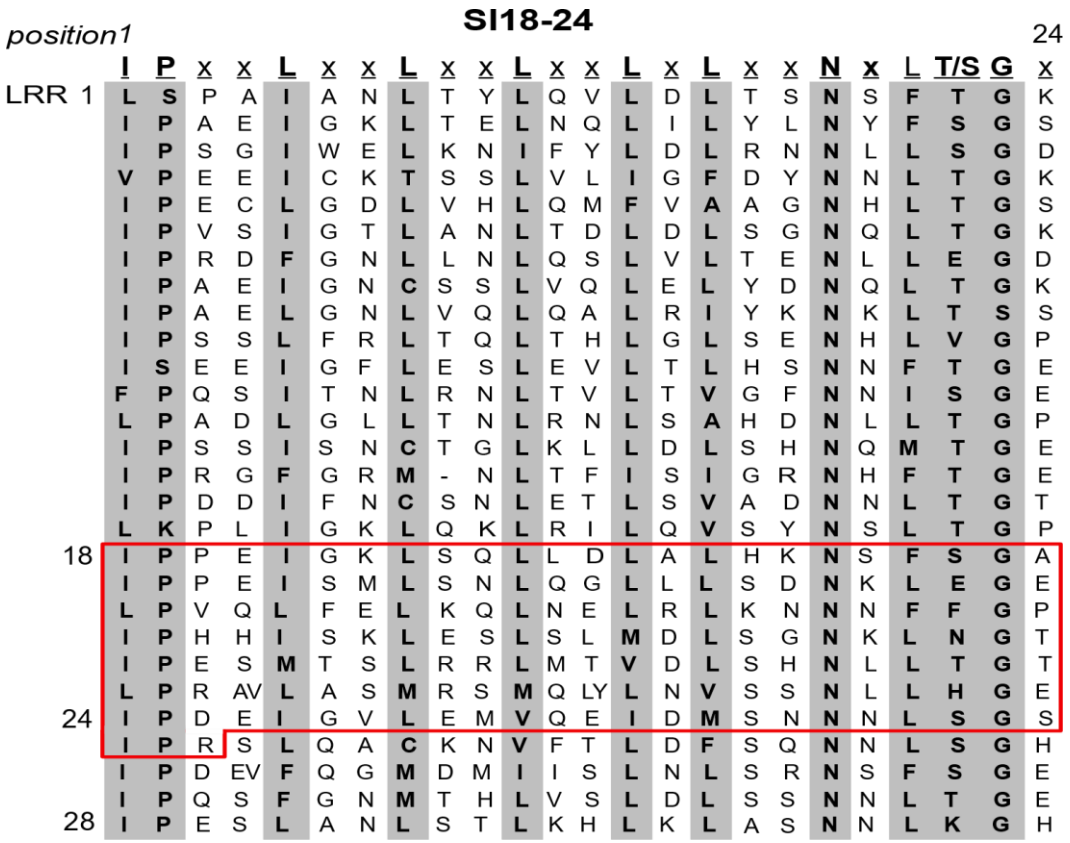
SI18-24
position1
24
I P x x L x x L x x L x x L x L x x N x L T/S G x
LRR 1
L S P A I A N L T Y L Q V L D L T S N S F T G K
I P A E I G K L T E L N Q L I L Y L N Y F S G S
I P S G I W E L K N I F Y L D L R N N L L S G D
V P E E I C K T S S L V L I G F D Y N N L T G K
I P E C L G D L V H L Q M F V A A G N H L T G S
I P V S I G T L A N L T D L D L S G N Q L T G K
I P R D F G N L L N L Q S L V L T E N L L E G D
I P A E I G N C S S L V Q L E L Y D N Q L T G K
I P A E L G N L V Q L Q A L R I Y K N K L T S S
I P S S L F R L T Q L T H L G L S E N H L V G P
I S E E I G F L E S L E V L T L H S N N F T G E
F P Q S I T N L R N L T V L T V G F N N I S G E
L P A D L G L L T N L R N L S A H D N L L T G P
I P S S I S N C T G L K L L D L S H N Q M T G E
I P R G F G R M - N L T F I S I G R N H F T G E
I P D D I F N C S N L E T L S V A D N N L T G T
L K P L I G K L Q K L R I L Q V S Y N S L T G P
18
I P P E I G K L S Q L L D L A L H K N S F S G A
I P P E I S M L S N L Q G L L L S D N K L E G E
L P V Q L F E L K Q L N E L R L K N N N F F G P
I P H H I S K L E S L S L M D L S G N K L N G T
I P E S M T S L R R L M T V D L S H N L L T G T
L P R AV L A S M R S M Q LY L N V S S N L L H G E
24
I P D E I G V L E M V Q E I D M S N N N L S G S
I P R S L Q A C K N V F T L D F S Q N N L S G H
I P D EV F Q G M D M I I S L N L S R N S F S G E
I P Q S F G N M T H L V S L D L S S N N L T G E
28
I P E S L A N L S T L K H L L K L A S N N L K G H

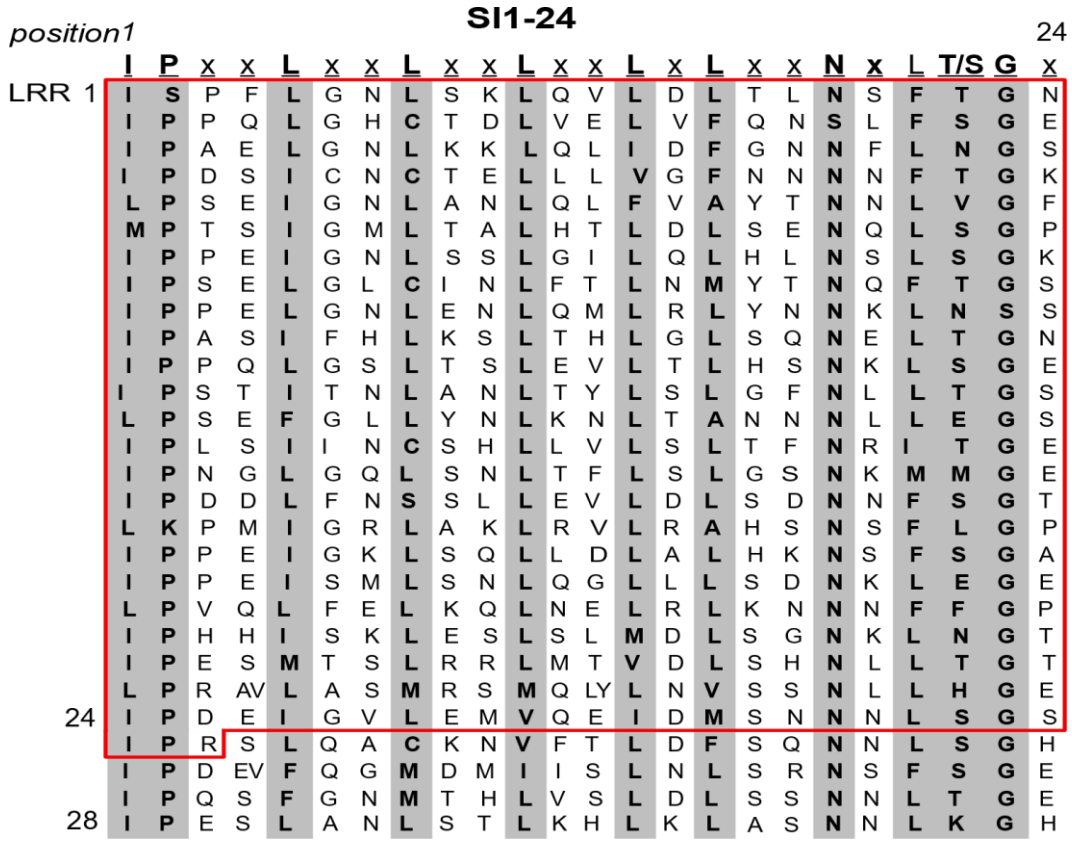
SI1-24
position1
24
I P x x L x x L x x L x x L x L x x N x L T/S G x
LRR 1
I S P F L G N L S K L Q V L D L T L N S F T G N
I P P Q L G H C T D L V E L V F Q N S L F S G E
I P A E L G N L K K L Q L I D F G N N F L N G S
I P D S I C N C T E L L L V G F N N N N F T G K
L P S E I G N L A N L Q L F V A Y T N N L V G F
M P T S I G M L T A L H T L D L S E N Q L S G P
I P P E I G N L S S L G I L Q L H L N S L S G K
I P S E L G L C I N L F T L N M Y T N Q F T G S
I P P E L G N L E N L Q M L R L Y N N K L N S S
I P A S I F H L K S L T H L G L S Q N E L T G N
I P P Q L G S L T S L E V L T L H S N K L S G E
I P S T I T N L A N L T Y L S L G F N L L T G S
L P S E F G L L Y N L K N L T A N N N L L E G S
I P L S I I N C S H L L V L S L T F N R I T G E
I P N G L G Q L S N L T F L S L G S N K M M G E
I P D D L F N S S L L E V L D L S D N N F S G T
L K P M I G R L A K L R V L R A H S N S F L G P
I P P E I G K L S Q L L D L A L H K N S F S G A
I P P E I S M L S N L Q G L L L S D N K L E G E
L P V Q L F E L K Q L N E L R L K N N N F F G P
I P H H I S K L E S L S L M D L S G N K L N G T
I P E S M T S L R R L M T V D L S H N L L T G T
L P R AV L A S M R S M Q LY L N V S S N L L H G E
24 I P D E I G V L E M V Q E I D M S N N N L S G S
I P R S L Q A C K N V F T L D F S Q N N L S G H
I P D EV F Q G M D M I I S L N L S R N S F S G E
I P Q S F G N M T H L V S L D L S S N N L T G E
28 I P E S L A N L S T L K H L K L A S N N L K G H

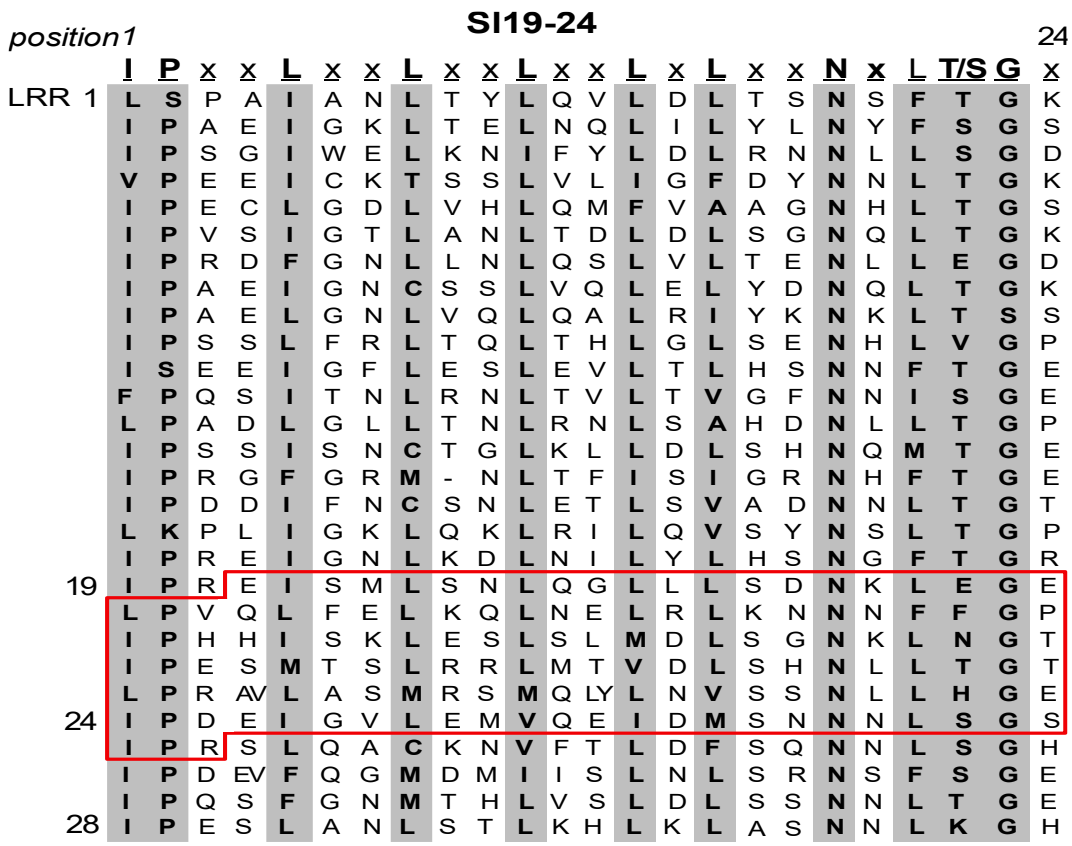
SI19-24
position1
24
I P x x L x x L x x L x x L x L x x N x L T/S G x
LRR 1
L S P A I A N L T Y L Q V L D L T S N S F T G K
I P A E I G K L T E L N Q L I L Y L N Y F S G S
I P S G I W E L K N I F Y L D L R N N L L S G D
V P E E I C K T S S L V L I G F D Y N N L T G K
I P E C L G D L V H L Q M F V A A G N H L T G S
I P V S I G T L A N L T D L D L S G N Q L T G K
I P R D F G N L L N L Q S L V L T E N L L E G D
I P A E I G N C S S L V Q L E L Y D N Q L T G K
I P A E L G N L V Q L Q A L R I Y K N K L T S S
I P S S L F R L T Q L T H L G L S E N H L V G P
I S E E I G F L E S L E V L T L H S N N F T G E
F P Q S I T N L R N L T V L T V G F N N I S G E
L P A D L G L L T N L R N L S A H D N L L T G P
I P S S I S N C T G L K L L D L S H N Q M T G E
I P R G F G R M - N L T F I S I G R N H F T G E
I P D D I F N C S N L E T L S V A D N N L T G T
L K P L I G K L Q K L R I L Q V S Y N S L T G P
I P R E I G N L K D L N I L Y L H S N G F T G R
19 I P R E I S M L S N L Q G L L L S D N K L E G E
L P V Q L F E L K Q L N E L R L K N N N F F G P
I P H H I S K L E S L S L M D L S G N K L N G T
I P E S M T S L R R L M T V D L S H N L L T G T
L P R AV L A S M R S M Q LY L N V S S N L L H G E
24 I P D E I G V L E M V Q E I D M S N N N L S G S
I P R S L Q A C K N V F T L D F S Q N N L S G H
I P D EV F Q G M D M I I S L N L S R N S F S G E
I P Q S F G N M T H L V S L D L S S N N L T G E
28 I P E S L A N L S T L K H L K L A S N N L K G H

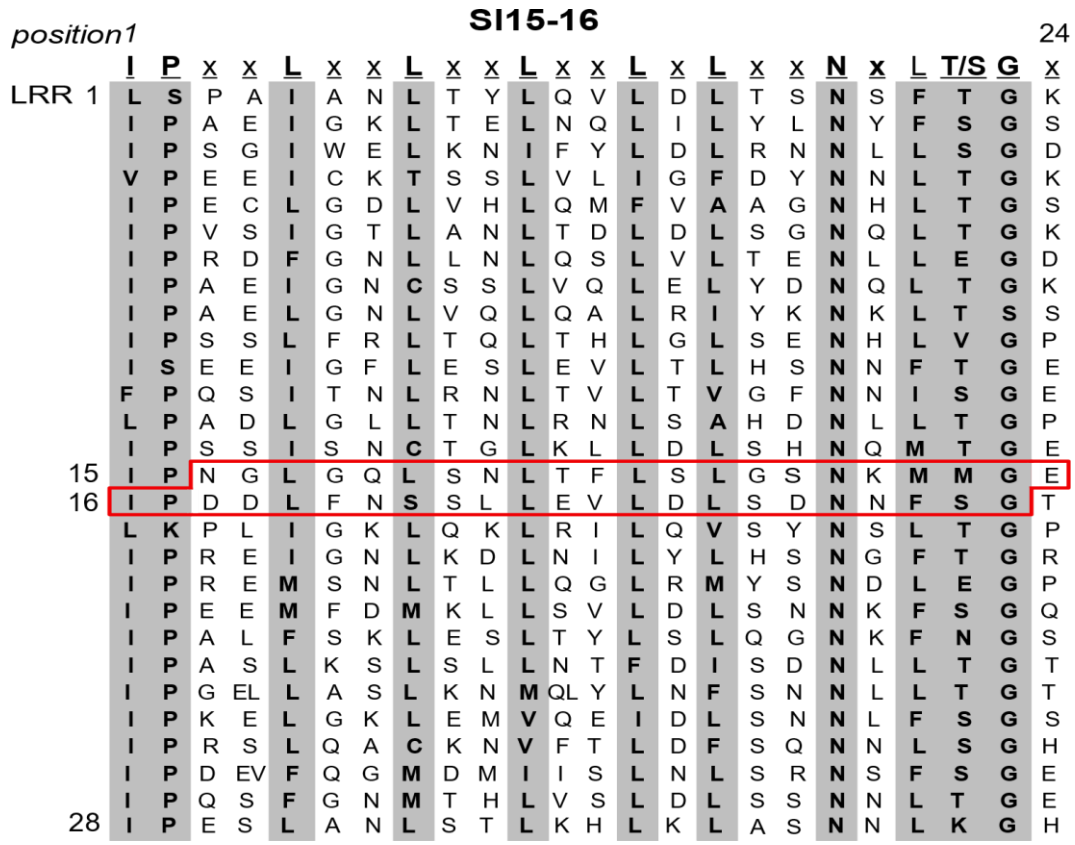
SI15-16
position1
24
I P x x L x x L x x L x x L x L x x N x L T/S G x
LRR 1 L S P A I A N L T Y L Q V L D L T S N S F T G K
I P A E I G K L T E L N Q L I L Y L N Y F S G S
I P S G I W E L K N I F Y L D L R N N L L S G D
V P E E I C K T S S L V L I G F D Y N N L T G K
I P E C L G D L V H L Q M F V A A G N H L T G S
I P V S I G T L A N L T D L D L S G N Q L T G K
I P R D F G N L L N L Q S L V L T E N L L E G D
I P A E I G N C S S L V Q L E L Y D N Q L T G K
I P A E L G N L V Q L Q A L R I Y K N K L T S S
I P S S L F R L T Q L T H L G L S E N H L V G P
I S E E I G F L E S L E V L T L H S N N F T G E
F P Q S I T N L R N L T V L T V G F N N I S G E
L P A D L G L L T N L R N L S A H D N L L T G P
I P S S I S N C T G L K L L D L S H N Q M T G E
15 I P N G L G Q L S N L T F L S L G S N K M M G E
16 I P D D L F N S S L L E V L D L S D N N F S G T
L K P L I G K L Q K L R I L Q V S Y N S L T G P
I P R E I G N L K D L N I L Y L H S N G F T G R
I P R E M S N L T L L Q G L R M Y S N D L E G P
I P E E M F D M K L L S V L D L S N N K F S G Q
I P A L F S K L E S L T Y L S L Q G N K F N G S
I P A S L K S L S L L N T F D I S D N L L T G T
I P G EL L A S L K N M QL Y L N F S N N L L T G T
I P K E L G K L E M V Q E I D L S N N L F S G S
I P R S L Q A C K N V F T L D F S Q N N L S G H
I P D EV F Q G M D M I I S L N L S R N S F S G E
I P Q S F G N M T H L V S L D L S S N N L T G E
28 I P E S L A N L S T L K H L K L A S N N L K G H

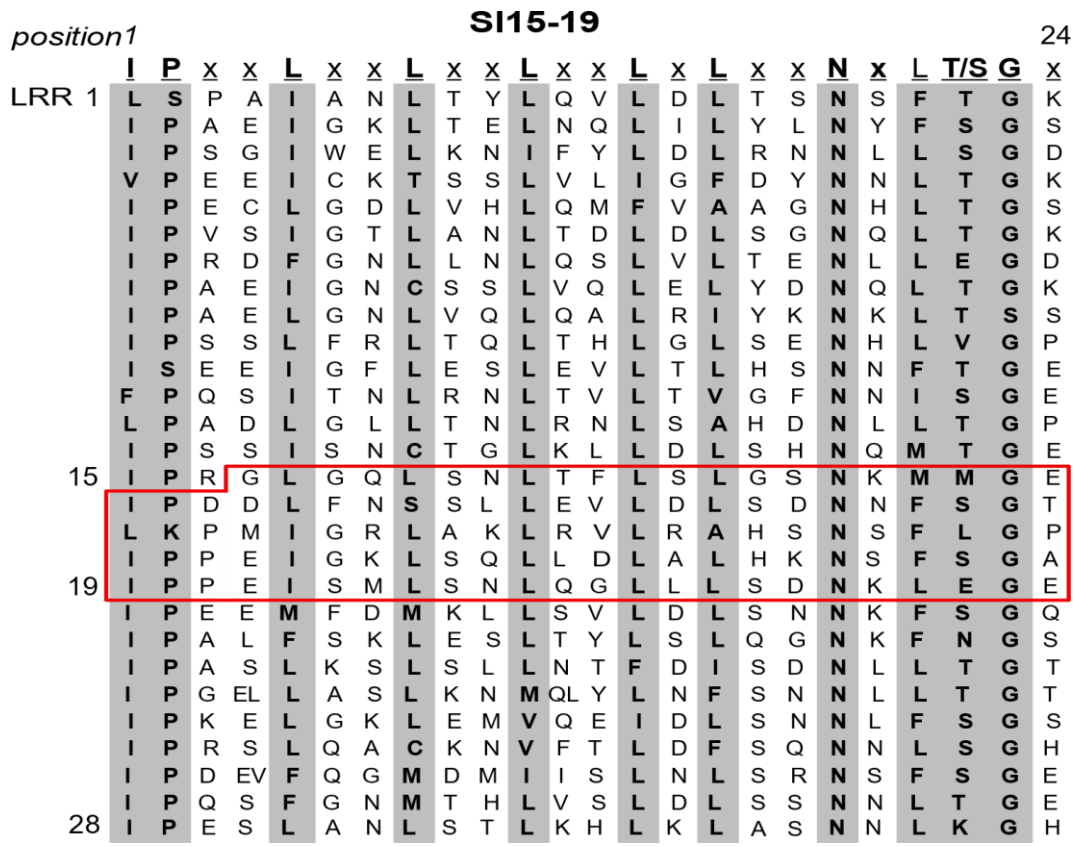
SI15-19
position1
24
I P x x L x x L x x L x x L x L x x N x L T/S G x
LRR 1 L S P A I A N L T Y L Q V L D L T S N S F T G K
I P A E I G K L T E L N Q L I L Y L N Y F S G S
I P S G I W E L K N I F Y L D L R N N L L S G D
V P E E I C K T S S L V L I G F D Y N N L T G K
I P E C L G D L V H L Q M F V A A G N H L T G S
I P V S I G T L A N L T D L D L S G N Q L T G K
I P R D F G N L L N L Q S L V L T E N L L E G D
I P A E I G N C S S L V Q L E L Y D N Q L T G K
I P A E L G N L V Q L Q A L R I Y K N K L T S S
I P S S L F R L T Q L T H L G L S E N H L V G P
I S E E I G F L E S L E V L T L H S N N F T G E
F P Q S I T N L R N L T V L T V G F N N I S G E
L P A D L G L L T N L R N L S A H D N L L T G P
I P S S I S N C T G L K L L D L S H N Q M T G E
15 I P R G L G Q L S N L T F L S L G S N K M M G E
I P D D L F N S S L L E V L D L S D N N F S G T
L K P M I G R L A K L R V L R A H S N S F L G P
I P P E I G K L S Q L L D L A L H K N S F S G A
19 I P P E I S M L S N L Q G L L L D N K L E G E
I P E E M F D M K L L S V L D L S N N K F S G Q
I P A L F S K L E S L T Y L S L Q G N K F N G S
I P A S L K S L S L L N T F D I S D N L L T G T
I P G EL L A S L K N M QL Y L N F S N N L L T G T
I P K E L G K L E M V Q E I D L S N N L F S G S
I P R S L Q A C K N V F T L D F S Q N N L S G H
I P D EV F Q G M D M I I S L N L S R N S F S G E
I P Q S F G N M T H L V S L D L S S N N L T G E
28 I P E S L A N L S T L K H L K L A S N N L K G H

SI18-23

	position1																						24
	I	**P**	x	x	**L**	x	x	**L**	x	x	**L**	x	x	**L**	x	**L**	x	x	**N**	x	L	**T/S**	**G**	x
LRR 1	L	S	P	A	I	A	N	L	T	Y	L	Q	V	L	D	L	T	S	N	S	F	T	G	K
	I	P	A	E	I	G	K	L	T	E	L	N	Q	L	I	L	Y	L	N	Y	F	S	G	S
	I	P	S	G	I	W	E	L	K	N	I	F	Y	L	D	L	R	N	N	L	L	S	G	D
	V	P	E	E	I	C	K	T	S	S	L	V	L	I	G	F	D	Y	N	N	L	T	G	K
	I	P	E	C	L	G	D	L	V	H	L	Q	M	F	V	A	A	G	N	H	L	T	G	S
	I	P	V	S	I	G	T	L	A	N	L	T	D	L	D	L	S	G	N	Q	L	T	G	K
	I	P	R	D	F	G	N	L	L	N	L	Q	S	L	V	L	T	E	N	L	L	E	G	D
	I	P	A	E	I	G	N	C	S	S	L	V	Q	L	E	L	Y	D	N	Q	L	T	G	K
	I	P	A	E	L	G	N	L	V	Q	L	Q	A	L	R	I	Y	K	N	K	L	T	S	S
	I	P	S	S	L	F	R	L	T	Q	L	T	H	L	G	L	S	E	N	H	L	V	G	P
	I	S	E	E	I	G	F	L	E	S	L	E	V	L	T	L	H	S	N	N	F	T	G	E
	F	P	Q	S	I	T	N	L	R	N	L	T	V	L	T	V	G	F	N	N	I	S	G	E
	L	P	A	D	L	G	L	L	T	N	L	R	N	L	S	A	H	D	N	L	L	T	G	P
	I	P	S	S	I	S	N	C	T	G	L	K	L	L	D	L	S	H	N	Q	M	T	G	E
	I	P	R	G	F	G	R	M	-	N	L	T	F	I	S	I	G	R	N	H	F	T	G	E
	I	P	D	D	I	F	N	C	S	N	L	E	T	L	S	V	A	D	N	N	L	T	G	T
	L	K	P	L	I	G	K	L	Q	K	L	R	I	L	Q	V	S	Y	N	S	L	T	G	P
18	I	P	P	E	I	G	K	L	S	Q	L	L	D	L	A	L	H	K	N	S	F	S	G	A
	I	P	P	E	I	S	M	L	S	N	L	Q	G	L	L	L	S	D	N	K	L	E	G	E
	L	P	V	Q	L	F	E	L	K	Q	L	N	E	L	R	L	K	N	N	N	F	F	G	P
	I	P	H	H	I	S	K	L	E	S	L	S	L	M	D	L	S	G	N	K	L	N	G	T
	I	P	E	S	M	T	S	L	R	R	L	M	T	V	D	L	S	H	N	L	L	T	G	T
23	L	P	R	AV	L	A	S	M	R	S	M	Q	LY	L	N	V	S	S	N	L	L	H	G	E
	I	P	K	E	L	G	K	L	E	M	V	Q	E	I	D	L	S	N	N	L	F	S	G	S
	I	P	R	S	L	Q	A	C	K	N	V	F	T	L	D	F	S	Q	N	N	L	S	G	H
	I	P	D	EV	F	Q	G	M	D	M	I	I	S	L	N	L	S	R	N	S	F	S	G	E
	I	P	Q	S	F	G	N	M	T	H	L	V	S	L	D	L	S	S	N	N	L	T	G	E
28	I	P	E	S	L	A	N	L	S	T	L	K	H	L	K	L	A	S	N	N	L	K	G	H

SI18-21

	position1																						24
	I	**P**	x	x	**L**	x	x	**L**	x	x	**L**	x	x	**L**	x	**L**	x	x	**N**	x	L	**T/S**	**G**	x
LRR 1	L	S	P	A	I	A	N	L	T	Y	L	Q	V	L	D	L	T	S	N	S	F	T	G	K
	I	P	A	E	I	G	K	L	T	E	L	N	Q	L	I	L	Y	L	N	Y	F	S	G	S
	I	P	S	G	I	W	E	L	K	N	I	F	Y	L	D	L	R	N	N	L	L	S	G	D
	V	P	E	E	I	C	K	T	S	S	L	V	L	I	G	F	D	Y	N	N	L	T	G	K
	I	P	E	C	L	G	D	L	V	H	L	Q	M	F	V	A	A	G	N	H	L	T	G	S
	I	P	V	S	I	G	T	L	A	N	L	T	D	L	D	L	S	G	N	Q	L	T	G	K
	I	P	R	D	F	G	N	L	L	N	L	Q	S	L	V	L	T	E	N	L	L	E	G	D
	I	P	A	E	I	G	N	C	S	S	L	V	Q	L	E	L	Y	D	N	Q	L	T	G	K
	I	P	A	E	L	G	N	L	V	Q	L	Q	A	L	R	I	Y	K	N	K	L	T	S	S
	I	P	S	S	L	F	R	L	T	Q	L	T	H	L	G	L	S	E	N	H	L	V	G	P
	I	S	E	E	I	G	F	L	E	S	L	E	V	L	T	L	H	S	N	N	F	T	G	E
	F	P	Q	S	I	T	N	L	R	N	L	T	V	L	T	V	G	F	N	N	I	S	G	E
	L	P	A	D	L	G	L	L	T	N	L	R	N	L	S	A	H	D	N	L	L	T	G	P
	I	P	S	S	I	S	N	C	T	G	L	K	L	L	D	L	S	H	N	Q	M	T	G	E
	I	P	R	G	F	G	R	M	-	N	L	T	F	I	S	I	G	R	N	H	F	T	G	E
	I	P	D	D	I	F	N	C	S	N	L	E	T	L	S	V	A	D	N	N	L	T	G	T
	L	K	P	L	I	G	K	L	Q	K	L	R	I	L	Q	V	S	Y	N	S	L	T	G	P
18	I	P	P	E	I	G	K	L	S	Q	L	L	D	L	A	L	H	K	N	S	F	S	G	A
	I	P	P	E	I	S	M	L	S	N	L	Q	G	L	L	L	S	D	N	K	L	E	G	E
	L	P	V	Q	L	F	E	L	K	Q	L	N	E	L	R	L	K	N	N	N	F	F	G	P
21	I	P	H	H	I	S	K	L	E	S	L	S	L	M	D	L	S	G	N	K	L	N	G	T
	I	P	A	S	L	K	S	L	S	L	L	N	T	F	D	I	S	D	N	L	L	T	G	T
	I	P	G	E	L	LA	S	L	K	N	M	M	Q	L	Y	L	NF	S	N	L	L	T	G	T
	I	P	K	E	L	G	K	L	E	M	V	Q	E	I	D	L	S	N	N	L	F	S	G	S
	I	P	R	S	L	Q	A	C	K	N	V	F	T	L	D	F	S	Q	N	N	L	S	G	H
	I	P	D	EV	F	Q	G	M	D	M	I	I	S	L	N	L	S	R	N	S	F	S	G	E
	I	P	Q	S	F	G	N	M	T	H	L	V	S	L	D	L	S	S	N	N	L	T	G	E
28	I	P	E	S	L	A	N	L	S	T	L	K	H	L	K	L	A	S	N	N	L	K	G	H

SI18

position1																						24
	I	P	x	x	L	x	x	L	x	x	L	x	x	L	x	L	x	x	N	x	L	T/S	G	x
LRR 1	L	S	P	A	I	A	N	L	T	Y	L	Q	V	L	D	L	T	S	N	S	F	T	G	K
	I	P	A	E	I	G	K	L	T	E	L	N	Q	L	I	L	Y	L	N	Y	F	S	G	S
	I	P	S	G	I	W	E	L	K	N	I	F	Y	L	D	L	R	N	N	L	L	S	G	D
	V	P	E	E	I	C	K	T	S	S	L	V	L	I	G	F	D	Y	N	N	L	T	G	K
	I	P	E	C	L	G	D	L	V	H	L	Q	M	F	V	A	A	G	N	H	L	T	G	S
	I	P	V	S	I	G	T	L	A	N	L	T	D	L	D	L	S	G	N	Q	L	T	G	K
	I	P	R	D	F	G	N	L	L	N	L	Q	S	L	V	L	T	E	N	L	L	E	G	D
	I	P	A	E	I	G	N	C	S	S	L	V	Q	L	E	L	Y	D	N	Q	L	T	G	K
	I	P	A	E	L	G	N	L	V	Q	L	Q	A	L	R	I	Y	K	N	K	L	T	S	S
	I	P	S	S	L	F	R	L	T	Q	L	T	H	L	G	L	S	E	N	H	L	V	G	P
	I	S	E	E	I	G	F	L	E	S	L	E	V	L	T	L	H	S	N	N	F	T	G	E
	F	P	Q	S	I	T	N	L	R	N	L	T	V	L	T	V	G	F	N	N	I	S	G	E
	L	P	A	D	L	G	L	L	T	N	L	R	N	L	S	A	H	D	N	L	L	T	G	P
	I	P	S	S	I	S	N	C	T	G	L	K	L	L	D	L	S	H	N	Q	M	T	G	E
	I	P	R	G	F	G	R	M	-	N	L	T	F	I	S	I	G	R	N	H	F	T	G	E
	I	P	D	D	I	F	N	C	S	N	L	E	T	L	S	V	A	D	N	N	L	T	G	T
	L	K	P	L	I	G	K	L	Q	K	L	R	I	L	Q	V	S	Y	N	S	L	T	G	P
18	I	P	P	E	I	G	K	L	S	Q	L	L	D	L	A	L	H	K	N	S	F	S	G	A
	I	P	R	E	M	S	N	L	T	L	L	Q	G	L	R	M	Y	S	N	D	L	E	G	P
	I	P	E	E	M	F	D	M	K	L	L	S	V	L	D	L	S	N	N	K	F	S	G	Q
	I	P	A	L	F	S	K	L	E	S	L	T	Y	L	S	L	Q	G	N	K	F	N	G	S
	I	P	A	S	L	K	S	L	S	L	L	N	T	F	D	I	S	D	N	L	L	T	G	T
	I	P	G	E	L	LA	S	L	K	N	M	M	Q	L	Y	L	NF	S	N	L	L	T	G	T
	I	P	K	E	L	G	K	L	E	M	V	Q	E	I	D	L	S	N	N	L	F	S	G	S
	I	P	R	S	L	Q	A	C	K	N	V	F	T	L	D	F	S	Q	N	N	L	S	G	H
	I	P	D	EV	F	Q	G	M	D	M	I	I	S	L	N	L	S	R	N	S	F	S	G	E
	I	P	Q	S	F	G	N	M	T	H	L	V	S	L	D	L	S	S	N	N	L	T	G	E
28	I	P	E	S	L	A	N	L	S	T	L	K	H	L	K	L	A	S	N	N	L	K	G	H

SI24

position1																						24
	I	P	x	x	L	x	x	L	x	x	L	x	x	L	x	L	x	x	N	x	L	T/S	G	x
LRR 1	L	S	P	A	I	A	N	L	T	Y	L	Q	V	L	D	L	T	S	N	S	F	T	G	K
	I	P	A	E	I	G	K	L	T	E	L	N	Q	L	I	L	Y	L	N	Y	F	S	G	S
	I	P	S	G	I	W	E	L	K	N	I	F	Y	L	D	L	R	N	N	L	L	S	G	D
	V	P	E	E	I	C	K	T	S	S	L	V	L	I	G	F	D	Y	N	N	L	T	G	K
	I	P	E	C	L	G	D	L	V	H	L	Q	M	F	V	A	A	G	N	H	L	T	G	S
	I	P	V	S	I	G	T	L	A	N	L	T	D	L	D	L	S	G	N	Q	L	T	G	K
	I	P	R	D	F	G	N	L	L	N	L	Q	S	L	V	L	T	E	N	L	L	E	G	D
	I	P	A	E	I	G	N	C	S	S	L	V	Q	L	E	L	Y	D	N	Q	L	T	G	K
	I	P	A	E	L	G	N	L	V	Q	L	Q	A	L	R	I	Y	K	N	K	L	T	S	S
	I	P	S	S	L	F	R	L	T	Q	L	T	H	L	G	L	S	E	N	H	L	V	G	P
	I	S	E	E	I	G	F	L	E	S	L	E	V	L	T	L	H	S	N	N	F	T	G	E
	F	P	Q	S	I	T	N	L	R	N	L	T	V	L	T	V	G	F	N	N	I	S	G	E
	L	P	A	D	L	G	L	L	T	N	L	R	N	L	S	A	H	D	N	L	L	T	G	P
	I	P	S	S	I	S	N	C	T	G	L	K	L	L	D	L	S	H	N	Q	M	T	G	E
	I	P	R	G	F	G	R	M	-	N	L	T	F	I	S	I	G	R	N	H	F	T	G	E
	I	P	D	D	I	F	N	C	S	N	L	E	T	L	S	V	A	D	N	N	L	T	G	T
	L	K	P	L	I	G	K	L	Q	K	L	R	I	L	Q	V	S	Y	N	S	L	T	G	P
	I	P	R	E	I	G	N	L	K	D	L	N	I	L	Y	L	H	S	N	G	F	T	G	R
	I	P	R	E	M	S	N	L	T	L	L	Q	G	L	R	M	Y	S	N	D	L	E	G	P
	I	P	E	E	M	F	D	M	K	L	L	S	V	L	D	L	S	N	N	K	F	S	G	Q
	I	P	A	L	F	S	K	L	E	S	L	T	Y	L	S	L	Q	G	N	K	F	N	G	S
	I	P	A	S	L	K	S	L	S	L	L	N	T	F	D	I	S	D	N	L	L	T	G	T
	I	P	G	E	L	LA	S	L	K	N	M	M	Q	L	Y	L	NF	S	N	L	L	T	G	T
24	I	P	D	E	I	G	V	L	E	M	V	Q	E	I	D	M	S	N	N	N	L	S	G	S
	I	P	R	S	L	Q	A	C	K	N	V	F	T	L	D	F	S	Q	N	N	L	S	G	H
	I	P	D	EV	F	Q	G	M	D	M	I	I	S	L	N	L	S	R	N	S	F	S	G	E
	I	P	Q	S	F	G	N	M	T	H	L	V	S	L	D	L	S	S	N	N	L	T	G	E
28	I	P	E	S	L	A	N	L	S	T	L	K	H	L	K	L	A	S	N	N	L	K	G	H

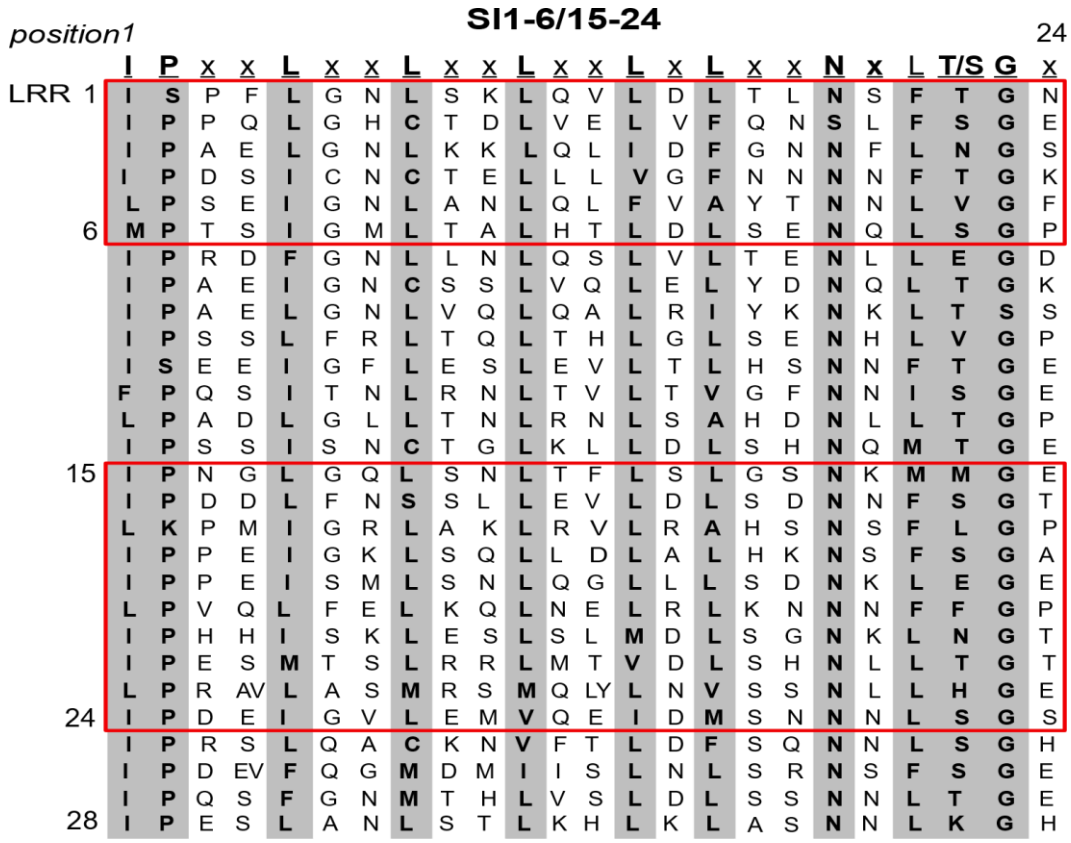
SI1-6/15-24
position1
24
I P x x L x x L x x L x x L x L x x N x L T/S G x
LRR 1
I S P F L G N L S K L Q V L D L T L N S F T G N
I P P Q L G H C T D L V E L V F Q N S L F S G E
I P A E L G N L K K L Q L I D F G N N F L N G S
I P D S I C N C T E L L L V G F N N N N F T G K
L P S E I G N L A N L Q L F V A Y T N N L V G F
6
M P T S I G M L T A L H T L D L S E N Q L S G P
I P R D F G N L L N L Q S L V L T E N L L E G D
I P A E I G N C S S L V Q L E L Y D N Q L T G K
I P A E L G N L V Q L Q A L R I Y K N K L T S S
I P S S L F R L T Q L T H L G L S E N H L V G P
I S E E I G F L E S L E V L T L H S N N F T G E
F P Q S I T N L R N L T V L T V G F N N I S G E
L P A D L G L L T N L R N L S A H D N L L T G P
I P S S I S N C T G L K L L D L S H N Q M T G E
15
I P N G L G Q L S N L T F L S L G S N K M M G E
I P D D L F N S S L L E V L D L S D N N F S G T
L K P M I G R L A K L R V L R A H S N S F L G P
I P P E I G K L S Q L L D L A L H K N S F S G A
I P P E I S M L S N L Q G L L L S D N K L E G E
L P V Q L F E L K Q L N E L R L K N N N F F G P
I P H H I S K L E S L S L M D L S G N K L N G T
I P E S M T S L R R L M T V D L S H N L L T G T
L P R AV L A S M R S M Q LY L N V S S N L L H G E
24
I P D E I G V L E M V Q E I D M S N N N L S G S
I P R S L Q A C K N V F T L D F S Q N N L S G H
I P D EV F Q G M D M I I S L N L S R N S F S G E
I P Q S F G N M T H L V S L D L S S N N L T G E
28
I P E S L A N L S T L K H L K L A S N N L K G H

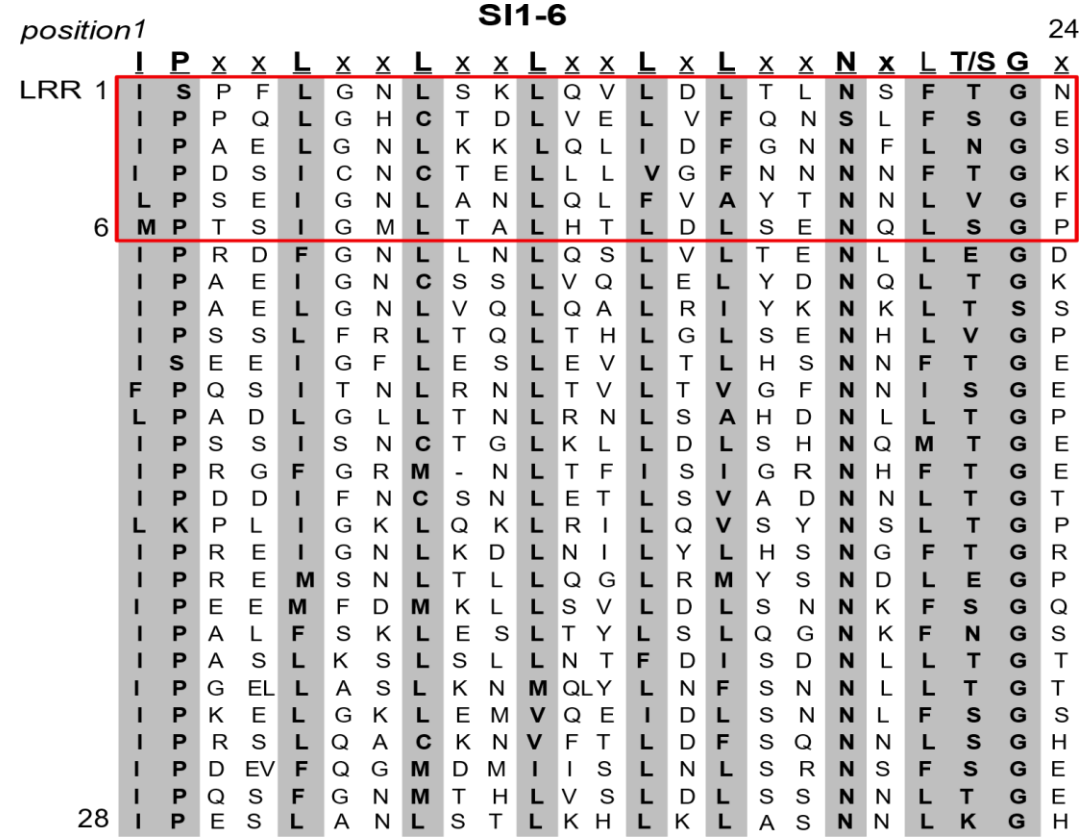
SI1-6
position1
24
I P x x L x x L x x L x x L x L x x N x L T/S G x
LRR 1
I S P F L G N L S K L Q V L D L T L N S F T G N
I P P Q L G H C T D L V E L V F Q N S L F S G E
I P A E L G N L K K L Q L I D F G N N F L N G S
I P D S I C N C T E L L L V G F N N N N F T G K
L P S E I G N L A N L Q L F V A Y T N N L V G F
6
M P T S I G M L T A L H T L D L S E N Q L S G P
I P R D F G N L L N L Q S L V L T E N L L E G D
I P A E I G N C S S L V Q L E L Y D N Q L T G K
I P A E L G N L V Q L Q A L R I Y K N K L T S S
I P S S L F R L T Q L T H L G L S E N H L V G P
I S E E I G F L E S L E V L T L H S N N F T G E
F P Q S I T N L R N L T V L T V G F N N I S G E
L P A D L G L L T N L R N L S A H D N L L T G P
I P S S I S N C T G L K L L D L S H N Q M T G E
I P R G F G R M - N L T F I S I G R N H F T G E
I P D D I F N C S N L E T L S V A D N N L T G T
L K P L I G K L Q K L R I L Q V S Y N S L T G P
I P R E I G N L K D L N I L Y L H S N G F T G R
I P R E M S N L T L L Q G L R M Y S N D L E G P
I P E E M F D M K L L S V L D L S N N K F S G Q
I P A L F S K L E S L T Y L S L Q G N K F N G S
I P A S L K S L S L L N T F D I S D N L L T G T
I P G EL L A S L K N M QLY L N F S N N L L T G T
I P K E L G K L E M V Q E I D L S N N L F S G S
I P R S L Q A C K N V F T L D F S Q N N L S G H
I P D EV F Q G M D M I I S L N L S R N S F S G E
I P Q S F G N M T H L V S L D L S S N N L T G E
28
I P E S L A N L S T L K H L K L A S N N L K G H

SI18 & 24

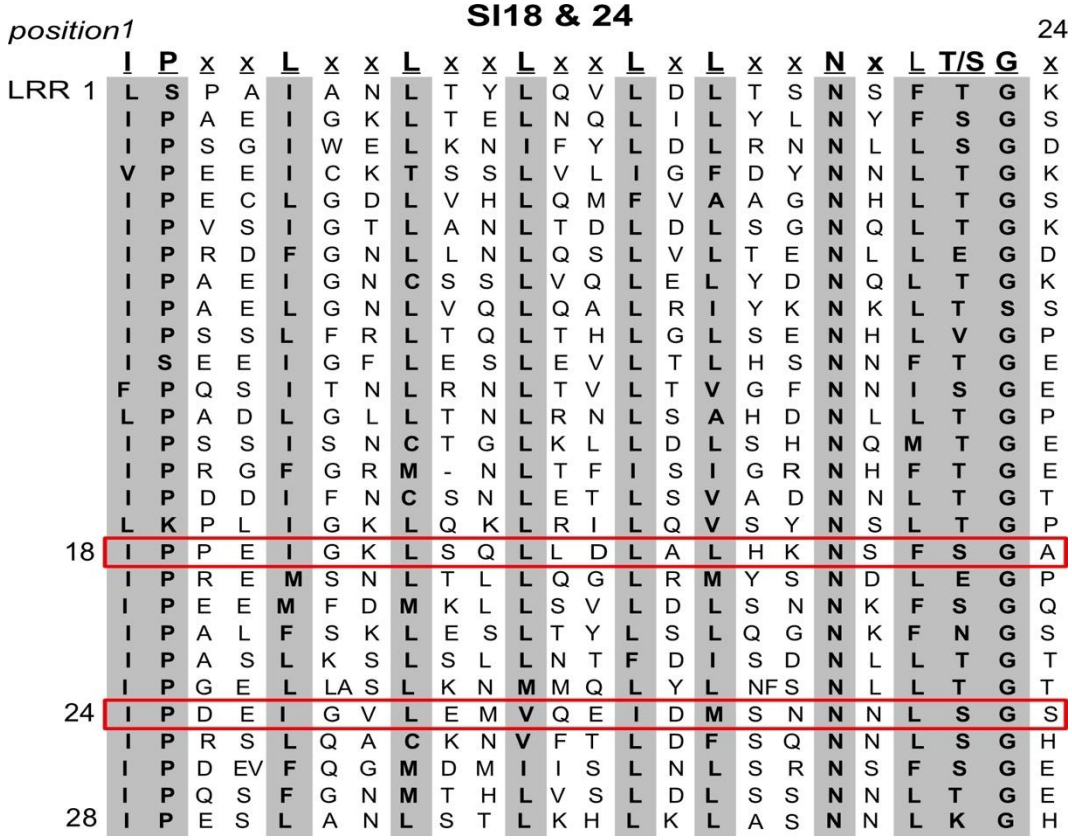

At15-24

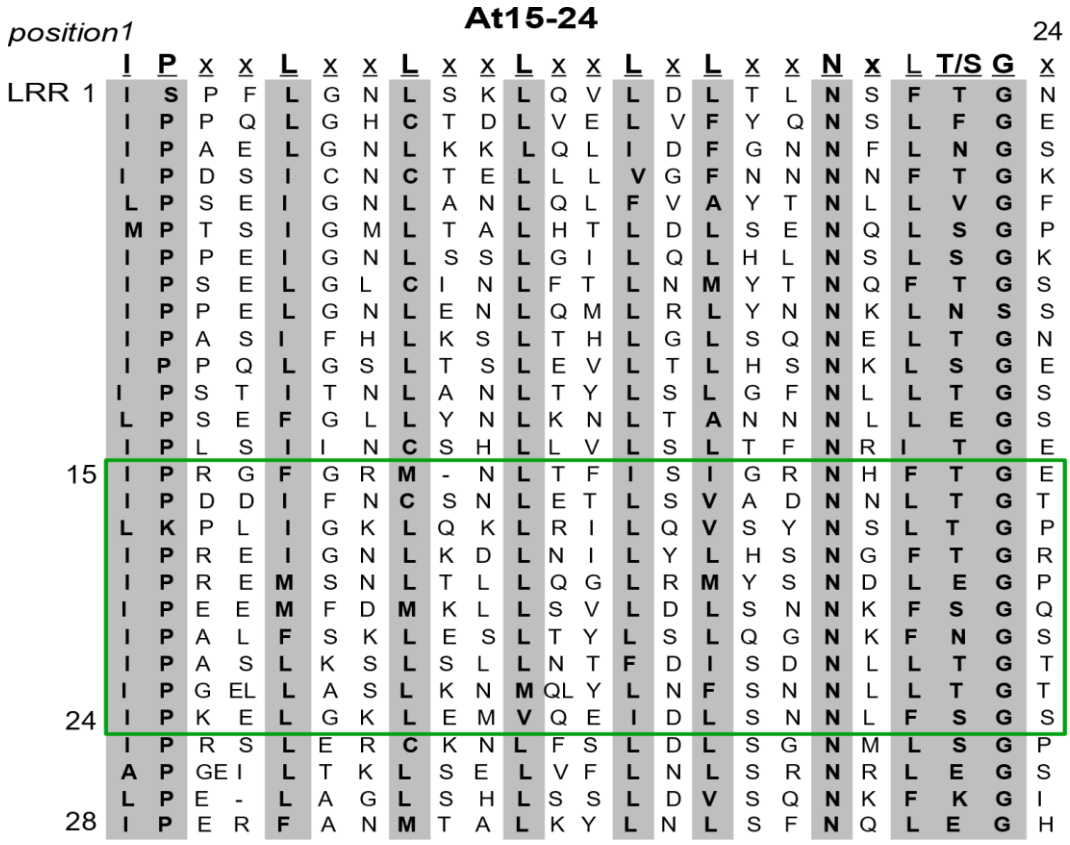

List of Abbreviations

Avr	Avirulence
Atpep1	Arabidopsis plant elicitor peptide 1
BAK1	Brassinosteroid insensitive 1-Associated receptor Kinase 1
BIK1	Botrytis-Induced Kinase 1
BIR	BAK1-Interacting Receptor like Kinase
BIR1t2	Chimera of BIR1 ectodomain-transmembrane domain and BIR2 kinase domain
BIR2t1	Chimera of BIR2 ectodomain-transmembrane domain and BIR1 kinase domain
BL	Brassinolide
BRI1	Brassinosteroid Insensitive 1
BtF	Chimera of AtBAK1 ectodomain-transmembrane domain and AtFLS2 kinase domain
CDPK	Calcium Dependent Protein Kinase
CEBiP	Chitin oligosaccharide Elicitor-Binding Protein
CERK1	Chitin Elicitor Receptor Kinase 1
Cf-4	*Cladosporium fulvum* resistance protein -4
Cf-9	*Cladosporium fulvum* resistance protein -9
co-ip	co-immunoprecipitation
DAMP	Damage-Associated Molecular Pattern
ECD	ectodomain
EFR	Elongation Factor Tu Receptor
EGF	Epidermal Growth Factor
EIX	Ethylene-Inducing Xylanase receptor
eMAX	Enigmatic MAMP of *Xanthomonas*
ETI	Effector-Tiggered Immunity
FLS2	Flagellin Sensing 2
KD	Kinase Domain
Lec	Lectin
LRR	Leucine-Rich Repeat
LYK5	Lysin Motif receptor Kinase 5
LysM	Lysin Motif
MAMP	Microbe-Associated Molecular Pattern
MAPK	Mitogen-Activated Protein Kinase
NLP	Necrosis and ethylene-inducing peptide 1-Like Proteins
PAMP	Pathogen-Associated Molecular Pattern
PEPR	Plant Elicitor Peptide Receptor
PGN	Peptidoglycan
PRR	Pattern Recognition Receptor

PTI	Pattern-Triggered Immunity
ReMax	Receptor of eMax
RLCK	Receptor-Like Cytoplasmic Kinase
RLK	Receptor-Like Kinase
RLP	Receptor-Like Protein
ROS	Reactive Oxygen Species
SERK	Somatic Embryogenesis Receptor Kinase
StB	Chimera of Sl15-24 ectodomain-transmembrane domain and AtBAK1 kinase domain
SOBIR1	Suppresser Of BIR1
SYR	Systemin Receptor
TMD	Transmembrane domain
WAK1	Wall-Associated Kinase 1
XA21	*Xanthomonas* resistance 21

List of Figures

Acknowledgements

I truly thank Prof. Georg Felix for giving me the chance to pursue my PhD in his group. I am grateful for his professional supervision and his patience on me. I appreciate very much his critical thinking and passion in science which influenced me and cultivated my interest in doing research. I also thank him for improving the written version of my thesis. I really appreciate working in his lab with a relax working style but extensive scientific discussion.

Thanks to Prof. Rosa Lozano-Durán for reviewing my thesis, thanks to Dr. Andrea Gust and Dr. Farid El-Kasmi for joining my thesis committee and helpful discussion.

Thanks to Dr. Lei Wang for teaching me laboratory techniques. The high standard experiment handling and useful skills I learned from him supported me to run my experiments smoothly.

Thanks to my thesis proofreading team: Dr. Judith Fliegmann, Dr. Chenlei Hua, Dr. Rory Pruitt, Rafee Ahamed, James Hunter.

Thanks to the whole Team Felix: Dr. Judith Fliegmann for revising my progress report slides and posters, sharing experiment protocols and giving helpful suggestions; Louis-Philippe Maier for sharing ideas and fruitful discussion, creating joyful atmosphere and having fun together, and truly thank him for providing economic support; Maike Osterhus for supportive conversation and having great time together; Nga Pham for soothing, calming and encouraging conversation; Ilonka Bock and Petra Neumann for all the assistance in the lab.

Thanks to whole plant biochemistry department: Prof. Thorsten Nürnberger for great discussion during progress report; Liane Schön for helping with complicated paperwork; Birgit Löffelhardt for accompany and being supportive; Ele, Sarina, Alex, Yanyue, Chenlei & Lisha, Katja, Peter, Rory…everyone for being supportive and having good time together. Thanks to the whole gardener team for great support with all the plant works.

Also faithfully, I thank my family in China: especially, my parents for unconditional love, encouragement and economic support; my cousin for helping me build up confidence and guiding me to go ahead. I thank my family in the UK: Qingsu Liu and Rafee Ahamed for friendly love, encouragement and being available all the time; James Hunter for comfort chat. I thank my family in Germany: Regina Jridi for motherly love and Renate K. Maier for encouraging chat; Anthony Chen for giving advice and being a good listener.

Thank you all for your support and help which take me to the end of my PhD!